INTELLIGENT BEHAVIOR OF AUTONOMOUS VEHICLES IN OUTDOOR ENVIRONMENT

Mechanical Engineering
Technical Report ME-TR-2

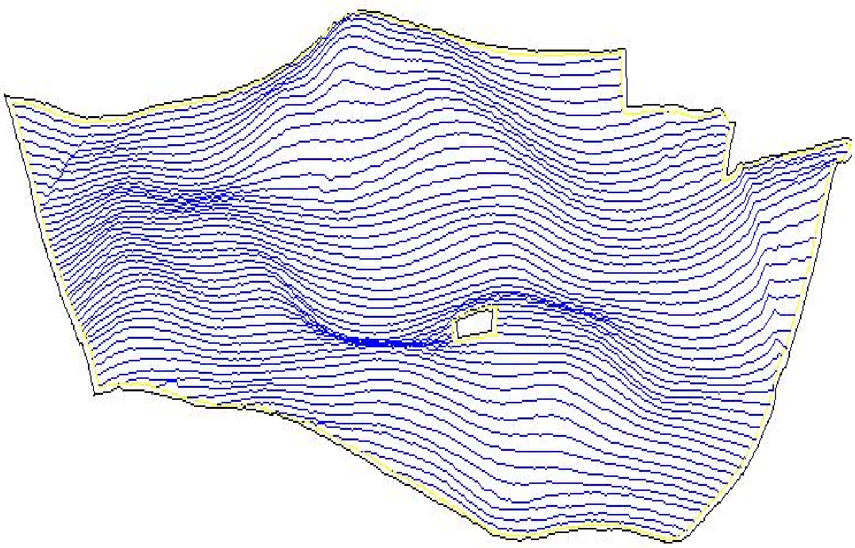

AARHUS UNIVERSITY
DEPARTMENT OF ENGINEERING

DATA SHEET

Title: Intelligent Behavior of Autonomous Vehicles in Outdoor Environment
Subtitle: Mechanical Engineering
Series title and no.: Technical report ME-TR-2

Author: Ibrahim Abdel Fattah Abdel Hameed, Department of Engineering – Mechanical Engineering, Aarhus University

Internet version: The report is available in electronic format (pdf) at the Department of Engineering website http://www.eng.au.dk.

Publisher: Aarhus University© **URL**: http://www.eng.au.dk

Year of publication: 2012 Pages: 98
Editing completed: June 2012

Abstract: The objective of this PhD-project has been to develop and enhance the operational behaviour of autonomous or automated conventional machines under out-door conditions. This has included developing high-level planning measures for the maximisation of machine productivity as an important element in the continued efforts of planning and controlling resource inputs in both arable and high value crops farming. The methods developed generate the optimized coverage path for any field regardless of its complexity on 2D or 3D terrains without any human intervention and in a manner that minimizes operational time, skipped and overlapped areas, and fuel consumption. By applying the developed approaches, a reduction of more than 20% in consumed fossil fuel together with a corresponding reduction in the emissions of CO2 and other greenhouses is achievable.

In this work, a software package for the autonomous navigation of field robotics over 2D and 3D field terrains and the optimization of field operations and machinery systems have been developed. a web-based version of the developed software package is currently under progress.

Keywords: automation, autonomous navigation, optimization, energy, environment, management of field operations, robotics in agriculture, machinery system, GPS, driving,

Supervisor: Claus Grøn Sørensen & Dionysis Bochtis

Please cite as: I. Hameed, 2012. Intelligent Behavior of Autonomous Vehicles in Outdoor Environment. Department of Engineering, Aarhus University. Denmark. 98 pp. - Technical report ME-TR-2

Cover image: Ibrahim Abdel Fattah Abdel Hameed

ISSN: 2245-4594 (ISBN:978-87-92869-38-8)

INTELLIGENT BEHAVIOR OF AUTONOMOUS VEHICLES IN OUTDOOR ENVIRONMENT

Ibrahim Abdel Fattah Abdel Hameed

Aarhus University, Department of Engineering

Abstract

The objective of this PhD-project has been to develop and enhance the operational behaviour of autonomous or automated conventional machines under out-door conditions. This has included developing high-level planning measures for the maximisation of machine productivity as an important element in the continued efforts of planning and controlling resource inputs in both arable and high value crops farming. The methods developed generate the optimized coverage path for any field regardless of its complexity on 2D or 3D terrains without any human intervention and in a manner that minimizes operational time, skipped and overlapped areas, and fuel consumption. By applying the developed approaches, a reduction of more than 20% in consumed fossil fuel together with a corresponding reduction in the emissions of CO_2 and other greenhouses is achievable.

In this work, a software package for the autonomous navigation of field robotics over 2D and 3D field terrains and the optimization of field operations and machinery systems have been developed. a web-based version of the developed software package is currently under progress.

Thesis committee

Thesis principal supervisor

Claus G. Sørensen	Associated Professor, Dept. of Engineering, Faculty of Science and Technology, Aarhus University, Denmark

Thesis scientific supervisor

Dionysis D. Bochtis	Associated Professor, Dept. of Engineering, Faculty of Science and Technology, Aarhus University, Denmak

Assessment committee

Peter Gorm Larsen	Professor, Dept. of Electronics and Computer Engineering, School of Engineering, Aarhus University, Denmark
Thomas Bak	Professor, Section for Automation & Control, Faculty of Engineering, Aalborg University, Denmark
Elisabeth Quendler	Assistant Professor, Division of Agricultural Engineering, University of Natural Resources and Life Sciences, Austria

This research was conducted under the auspices of the Graduate School of Science anAgriculture, Food and Environment (SAFE), Faculty of Science and Technology, Aarhus University.

Summery

The application of global positioning systems (GPS) in agriculture is currently a key issue as the basis for all-weather and high accuracy navigation systems. The development of automatic guidance and enhanced steering systems has advanced rapidly with the introduction of satellite technology and GPS supplemented with correction signals. One of the main reasons behind the increased interest in automatic guidance systems is the significant potential of these systems in finding the optimal coverage path that minimizes costs and environmental impacts from field operations. These guidance systems are the core components of any GPS-based automated guided vehicle, autonomous system, or robots, and understood as intelligent machines capable of self-management and designed to operate independently in a dynamic environment with minimal or no remote human intervention.

The aim of the PhD project was to develop reliable, robust, timely, and complete coverage path planning algorithms and models for both convex and non-convex field polygons and regardless of the complexity of the field boundary. The pursued approach build on the basic method of minimizing the non-working time or distance by optimizing the driving angle and the sequence of the field-work tracks, instead of following current standard motifs. The method is based on the field coverage problem being expressed as the traversal of a weighted graph allowing for finding the optimal track sequences by deriving the shortest traversal in the graph. The weight of the graph arcs could be based on any relative optimisation criterion, such as total or non-working travelling distance, total or non-productive operational time, a dedicated soil compaction measure, etc. Building on these basic path coverage measures, a complete tool that generates the geometrical representation of the field and the subsequent optimal coverage plan was developed.

The developed geometrical representations and algorithms are capable of dealing with both 2D and 3D field terrains as a way to fully represent the topographical characteristics of specific fields. Also, the developed suite of algorithms are computationally efficient with an enhanced optimization performance and compatible with the often low computing power of the on-board computers that controls and monitors the vehicle's various operating parameters. Specifically, a set of 2D coverage path planning algorithms are developed that can generate straight and curved field tracks parallel to an edge of a field or, alternatively, parallel to a user defined driving or steering angle. Based on specific field characteristics, the developed methods can divide a field into sub-regions and find the optimal path in each sub-region. Also, a simplified 2D coverage path planning algorithm was developed which significantly reduces computing time to around 30% of the computing time of the original algorithms and therefore suits the often low-computing power of on-board computers. Specific applications of the coverage path planning tool involve the management and planning of autonomous operations such as grass cutting, lawn striping, pitch marking in football stadiums, etc. As a way to minimize operations time and driving distance on headlands, driving angle and track sequencing optimization algorithms are invoked together with a complete coverage path planning algorithm that clusters field tracks into blocks and finds the optimum sequence of blocks in a manner that minimizes the driving distance between these blocks and avoids collision with field obstacles. As part of more accurately representing the topography of specific fields, a 3D terrain coverage path planning algorithm was developed that considers the elevation of field terrain that can be used for minimizing fuel consumed in various field operations and for various soil surface conditions. In 2D field representation, an optimal driving pattern is derived by which field operations are done in a manner which minimizes the amount of driving over field area and hence reducing soil compaction and fuel consumption. In 3D field representation, power models which consider elevation of field terrain are used to accurately estimate fuel consumption and hence finding the optimal driving pattern to drive up and down field hills in a manner which minimizes total fuel consumption. Simulation results showed that a reduction of fuel consumption in the range of 10-15% can be achieved when applying the optimized 2D coverage path planning in field operations. Reduction in fuel consumptions can exceed 20% in case of applying the optimized 3D coverage path planning in field operations. In addition to the economical impact of energy savings as a result of the application of the optimized coverage planning, environmental impact represented by a similar amount of reduced emissions of CO_2 and greenhouse gases are achieved.

Key words: automation, autonomous, optimization, energy, environment.

Sammenfatning

Anvendelsen af GPS (global positioneringssystem) i landbruget er i øjeblikket i fokus som grundlag for stor præcision i navigationssystemer til landbrugsmaskiner. Indførelsen af satellitteknologi og GPS med korrektionssignaler har ført til en hurtig udvikling af automatisk styring. Styresystemerne er de centrale elementer i ethvert GPS-baseret, automatisk styret køretøj, autonom maskine eller robot, som er beregnet til at operere selvstændigt i et dynamisk miljø med minimal eller ingen menneskelig indgriben gennem f.eks. fjernbetjening.

En af de vigtigste årsager til den øgede interesse for automatiske styresystemer er det betydelige potentiale for ved hjælp af disse systemer at finde den optimale rute, som minimerer omkostninger og miljøpåvirkninger fra markarbejdet.

Formålet med ph.d.-projektet var at udvikle pålidelige, robuste og præcise algoritmer og modeller til planlægning af kørselsruter i uregelmæssige marker. De udviklede geometriske beskrivelser og algoritmer er i stand til at håndtere markoverfalder i både 2D og 3D og dermed tage højde for de topografiske forhold på marken. Algoritmerne er samtidig beregningsmæssigt effektive og i stand til at optimere ydeevnen af den ofte begrænsede kapacitet i de påmonterede computere, der styrer og overvåger køretøjets forskellige funktioner.

Udviklingen af et specielt sæt algoritmer til 2D dækning skal fremhæves, idet det kan generere både lige og buede ruter parallelt med en markgrænse, eller parallelt med en brugerdefineret kørselsvinkel. De udviklede metoder kan opdele en mark i flere, mindre områder, baseret på markens karakteristika. Desuden er en alternativ, forenklet 2D algoritme udviklet til ruteplanlægning. Af hensyn til de påmonterede computeres ofte begrænsede ydeevne vil algoritmen reducere behovet for computerkapacitet til omkring 30% af beregningstiden for de oprindelige algoritmer.

Af specifikke anvendelsesområder kan nævnes græsslåning, stribeslåning af plæner og opmærkning på fodboldstadioner.

For at minimere køretiden og kørsel på forageren kan benyttes algoritmer, som ud fra kørevinkel og køresporenes rækkefølge optimerer kørselen ved at samle sporene i blokke og finde den optimale rækkefølge af blokke på en måde, der minimerer kørselsafstand mellem blokkene og samtidig undgår kollision med forhindringer på marken.

Ved at planlægge markarbejdet ud fra en mere præcis topografi for den enkelte mark vil energibehovet kunne nedbringes, og derfor blev en 3D algoritme udviklet til at beskrive stigninger i terrænet. Algoritmen kan ved hjælp af trækkraftmodeller med stor præcision vurdere det direkte energibehov og dermed finde den optimale rute gennem en ujævn mark. Resultaterne har vist en reduktion af energibehovet på 6,5% ved brug af den nævnte 3D konfiguration i forhold til det tilfælde, hvor ruteplanlægningen foretages ud fra en antagelse om helt plane marker. Reduktionen i samlet energibehov fører til reduceret brændstofforbrug og direkte CO_2-udledning.

Nøgleord: automatisering, autonom, optimering, energi, miljø

Preface

I owe a very special thanks to my supervisor Claus Aage Grøn Sørensen at Dept of Engineering (DoE), Faculty of Science and Technology, who gave me the possibility and motivation to start this PhD project on developing innovative methods to improve the behaviour of autonomous vehicles in outdoor environment. The basic idea was to develop an intelligent mobile robot or an autonomous vehicle to be entirely able to find its way from the barn to the field and vice versa, avoiding collision with obstacles and carrying out a specific field operation upon reaching the targeted field such as seeding, spraying, harvesting, etc. The vehicle should be able to generate the optimal coverage path planning required for its navigation throughout the entire field carrying out its task in a manner which reduces operational cost, increasing yield and reducing its environmental implication.

Thank you very much to my thesis co-supervisor, Dionysis D. Bochits, for guiding the progress of this work to its final destination. I would like also to thank my former co-supervisor Michael Nørremark for his sincere guidance and effort in defining the reach goal in the early phase of this project. In this regard, it is worth noting that the support and motivation from Morten D. Rasmussen, the former head of Department of Biosystems Engineering and the current head of Biological and Chemical Engineering (BCE) Section of DoE, and Ole Green, the head of Automation and System Technology (AUS) research group, have played a significant rule in putting me on track and helping me to accomplish my task.

Additional thanks are due to my colleagues in AUS group who motivated me to proceed to my destination. I cannot end that without pointing out to the secretary of Department, Anja Torup Hansen, without her continuous and sincere help I had been drowned in details and life would be unbelievably complex. Finally, a bunch of thanks and love go to my wife, Abeer Badawy (MBBS, MSc), and my sons, Mohamed and Omar for their patience and encouragement. My stay in Denmark and the work conducted in this thesis were financially support from Aarhus University so thanks to everyone who has made this possible.

I am sure that this thesis is interesting for many, and I hope it can contribute to further understanding and knowledge to the area of autonomous navigation, autonomous vehicles and robotics in agriculture.

Ibrahim A. Hameed

Foulum, February 2012

Contents

Chapter 1

General Introduction

1.1 Introduction

Currently, new technologies and equipments are being developed as a way to increase productivity, safety and reduce human workload in agricultural operations (Rovira-Mas et al., 2008). These technologies are ranging from navigation-aiding devices that assist the vehicle's driver in following field-work tracks to automated auto-steering systems and fully autonomous vehicles. Auto-steering systems are specifically designed to increase productivity thorough increased speed, the capability to use wider implements, the ability to perform multiple functions with increased precision and accuracy and reduce operator fatigue (O'Connor et al., 1996). However, the drawback of the commercially available auto-steering systems is that they rely on the experience of the driver in selecting the field area coverage strategy. These strategies may not be the optimum ones and following it a year after a year would lead to accumulated reductions of operations productivity. Moving to the fully autonomous agricultural vehicles, a more complex motion framework consisting of navigation sensors, navigation planner, vehicle motion models, and steering controllers are required (Cariou et al., 2009). The advent of autonomous system is expected to provide farmers with a complete new range of smart agricultural equipment that can do the right thing, in the right place, at the right time and in the right way requiring minimal or no human supervision (Blackmore et al., 2005). In both cases, involving automated and envisioned fully autonomous agricultural vehicles, explicitly formulated plans are needed. For example, explicitly formulated coverage plans make it possible to execute field operations in a manner that minimizes operational time, reduce skips or overlaps, reduce soil compaction, etc. Therefore, optimized coverage path planning can be considered as a core component of any autonomous or semi-autonomous system. Currently, there is no reliable and complete tools which can provide the optimized coverage path for multiple field shapes regardless of its complexity, the number of the in-field obstacles, and that are applicable to both 2D and 3D field terrain (Oksanen, 2007; Slaughter et al., 2008). In this Thesis, the aim is to develop robust, fast and reliable software tools that can provide optimized coverage path planning for agricultural vehicles so that field operations can be done in a manner that minimizes time, cost, and environmental implications.

1.2 Automatic guided vehicles (AGVs) in agriculture

Automated guided vehicles (AGVs) are vehicles that can perform desired tasks in unstructured environments without continued human guidance. Each type of AVs or robots has a certain degree of autonomy and therefore requires a proportional degree of human guidance. In agriculture, AVs are designed to reduce labour input and reduce intensive, repetitive, and dangerous work and increase farming efficiency and productivity. Research into the automation of agricultural vehicles is widely pursued. Some researchers have looked at GPS-based techniques for guidance (Erbach et al., 1991; O'Conner et al., 1996; Reid et al., 2000), others have pursued computer vision approaches (Billingsley et al., 1995; Gerrish, et al., 1997; Southall, et al., 1999; Tillett et al., 2002), and others have investigated a combination of vision with other techniques (Pilarski, et al., 1999; Zhang et al., 1999; Li et al., 2009). The main areas of scientific research currently being pursued in terms of application of AVs in agriculture include:

- Crop scouting and collecting of field data
- Mechanical weeding and micro spraying
- GPS guided planting, seedbed preparation, spraying, cultivation, etc.
- Harvesting

In essence, agricultural robotics uses on-farm sensing and control to actuate autonomous farm machinery with the aim of satisfying agronomy-based objectives (Eaton et al., 2008). On the other hand, there are standalone guidance systems which are developed to remove the need for a human driver to be physically on agricultural equipments and machines or at least to assist him/her to operate it more efficiently. These guidance systems are now deployed in most of the newly manufactured agricultural equipments and even can be mounted on old equipments. Global positioning system (GPS) is the most widely used position estimation sensor in these systems. Some GPS systems can guide massive agricultural machines as accurately as +/- 2.5cm or closer from an established row while moving at speeds of 19km/h or higher (Buick, 2006; Li et al., 2009). The rapid adoption of these GPS systems is being driven by various factors, including the tangible payback that customers receive from their GPS-based guidance systems, improved in-field productivity, reduced crop inputs such as fuel, fertilizer and chemicals, reduced operator fatigue, and the ability to operate machinery longer hours, simple installation, operation and lower cost of guidance technology (Heraud & Lange, 2009). With the advent of these technologies, GPS-based guidance systems provide the ability to work efficiently around the clock and eliminated the hazards in operations such as spraying pesticides by conducting it at night.

For autonomous equipments to work efficiently and robustly, it should be able to accurately drive along a calculated route obtained through the application of the optimized coverage path planning algorithms. In this regard, various position sensing types are used and therefore sensor fusion is widely used to combine information from various sensing sources since no individual sensing technology is ideally suited for vehicle automation under all modes of use (Bento et al., 2005). The appropriate sensor will depend on the field status at the time of operation. But even under a given field operation, the availability of data from multiple sensors provides opportunities to better integrate the data to provide a result superior to the use of the individual sensor. Autonomous equipment is usually equipped with a GPS receiver, heading gyroscope, Droppler radar, and four-wheel odometry for positioning, a pair of cameras and infrared (IR) sensors for obstacle detection and identification (Stentz, 2001). Due to the complexity of the obstacle detection problem, many types of sensor data are needed to discriminate obstacles from normal terrain conditions. Sufficient information about permanent obstacles can be obtained and identified using the field boundaries provided in the shape files used for generating the optimized coverage path throughout the entire field. The concept of coverage path planning will normally be controlled by GPS information only and therefore the reliability and accuracy of GPS information is the key to successful agricultural operations. Due to the open nature of the field terrain, GPS provides position estimates of sufficient accuracy enough for accurately executing coverage patterns. Since field boundaries are fixed over years, it is much more suitable to provide a software system that can provide the vehicle with the optimized coverage path planning over 2D and 3D field terrains. The optimized coverage path can be provided as a sequence of GPS waypoints representing field tracks and headland polygons. It can also be provided in the form of a standard shape or KML files.

1.3 Optimized coverage planning

Coverage path planning is the determination of a path that a mobile unit or robot has to follow in order to pass over each point in a given environment or region (Oksanen & Visala, 2009). Ultimately, a coverage path will minimize some cost function/s, such as time or travelled distance. Automated path planning has been studied for the optimization of field operations and should be coordinated with specific field operation requirements like machine characteristics, and topographic features of the field (Jin & Tang, 2010). Current applications of automatically guided field equipment enable the machine to follow straight or curved paths that provide complete field coverage, and little operational optimization has been taken into account, especially when irregular field boundaries are present. To improve field efficiency and, in particular, to fully utilize the advantages provided by automatically guided farming equipment, an optimal coverage path planner is considered a key requirement (Sørensen & Bochtis, 2010; Jin & Tang, 2011).

During the last decade, a number of methods for the representation of the field as a geometrical entity for field operations planning have been introduced. Fabre et al. (2001) presented a coverage path planning approach that minimizes the overlapping between successive tracks. In this approach, a driving direction was chosen as a direction to which successive filed work tracks are guided followed by the collection of a set of characteristic points in the headland and an associated heuristic greedy algorithm was used to find the covering trajectory. However, this work did not report the criteria of how the steering edge was chosen. Palmer et al. (2003) introduced a method to generate pre-defined field tracks to reduce the amount of overlapped and missed areas and thereby improve operational efficiency. The field and obstacle boundaries were obtained by driving a vehicle around the field perimeter while logging the visited coordinates using a positioning system and the preferred working direction was defined with the use of an initial operator-defined straight line. From this line, a grid of parallel lines was generated and the lines were spaced at one implement width from each other in order to cover the entire field. A drawback of this approach is that for complex situations, human intervention may be required to complete the generation of the course. Ta ïx et al. (2006) proposed a field coverage algorithm for convex polygonal fields with at most one vertex of concavity. The field is split into a work area and a turning area. The driving direction is given as input (i.e., not computed) and the work area is covered by parallel non-overlapping swaths. Non-convex fields and fields with large obstacles are subdivided along the boundary segments defined by the concave vertices, and are treated separately. Ryerson and Zhang (2007) used grid representation for the field and a genetic algorithm was used to find the optimal path (i.e., only one path) travelling through all the field grids covering the entire field area. Although this method can be used in grass mowing, it cannot be used for covering row crops. In addition, there is no guarantee that it can fully cover the while field area and it is suitable only for simple field shapes. Oksanen and Visala (2007) introduced an algorithmic field decomposition method based on trapezoidal split of a complex-shaped field plot into simple shaped subfields. Then, using a heuristic search approach, the optimum driving direction in each subfield was selected among a set of 6 possible driving directions (0, 30, 60, 90, 120 and 150). The cost function used was related to the weighted sum of area, distance and efficiency (i.e., turning time in headlands). The devised algorithm uses only straight driving direction and therefore it works efficiently only for fields with straight edges. Oksanen and Visala (2009) used two greedy algorithm approaches to find as efficient a 2D coverage route as possible. Their method adopted the trapezoidal decomposition method and searched for the best driving direction. The disadvantage of this approach is its long computational time and in addition it requires human intervention for completing the route in case of complex shaped fields. de Bruin et al. (2009) proposed an elementary method for optimizing the spatial configuration of field tracks within agricultural fields while creating space for field margins. The approach assumed straight tracks and the optimisation involved an exhaustive search over a discrete set of track orientations and positional shifts that are derived from measured field geometry. Also, Hofstee et al. (2009) developed a tool for determining the optimum path for field operations in single convex fields. Jin and Tang (2010) developed an optimization algorithm which decomposes the field into regions and finding the optimal driving direction in each region. The developed algorithms did not provide the optimal positions for entering and exiting the field, nor does it provide the best solution for travelling between different sub-regions. Jin and Tang (2011) developed 3D terrain coverage path planning algorithm for reducing headland turning cost and soil erosion. A common characteristic of the abovementioned methods is that an optimal solution cannot be guaranteed. It can be summarised that although coverage path planning is a very straight forward problem, most of the described approaches are not implemented and therefore the need arises for developing more formalised approaches based on a strong mathematical foundation suitable for implementation.

Recently, the idea of minimizing the non-working time or distance by optimizing the sequence of the field-work tracks, instead of following standard motifs has been introduced and a new type of algorithmically-computed optimal fieldwork patterns (*B-patterns*) have been presented (Bochtis 2008). The method is based on an approach according to which the field coverage is expressed as the traversal of a weighted graph, and the problem of finding optimal track traversal sequences is equivalent to finding the shortest tours in the graph. The weight of the graph arcs could be based on any relative optimisation criterion, such as total or non-working travelling distance, total or non-productive operational time, a dedicated soil compaction measure, etc. The first experimental implementation of optimal path planning on a field robot showed that by using *B-patterns* instead of traditional fieldwork patterns, the total non-working distance can be reduced by up to 50% (Bochtis et al., 2009). Nevertheless, a complete tool that generates the geometrical representation of the field and the subsequent optimal coverage plan has not been developed yet. Also, a tool or software for coverage path planning is required to be available as an open source code for end-users and for developers as well.

1.4 Aims and objectives

The general objective of this study was to develop robust, reliable, simple, fast and complete methodologies and models for optimized coverage path planning involving both 2D and 3D field terrains. These algorithms will be able to take into account all field shapes regardless of its complexity and without human intervention. Under the direction of such optimized coverage path planning measures, field operations will be executed in a manner that reduces operational time, driving distances, and consequently, fuel consumption. The perspective is to provide the data outputs from these algorithms to the automatic guidance systems, robots, auto-steering systems, or even to farmers using a suitable format. For consultation and visualization, it will be possible to integrate these data outputs into web-based services such as Google maps. Also, these algorithms and models will be combined with simulators of machinery systems and integrated into model based decision support systems (DSS) that gives a farmer the opportunity to improve his/her understanding of the entire field operation and to test various operational scenarios before going to the field, for example, to select the most appropriate functional characteristics of his/her new machinery system.

The expected beneficiaries of this project will include manufacturers and developers of agricultural equipments, farmers who are interested in reducing operations cost and human workload and maximizing the use resources in arable farming, and researchers who are interested in further exploring and researching the potential of resource optimisation, reduction of environmental impact, etc. in the realm of agricultural operations.

1.5 Outline of the thesis

The outline of the Thesis is schematically represented in Fig. 1. After the introduction (Chapter 1), each research point will be presented in a separate Chapter. In general, the Thesis is presented in three main Parts: geometrical field representation of the operational environment is presented in Part I, the development of the optimization of coverage path planning is presented in Part II and the integration of the planning models into decision support systems (DSS) is presented in Part III. In Part I, a set of geometrical representation algorithms for 2D field terrains are presented (Chapter 2). These algorithms are capable of generating both straight and curved tracks and parallel to the longest edge/side of the field or parallel to a user defined driving angle. Besides, it can divide a field into sub-regions and subsequently generate the optimal path planning in each sub-region.

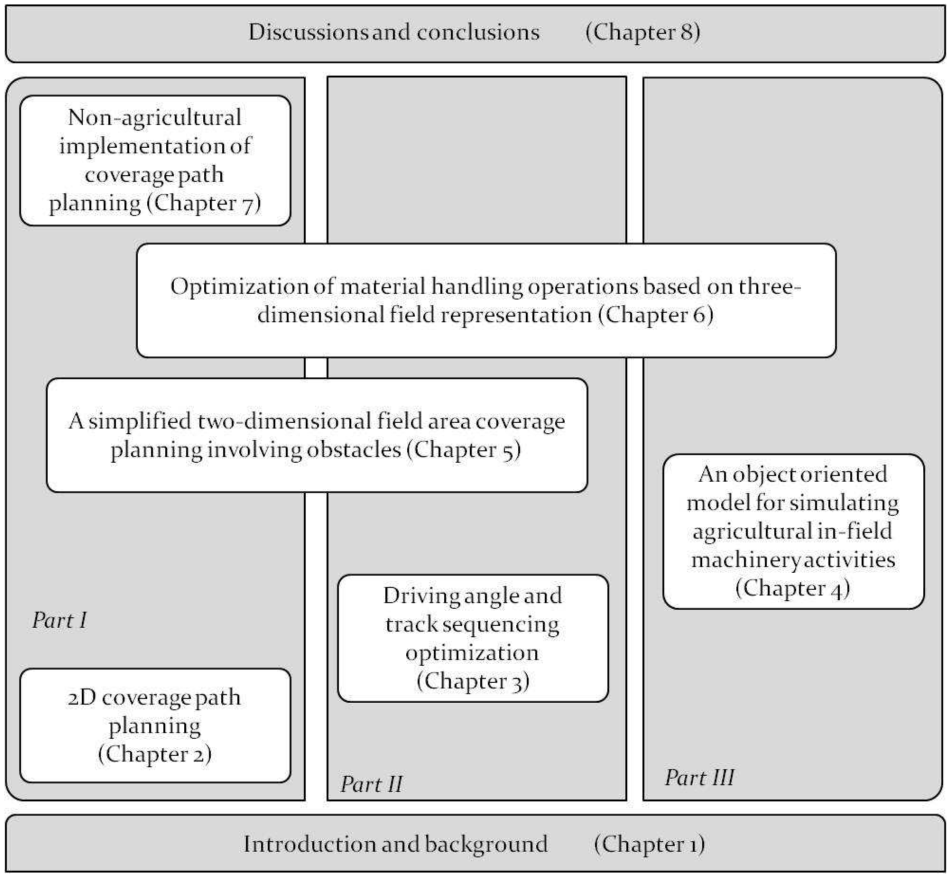

Fig. 1 – Schematic representation of the outline of the Thesis.

For field operation to be done in a manner that minimizes driving time and distance over field surface, driving angle and track sequencing optimization is presented (Chapter 3, Part II). As a result of the reduced driving over field surfaces, soil compaction and fuel consumption can be reduced. Coverage path planning and optimization are combined with a simulation model of a machinery system in order to build a decision support system (DSS) is presented (Chapter 4,Part III). The developed simulation system can help a farmer/farm manger to better understand the entire field operation and to test various operational scenarios and to test and select mechanical specifications which satisfy his/her needs optimally before going to the field. A simplified geometrical representation (SGR) algorithm was developed in an attempt to improve the performance of the optimization algorithms used to optimize path planning. The developed SGR approach requires low computing power of on-board computers and hence timely output can be obtained. In the same context, a complete field coverage approach is developed to enable field obstacles avoidance. In this approach, field tracks are clustered into blocks where each block consists of a number of tracks. The sequence of blocks is optimized in a manner that minimizes the connection distance between blocks and avoids collision with permanent obstacles defined the field shape file as well (Chapter 5, Parts I & II). Coverage path planning on 3D terrain is introduced in connection with the direct energy consumption optimization (Chapter 6, Parts I, II & III). In this approach, 3D field representation is developed and driving angle is optimized in a manner which minimizes the total power consumed in driving over the field area. Specific models which consider elevation of field terrain in estimating power consumptions are used. A specific non-agricultural application of coverage path planning for cutting the grass, grass stripping, etc. is presented in Chapter 7, Part I). Discussion and conclusions are then presented (Chapter 8).

References

Bento, C. L., Nunes, U., Moita, F. & Surrecio, A.-O. (2005). Sensor fusion for precise autonomous vehicle navigation in outdoor semi-structured environments. In: *Proceedings of the 8th International IEEE Conference on Intelligent Transportation Systems*, Austria, 245-250.

Billingsley, J., Schoenfisch, M. (1995). Vision Guidance of Agricultural Vehicles. *Autonomous Robots*, (2).

Blackmore, B. S. (2009). New concepts in agricultural automation. In: *Proceedings of HGCA conference*, Precision in arable farming - current practice and future potential,

Blackmore, B. S., Stout, W., Wang, M., & Runov, B. (2005). Robotic agriculture – the future of agricultural mechanisation?. In: *Proceedings of the 5th European Conference on Precision Agriculture*, ed. J. Stafford, V. The Netherlands, Wageningen Academic Publishers, 621-628.

Bochtis, D. 2008. Planning and control of a fleet of agricultural machines for optimal management of field operations. Ph.D. Thesis. AUTh, Department of Agricultural Engineering, Greece.

Bochtis, D. D., Vougioukas, S. G., and H. W. Griepentrog. 2009. A mission planner for an autonomous tractor. T ASABE. 52(5): 1429-1440.

Buick, R. (2006). GPS guidance and automated steering renew interest in precision farming techniques. Trimble Navigation Limited, 1-10 (retrieved in December 2011 from http://www.gpsags.com/media/Precision-Farming-Whitepaper.pdf).

Cariou, C., Lenain, R., Thuilot, B. & Berducat, M. (2009). Automatic guidance of a four-wheel-steering mobile robot for accurate field operations. *Journal of Field Robotics*, 26(6–7), 504–518.

Choset, H. & Pignon, P. (1997). Coverage path planning: The boustrophedon cellular decomposition. In: *Proceedings of the International Conference on Field and Service Robotics*, Canberra, Australia.

de Bruin, S., Lerink, P., Klompe, A., van der Wal, T., & Heijting, S. (2009). Spatial optimisation of cropped swaths and field margins using GIS. *Computers and Electronics in Agriculture*, 68, 185-190.

Eaton, R., Katupitiya, J., Siew, K. W. & Howarth, B. (2008). Autonomous Farming: Modeling and Control of Agricultural Machinery in a Unified Framework. In: Proceedings of the 15th International Conference on Mechatronics and Machine Vision in Practice, 499 – 504.

Erbach, D.C., Choi, C.H., Noh, K. (1991). Automated Guidance for Agricultural Tractors. *Automated Agriculture for the 21st Center*, ASAE, 1991.

Fabre, S., Soures, P., Taix, M., & Cordesses, L. (2001). Farmwork path planning for field coverage with minimum overlapping. In: *Proceedings of the IEEE Conference on Emerging Technologies and Factory Automation*, France, 2, 691-694.

Gerrish, J. B., Fehr, B. W., Van Ee, G. R., Welch, D. P. (1997). Self-Steering Tractor Guided by Computer Vision. *Applied Engineering in Agriculture*, 13(5).

Heraud, J. A. & Lange, A. F. (2009). Agricultural Automatic Vehicle Guidance from Horses to GPS: How We Got Here, and Where We Are Going. In: Proceedings of thew Agricultural Equipment Technology, ASABE Distinguished Lecture #33, USA, pp. 1-67.

Hofstee, J. W., Spa¨ tjens, L. E. E. M., & Ijken, H. (2009). Optimal path planning for field operations. In: *E. J. Van Henten, D. Goense, & C. Lokhorst (Eds.), Proc. Joint International Agricultural Conference*, JIAC 2009, Precision Agriculture 09 (pp. 521e529), Netherlands: Wageningen.

Jin, J. & Tang, L. (2010). Optimal coverage path planning for arable farming on 2D surfaces. *Transactions of the ASABE*, 53(1), 283–295.

Jin, J. & Tang, L. (2011). Coverage path planning on three-dimensional terrain for arable farming. *Journal of Field Robotics*, 28(3), 424–440.

Julian, A. P. (1971). Design and performance of a steering control system for agricultural tractors. *Journal of Agricultural Engineering Research*, 16(3), 324-336.

Larsen, W. E., Nielsen, G. A., & Tyler, D. A. (1994). Precision navigation with GPS. *Computers and Electronics in Agriculture*, 11(1), 85-95.

Li, M., Imou, K., Wakabayashi, K. & Yokoyama, S. (2009). Review of research on agricultural vehicle autonomous guidance. International Journal of Agricultural and Biological Engineering, 2(3), 1—16.

Martinet, P., Bonton, P., Gallice, J., Berducat, M., Debain, C., Rouveure, R., (1998). Automatic guided vehicles in agricultural and green space fields. In: *Proceedings of 4th French-Israeli Symposium on Robotics*, France, pp. 87–92.

Nebot E. (1999). *Sensors used for autonomous navigation*. Advances in Intelligent Autonomous Systems, Kluwer Academic Publishers, Dordrecht, Chapter 7, 135-156.

O'Connor, M., Bell T., Elkaim G., & Parkinson B. (1996). Automatic steering of farm vehicles using GPS. In: *Proceedings of the 3rd international conference on precision agriculture*, Minneapolis, MN, June 23–26.

O'Connor, M., Bell, T., Elkaim, G. & Parkinson, B. (1996). Automatic steering of farm vehicles using GPS. In: *Proceedings of the 3rd International Conference on Precision Agriculture*, 3, 767-777.

Oksanen, T. & Visala, A. (2009). Coverage path planning algorithms for agricultural field machines. *Journal of Field Robotics*, 26(8), 651–668.

Oksanen, T. (2007). *Path planning algorithms for agricultural field machines*. PhD dissertation, Department of Automation and Systems Technology, Helsinki university of technology, Finland.

Oksanen, T., & Visala, A. (2007). Path planning algorithms for agricultural machines. *Agricultural Engineering International: the CIGR Ejournal*, vol. IX. Manuscript ATOE 07 009.

Palmer, R. J., Wild, D., & Runtz, K. (2003). Improving the efficiency of field operations. *Biosystems Engineering*, 84(3), 283-288.

Pilarski, T., Happold, M., Pangels, H., Ollis, M., Fitzpatrick, K., & Stentz, A. (1999). The DEMETER System for Autonomous Harvesting. In: *Proceedings of the 8th International Topical Meeting on Robotics and Remote Systems*.

Reid, J. F., Zhang, Q., Noguchi, N., & Dickson, M. (2000). Agricultural automatic guidance research in North America. *Computers and Electronics in Agriculture*, 25(1-2), 155-167.

Rovira-Mas, F., Shufeng H., & Reid, J. F. (2008). Evaluation of automatically steered agricultural vehicles. In: Proceedings of the IEEE/ION position, location and navigation symposium, 2008 IEEE/ION, Monterey, CA, 473 – 478.

Ryerson, A. E. F. & Zhang, Q. (2007). Vehicle path planning for complete field coverage using genetic algorithms. *Agricultural Engineering International: CIGR Ejournal*, 4, manuscript ATOE 07 014.

Slaughter, D. C., Giles, D. K., & Downey, D. (2008). Autonomous robotic weed control systems: A review. *Computers and Electronics in Agriculture*, 61(1), 63–78.

Sørensen, C.G. & Bochtis, D. D. (2010). Conceptual model of fleet management in agriculture. Biosystems Engineering, 105(1), 41-50.

Southall, B., Hague, T., Marchant, J. A., & Buxton, B. F. (1999). Vision-aided Outdoor Navigation of an Autonomous Horticultural Vehicle. In: *Proceedings of the 1st International Conference on Vision Systems* (ICVS).

Stentz, A. (2001). Robotic Technologies for Outdoor Industrial Vehicles. In Proceedings of SPIE AeroSense.

Stentz, A. (2001). Robotic technologies for outdoor industrial vehicles. In: *Proceedings of SPIE AeroSense.*

Taïx, M., Soueres, P., Frayssinet, H., & Cordesses, L. (2006). Path planning for complete coverage with agricultural machines. In: *S. Yuta, et al. (Eds.), Field and service robotics*, STAR, Vol. 24 (pp. 549-558).

Tillett, N. D., Hague, T., & Miles, S. J. (2002). Inter-row vision guidance for mechanical weed control in sugar beet. *Computers and Electronics in Agriculture*, 33(3), 163–177.

Zhang, Q., Reid, J. F., & Noguchi, N. (1999). Agricultural Vehicle Navigation Using Multiple Guidance Sensors. In: *Proceedings of the International Conference on Field and Service Robotics*.

Chapter 2

Automated Generation of Guidance Lines for Operational Field Planning

Hameed, I. A., Bochtis, D. D., Sørensen, C. G., & Nørremark, M.

Journal of Biosystems Engineering, 2010, 107(4), 294-306.

BIOSYSTEMS ENGINEERING 107 (2010) 294–306

Available at www.sciencedirect.com

ScienceDirect

journal homepage: www.elsevier.com/locate/issn/15375110

Research Paper

Automated generation of guidance lines for operational field planning

I.A. Hameed, D.D. Bochtis, C.G. Sørensen, M. Nøremark*

University of Aarhus, Faculty of Agricultural Sciences, Dept. of Biosystems Engineering Blichers Allé 20, P.O box 50, 8830 Tjele, Denmark

ARTICLE INFO

Article history:
Received 7 January 2010
Received in revised form
7 May 2010
Accepted 15 September 2010

A number of advanced satellite positioning based systems for agricultural machines have been developed and are commercial available for aiding and supporting navigation efforts up to full auto-steering. Furthermore, in terms of the route planning for agricultural field operations, advanced methods based on combinatorial optimisation of fieldwork patterns have recently been introduced. In order to apply and implement these methods in the high-level control system of agricultural machines, an appropriate representation of the field as a geometrical entity made up of discrete geometric primitives, such as points, lines, and polygons is needed. Preferably, such a representation must be generated in real-time providing the input to the whole accuracy range of navigation systems as well as the range of operation types, equipment characteristics, and machinery kinematics.

Here, a method for real-time generation of field geometrical representation for operational planning is presented. The representation regards simple or complex fields for both convex and non-convex field boundaries, where generated tracks can be straight or curved. As demonstration cases for the method, 15 different field types were evaluated. According to the experimental results, the computational time of the method was in the range of 0.11–239.73 s for the case of single-block fields and in the range of 2.24–402.59 s for multiple-blocks fields. The tested fields were of different shapes and the area ranged from 0.21 ha to 44.93 ha.

1. Introduction

The maximisation of agricultural machine productivity is an important element in the continued efforts of planning and controlling resource inputs in both arable and high value crops farming (e.g., Sørensen & Nielsen, 2005). A preliminary step in the direction of achieving increasing operational efficiency is a renewed focus on the usage of advanced systems both in terms of technology and management measures. A number of satellite positioning based systems for agricultural machines have been developed ranging from aiding and supporting navigation efforts to full auto-steering systems (Earl, Thomas, & Blackmore, 2000; Keicher & Seufert, 2000; Klee, Hofmann, & Pickle, 2003; Nørremark, Griepentrog, Nielsen, & Søgaard, 2008). Although the primary objective of these systems is to help operators to relieve stress and relax during driving and focus only on important tasks such as the machine implement, optimised route and path planning is one of the most important requirements voiced by farm managers and machine contractor managers as a way to develop an advanced integrated fleet management system (Sørensen & Bochtis, 2010).

On the other hand, in recent years the development of autonomous vehicles in agriculture has experienced increased interest. There are a number of prototypes that have been developed for field crops, such as the Demeter system for

* *Corresponding author.*
E-mail address: Dionysis.Bochtis@agrsci.dk (D.D. Bochtis).
1537-5110/$ – see front matter © 2010 IAgrE. Published by Elsevier Ltd. All rights reserved.
doi:10.1016/j.biosystemseng.2010.09.001

Nomenclature

${}_kB_j$	the set of the (indices) of the points constitute the jth boundary, $j \in \{0,1\ldots,h+1\}$ of the kth field block, $k \in \{1,\ldots,b\}$. In the case of $k \equiv \varnothing$ the symbol refers to a single-block field
${}_k\mathbf{B}_j^i$	a point of the boundary ${}_kB_j$ where $i \in \lvert {}_kB_j \rvert$ and $k \in \{1,\ldots,b\}$. In the case of $k \equiv \varnothing$ the symbol refers to a single-block field
b	the number of the field blocks
$({}_kb_x^i, {}_kb_y^i)$	the coordinates of the point ${}_k\mathbf{B}_j^i$ in a 2-dimensional coordinate system. In the case of $k \equiv \varnothing$ the symbol refers to a single-block field
$H_{\mathbf{pp}'}$	the half-plane that is defined as the subset $H_{\mathbf{pp}'} = \{(x,y) \in \mathbb{R}^2 \mid \varphi_{\mathbf{pp}'}(x,y) \le 0\}$ where $\mathbf{P}$ and $\mathbf{P}'$ are two points
${}_i\mathcal{H}_B$	the family of sets of the internal boundaries that are created by the headland passes in block i ${}_i\mathcal{H}_B = \cup_{j=1}^{h} {}_iB_j, i \in \{1,\ldots,b\}$. In the case of $i \equiv \varnothing$ the symbol refers to a single-block field
${}_i\mathcal{H}_O$	the family of sets of the external boundaries that are created of the passes around the obstacle area $i \in \{1,\ldots,o\}$
F	the field area
h	number of headland passes for the headland creation
L	the length of the diagonal of the MBB of the field polygon
l_i	the length of the track $i \in T$, $l_i = \sum_{j=2}^{n_i} \lVert \mathbf{\Gamma}_j^i - \mathbf{\Gamma}_{j-1}^i \rVert$
n_i	the number of points that describe a track, $i \in T$
S	the set of the points of a curved edge; a curved edge is defined as the collection of sequential straight edges satisfying the criterion that the angle between two successive edges is less than or equal to a threshold value, ϑ
$\mathfrak{S}$	the family of sets, S_i, representing the field boundary curved edges
${}_iT$	the family of the sets of the field of field blocks $i \in \{1,\ldots,b\}$. In the case of $i \equiv \varnothing$ the symbol refers to a single-block field
$\mathcal{T}$	the family of the sets of the tracks of all field blocks, $\mathcal{T} = \cup_{i=1}^{b} {}_iT$
w	the effective operating width
$\mathbf{\Gamma}_j^i$	a point of the track $i \in T, j \in \{1,n_i\}$
$(\gamma_{jx}^i, \gamma_{jy}^i)$	the x- and y-coordinate of a point $\mathbf{\Gamma}_j^i$, $i \in T, j \in \{1,n_i\}$
Δ	the operator which given two lines returns their intersection point, $\Delta : \mathbb{R}^3 \times \mathbb{R}^3 \mapsto \mathbb{R}^2 \cup \varnothing$
$\varepsilon_{\mathbf{pp}'}$	the straight line that passes through points $\mathbf{P}$ and $\mathbf{P}'$
Θ	the operator that returns the angle between two (oriented) line segments, $\Theta : \mathbb{R}^3 \times \mathbb{R}^3 \mapsto [0, 360)$
ϑ	the threshold angle; a curved edge is considered as the collection of sequential straight edges satisfying the criterion that the angle between two successive edges is less than or equal to ϑ
κ	the threshold distance used in filtering headland area generation
Π	the operator which, given a line, returns a parallel line at a given distance from the side corresponding either to the interior of the area defined by the boundary the line belongs to, using as argument: -1, or to the exterior, using as argument: $+1$, $\Pi : \mathbb{R}^3 \times \mathbb{R} \times \{-1,+1\} \mapsto \mathbb{R}^3$
$\lVert\rVert$	the operator that returns the Euclidean distance between any two points $\lVert\rVert : \mathbb{R}^2 \times \mathbb{R}^2 \mapsto \mathbb{R}$

automated harvesting equipped with a video camera and GPS for navigation (Pilarski et al., 2002), the autonomous Christmas tree weeder (Have, Nielsen, Blackmore, & Theilby, 2005) and the API platform for patch spraying (Bak & Jakobsen, 2004).

Regarding the route planning for agricultural field operations, advanced methods based on combinatorial optimisation have recently been introduced. Bochtis (2008) introduced a new type of algorithmically-computed optimal fieldwork patterns (*B-patterns*) based on an approach according to which the field coverage is expressed as the traversal of a weighted graph, and the problem of finding optimal traversal sequences is shown to be equivalent to finding the shortest tours in the graph. The implementation of *B-patterns* in conventional agricultural machines, supported by auto-steering systems, was presented by Bochtis and Vougioukas (2008). The experimental results showed that, by using a specific set of algorithmically-computed optimal sequences based on the proposed approach, the total non-working distance can be reduced significantly, by up to 50%. The same approach has been implemented for the mission planning of an autonomous tractor for area coverage operations such as grass mowing, seeding and spraying (Bochtis, Vougioukas, & Griepentrog, 2009). A generalisation of the above approach covering the majority of field operation types is presented in Bochtis and Sørensen (2009). In that article, a dedicated classification of agricultural field operations was devised in terms of the machinery system (single or multiple-machinery system), the operation characteristic (deterministic, stochastic, and dynamic) and the facility units' characteristics (single or multiple, mobile or stationary), and tailored to a conceptual application of the well-known vehicle routing problem (VRP) (Toth & Vigo, 2002). The concept regarded the operations of primary agricultural machines, with the traversed tracks in the field abstractively representing the "customers" in the VRP methodology. Regarding route planning for service units in agricultural field operations (e.g., transport wagons in a harvesting operation), Bochtis and Sørensen (2010) showed that it can be cast as instances of VRP with time windows by using the abstractive representation of the supported primary machines as the "customers" in the methodology of this specific constrained type VRP. Alia, Verlindena, and Oudheusdena (2009) proposed a combination of VRP and minimum cost network flow problems in order to determine the optimal covering routes for combine harvesters as well as feasible positions for grain transfer between the combine harvesters and tractors.

In order to automate the implementation of the above mentioned methods in the auto-steering or navigation-aiding systems mounted in agricultural machines or in the high-level control system of field robots, an appropriate representation of the field as a geometrical entity is required (Bochtis & Oksanen, 2009). A geometrical representation is made up of discrete geometric primitives, such as points, lines, polygons, splines, and polynomial functions. This type of map is highly space-efficient because an arbitrarily large region of space can be represented by a model with only a few numerical parameters, and it is possible to store occupancy data with almost arbitrarily high resolution (Dudek & Jenkin, 2000). A geometrical representation provides a concise representation of environmental data that can be readily used for higher-level processing.

During the last decade, a number of methods for the representation of the field as an environment for field operations planning have been introduced. Palmer, Wild, and Runtz (2003) introduced a method to generate pre-defined field tracks to reduce the amount of overlapped and missed areas and thereby improve operational efficiency. The field and obstacle boundaries are obtained by driving a vehicle around the field perimeter while logging the visited coordinates using a positioning system. The preferred working direction is defined with the use of an initial operator-defined straight line. From this line, a grid of parallel lines is generated. The lines are spaced at one implement width from each other in order to cover the entire field. A drawback of this approach is that for complex situations, human intervention may be required to complete the generation of the course. Oksanen and Visala (2007) introduced an algorithmic field decomposition method based on trapezoidal split of a complex-shaped field plot into simple shaped subfields. Then, using a heuristic search approach, the optimum driving direction in each subfield was selected among a set of 6 possible driving directions (0, 30, 60, 90, 120 and 150°). The cost function used was related to the weighted sum of area, distance and efficiency (i.e., turning time in headlands). This algorithm uses only straight driving direction and therefore it works well only for fields with straight edges. Taix, Soueres, Frayssinet, and Cordesses (2006) proposed a field coverage algorithm for convex fields based on the treatment of convex cells. de Bruin, Lerink, Klompe, van der Wal, & Heijting, 2009 proposed an elementary method for optimising the spatial configuration of field tracks within agricultural fields while creating space for field margins. The approach assumed straight tracks and the optimisation involved an exhaustive search over a discrete set of track orientations and positional shifts that are derived from measured field geometry. Also, Hofstee, Spätjens, and Ijken (2009) developed a tool for determining the optimum path for field operations in single convex fields.

A common characteristic of the above mentioned methods is that an optimal solution cannot be guaranteed. This is expected due to the characteristics of agricultural field operations, where a number of constraints must be complied with, including soil compaction, operating while following contour lines, the fact that a typical agricultural machine usually cannot operate while manoeuvring, the fieldwork pattern followed in previous treatments or by other machinery types, etc. The presence of these agronomic constraints also explains the fact that, though the area coverage and area decomposition are well-known problems in the robotics discipline and a large number of successful methods have been provided (see e.g., Choset (2001) for a literature review), the pursued approaches cannot be directly adopted in the case of agricultural operations.

Here, a method for real-time generation of field geometrical representation for operational planning is presented. The geometrical representation regards simple or complex fields for both convex and non-convex field boundaries, and where the tracks generated can be straight or curved. It is worth noting that the idea of the geometrical representation of a field area for a point-to-point path plan generation or area coverage planning for agricultural vehicles is not new in itself. Various methods and system descriptions have been presented in a number of patents, covering aspects such as headlands creation (Sachs, Roszhart, Schleicher, Beck, & Bezdek, 2009), a contour path planning (Flann, Hansen, & Gray, 2007), generation of headland turns (Birnie, 2009; Senneff, Leiran, & Roszhart, 2009), and selecting optimal driving direction in terms of minimised energy consumption (Anderson 2004). Nevertheless, in the patents the proposed methods and systems are presented without giving the actual approaches for solving the problem at hand, either because it is not the general purpose of a patent or because the appropriate approaches have not been developed yet. However, here the attempt is to provide a formalised mathematical description of a field geometrical representation and to present the proposed approach in sufficient mathematical detail as a basis for a reproducible and extensible "open source" for further implementation and/or improvement.

2. Preliminaries

A geometrical representation is characterised by two properties (Dudek & Jenkin, 2000):

- The set of basic primitives used for describing objects
- The set of composition and deformation operators used to manipulate objects or primitives

Here, the set of the geometric primitives is composed by points, line segments and polygons. The operators used are given in a following section.

The field in question is considered as a 2-dimensional closed area which may contain a number of obstacles considered also as 2-dimensional closed areas. A field is completely defined by an ordered set of points where their sequential pair-wise connections constitute the field boundary (polygon). Let B_0 denote the set of the (indices) of the boundary points, each referent as $\mathbf{B}_0^i, i\in|B_0|$, and (b_x^i, b_y^i) denotes the coordinates of point $\mathbf{B}_0^i$ in relation to a 2-dimensional coordinate system, which can be either relative/local or absolute/global, e.g., the Universal Transverse Mercator (UTM) system.

2.1. Line representation

Let $\varepsilon_{\mathbf{PP}'}$ denote the straight line passing through points $\mathbf{P}$ and $\mathbf{P}'$. A general equation of a straight line can be determined to be of the form $a_{\mathrm{PP}'}x + b_{\mathrm{PP}'}y + c_{\mathrm{PP}'} = 0$, in which $a_{\mathrm{PP}'}, b_{\mathrm{PP}'}, c_{\mathrm{PP}'} \in \mathbb{R}$ are constants determined from the coordinates p_x, p_y, p'_x and p'_y. By doing so, a straight line $\varepsilon_{\mathbf{PP}'}$ can be represented as an $\mathbb{R}^3$ entity $(a_{\mathrm{PP}'}, b_{\mathrm{PP}'}, c_{\mathrm{PP}'})$.

2.2. Field area representation

Let $\varphi_{PP'}: \mathbb{R}^2 \times \mathbb{R}^2 \to \mathbb{R}$ be the function given by: $\varphi_{PP'}(x, y) = a_{PP'}x + b_{PP'}y + c_{PP'}$ and H represent a half-plane defined as the subset: $H_{PP'} = \{(x, y) \in \mathbb{R}^2 | \varphi_{PP'}(x, y) \leq 0\}$.

The field area can then be defined as:

1) For the case of a convex $|B_0|$-sided polygonal region: $F = H_{B_0^1 B_0^2} \cap H_{B_0^2 B_0^3} \cap \ldots \cap H_{B_0^{|B|-1} B_0^{|B|}} \cap H_{B_0^{|B|} B_0^1}$
2) For the case of non-convex region, the field area can be expressed as: $F = F_1 \cup F_2 \cup \ldots \cup F_n$, in which each of F_n is a convex polygonal set that is expressed in terms of half-plane as previously.

2.3. Track representation

The fieldwork pattern that the presented geometrical representation refers to is the "headland pattern". The term "headland pattern" refers to the complete covering, in a geometrical sense, of the main field area (or of a block of a field), that is the field area (or block area) excluding the headland area by a set of parallel tracks. Let T denote the set of the field tracks.

A track is determined geometrically by a number, n_i, of points and is described by the vector $\langle(\gamma_{1x}^i, \gamma_{1y}^i), (\gamma_{2x}^i, \gamma_{2y}^i), \ldots, (\gamma_{n_i x}^i, \gamma_{n_i y}^i)\rangle$, $i \in T$, where γ_{jx}^i and, γ_{jy}, $j \in \{1, n_i\}$ are the x- and y-coordinates of point $\boldsymbol{\Gamma}_j^i$. In the simplest case, when tracks are straight lines, two points describe each track, corresponding to its two endings. The length of a track is approximated by $l_i = \sum_{j=2}^{n_i} \|\boldsymbol{\Gamma}_j^i - \boldsymbol{\Gamma}_{j-1}^i\|$, where $\|\mathbf{P} - \mathbf{P'}\|$ denotes the Euclidean distance between any two points $\mathbf{P}$ and $\mathbf{P}'$ in $\mathbb{R}^2$.

2.4. Headland representation

In a field operation, headlands are created by the sequential passes that the agricultural machine has to perform peripheral to the main field area before or after (depending on the operation) the operation in the main field area. Thus, the headland width results from the multiplication of the effective operating width of the machine by the number of the peripheral passes. Let h denote the number of the passes. As a geometrical entity, a headland is defined as the set of sets of the internal boundaries that are created by the headland passes: $\mathcal{H}_B = \cup_{i=1}^{h} B_i$.

2.5. Obstacles

An obstacle area in the field area is described analogously to the field area by an ordered set of points where their sequential pair-wise connections constitute its boundary, i.e., $O_0 = \{1,2,3,\ldots\}$.

The headland area of an obstacle is defined as the set of sets of the external boundaries that are created of the passes around the obstacle area: $\mathcal{H}_O = \cup_{i=1}^{h_O} O_i$.

2.6. Operators

As was previously mentioned, one of the properties characterising a geometrical representation is the set of composition and deformation operators used to manipulate the geometric primitives. We define the following operators:

- $\Pi: \mathbb{R}^3 \times \mathbb{R} \times \{-1, +1\} \mapsto \mathbb{R}^3$ which, given a line, returns a parallel line at a given distance from the side corresponding either to the interior of the area defined by the boundary the line belongs to, using as argument: -1, or to the exterior, using as argument: $+1$.
- $\Delta: \mathbb{R}^3 \times \mathbb{R}^3 \mapsto \mathbb{R}^2 \cup \varnothing$ which, given two lines, returns their intersection point.

2.7. Minimum bounding box

For a 2-dimentional polygon, the minimum bounding box (MBB), in computational geometry, is defined as the minimum-area rectangle enclosing the set of points that a polygon consists of (O'Rourke, 1985). Consequently, the MBB of the polygon representing a field (namely the boundary B_0) is the rectangular area defined by the points:

$$\left\langle \left(\min\left[b_{0x}^i\right], \min\left[b_{0y}^i\right]\right), \left(\max\left[b_{0x}^i\right], \min\left[b_{0y}^i\right]\right), \right.$$
$$\left. \times \left(\max\left[b_{0x}^i\right], \max\left[b_{0y}^i\right]\right), \left(\min\left[b_{0x}^i\right], \max\left[b_{0y}^i\right]\right) \right\rangle$$

As will be clear later, the generated tracks are produced in a way that they must cover the MBB of the field ensuring that there will not be any skipped areas within the field area in the case of very complex fields.

2.8. Generalisation of sets

For simplicity, the above mentioned terms and corresponding symbols were referenced to the case of single-block fields and single-obstacle area presence. In the case where a field consists of more than one block and in the presence of more than one obstacle area, symbols are modified as follows.

The set of tracks is a union of sets, $\mathcal{T} = \cup_{i=1}^{b} {}_iT$, where ${}_iT$ is the set of the tracks of block i and b denotes the number of the blocks that the field area consists of.[1]

Analogously, the boundary of each block is denoted by ${}_iB, i \in \{1, \ldots, b\}$ and the headlands are denoted by ${}_i\mathcal{H}_B = \cup_{j=1}^{h} {}_iB_j, i \in \{1, \ldots, b\}$. Similarly, for the obstacles the symbols ${}_iO_o$ and ${}_i\mathcal{H}_O, i \in \{1, \ldots, o\}$, are used, where o denotes the number of obstacle areas within the field area. It has to be noted that the number h remains the same for all blocks or obstacles since it is determined by the geometrical (i.e., size) and kinematical (i.e., turning radius) features of the machine carried out the operation.

3. The algorithmic approach

3.1. Headland area generation

The distance between the first headland pass and the field boundaries is half of the implement width, $w/2$, and between subsequent headland passes is an implement width, w, where w denotes the (effective) operating width of the machine which carries out the operation. As previously mentioned, a headland consists of a sequence of internal (or external in

[1] Note that $\cap_{i=1}^{b} {}_iT = \varnothing$. The indices follow the rule: ${}_iT = \{|{}_{i-1}T| + 1, \ldots, |{}_{i+1}T| - 1\}$, $i \neq 1, b$, ${}_1T = \{1, \ldots, |{}_2T| - 1\}$, ${}_bT = \{|{}_{b-1}T| + 1, \ldots, |{}_bT|\}$.

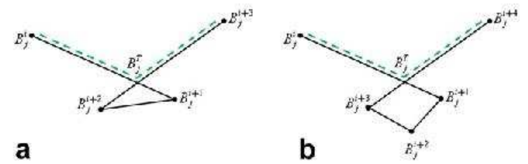

Fig. 1 – Dissolving of segments after the operation of filter 2 in chosen (example) groups of (a) $m = 3$, and (b) $m = 4$, segments.

the case of an obstacle area) boundaries corresponding to headland passes. A headland pass is then obtained by getting the intersection points between segments of lines parallel to the segments of lines of the previous headland pass at distance d from the interior of the field area (using the Δ operator with argument -1) or the area exterior in the case of an obstacle (using the Δ operator with argument $+1$). The distance d for the first headland boundary is set to $w/2$, while for the rest of the boundaries it is set to w. Consequently, the generation of the internal field boundaries that compose the headland is described by the set of the following points:

$$\mathbf{B}_j^i = \Delta[\Pi(\varepsilon_{\mathbf{B}_{j-1}^i \mathbf{B}_{j-1}^{i+1}}, d, -1), \Pi(\varepsilon_{\mathbf{B}_{j-1}^{i+1} \mathbf{B}_{j-1}^{i+2}}, d, -1)],$$

$$d = \begin{cases} w/2 & \text{if } j = 1 \\ w & \textbf{otherwise} \end{cases}, \quad 1 \le j \le h, \quad i \in |B_0|,$$

An additional (virtual) headland pass is generated at distance $w/2$ from the last headland pass to be used as the internal boundary of the main field area. As part of the headland area generation, two filtering operations take place in order to avoid irregularities in the configuration of the generated boundaries. These operations are described in the following section.

3.1.1. *Filter1*

Headland passes are created sequentially towards the field interior. For each new resulting pass (boundary) $B_j, j \in \{1, \ldots h\}$, this filter creates all the possible groups of m sequential segments, where $m \in \{3, 4, \ldots, |\mathbf{B}_j| - 1\}$ and checks if there is an intersection between the first and last segment of each group. If this is the case, the in-between segments have to be dissolved replacing their vertices with the coordinates of their intersection point:

$$\left.\begin{array}{c} \|\Delta(\varepsilon_{\mathbf{B}_j^i \mathbf{B}_j^{i+1}}, \varepsilon_{\mathbf{B}_j^{i+m-1} \mathbf{B}_j^{i+m}}) - \mathbf{B}_j^i\| + \|\Delta(\varepsilon_{\mathbf{B}_j^i \mathbf{B}_j^{i+1}}, \varepsilon_{\mathbf{B}_j^{i+m-1} \mathbf{B}_j^{i+m}}) - \mathbf{B}_j^{i+1}\| \le \|\mathbf{B}_j^i - \mathbf{B}_j^{i+1}\| \\ \wedge \\ \|\Delta(\varepsilon_{\mathbf{B}_j^i \mathbf{B}_j^{i+1}}, \varepsilon_{\mathbf{B}_j^{i+m-1} \mathbf{B}_j^{i+m}}) - \mathbf{B}_j^{i+m-1}\| + \|\Delta(\varepsilon_{\mathbf{B}_j^i \mathbf{B}_j^{i+1}}, \varepsilon_{\mathbf{B}_j^{i+m-1} \mathbf{B}_j^{i+m}}) - \mathbf{B}_j^{i+m}\| \le \|\mathbf{B}_j^{i+m-1} - \mathbf{B}_j^{i+m}\| \end{array}\right\} \Rightarrow \mathbf{B}_j^{i+1} \equiv \mathbf{B}_j^{i+2} \equiv \ldots \equiv \mathbf{B}_j^{i+m-1} \equiv \Delta(\varepsilon_{\mathbf{B}_j^i \mathbf{B}_j^{i+1}}, \varepsilon_{\mathbf{B}_j^{i+m-1} \mathbf{B}_j^{i+m}})$$

Fig. 1 illustrates an example of the filter implementation in groups of 3 (Fig. 1a) and 4 (Fig. 1b) segments. The pseudo-code of the filter is given in Appendix I.

3.1.2. *Filter2*

This filter also operates on all possible groups of m sequential line segments. It checks if the intersection point of the first and last segments of the group in question is located on either the first or last line segment and at distance less than a threshold distance κ from the end point of the corresponding line segment. In this case, all the in-between points are replaced with the intersection point (m identical points). The threshold distance κ is determined by the features of the agricultural machinery that has to carry out the operation being planned. The value of $w/2$ was selected as threshold, since in this case the coverage of the area corresponding to the deleted points remains secured. The operation of the filter is described by the following equation:

$$\|\Delta(\varepsilon_{\mathbf{B}_j^i \mathbf{B}_j^{i+1}}, \varepsilon_{\mathbf{B}_j^{i+m-1} \mathbf{B}_j^{i+m}}) - \mathbf{B}_j^i\| \le \kappa \Rightarrow \mathbf{B}_j^{i+1} \equiv \mathbf{B}_j^{i+2} \equiv \ldots \equiv \mathbf{B}_j^{i+m-1} \equiv \Delta(\varepsilon_{\mathbf{B}_j^i \mathbf{B}_j^{i+1}}, \varepsilon_{\mathbf{B}_j^{i+m-1} \mathbf{B}_j^{i+m}})$$

Fig. 2 illustrates an example of the filter implementation in groups of 3 (Fig. 2a), 4 (Fig. 2b), and 5 (Fig. 2c) segments. The pseudo-code of the filter is given in Appendix II.

3.2. *Track generation*

3.2.1. *Determination of the longest "curved" edge*

Track generation refers to the process of generating parallel tracks to cover the main field area (the whole area excluding the headland area and the obstacle areas, if any) of a field (or of the field block in the case of a multiple-blocks field). The generated tracks are parallel to the longest "curved" edge of the field block. A curved edge is a collection of sequential straight edges satisfying the criterion that the angle between two successive edges is less than or equal to a threshold angle, ϑ. Note that when the threshold value is set to be zero, the generated tracks are parallel to the longest straight edge of the field block. A general flowchart of the track generation process is shown in Fig. 3.

Let $\mathfrak{I}$ denotes the family of sets, S_i, representing the field curved edges, $\mathfrak{I} = \{S_1, S_2, \ldots\}$. A curved edge of the main field boundary, s_i, is defined as the set of points as follows

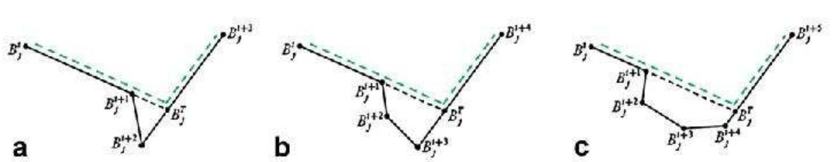

Fig. 2 – Dissolving of segments after the operation of filter 2 in the chosen groups of (a) $m = 3$, (b) $m = 4$, and $m = 5$ segments.

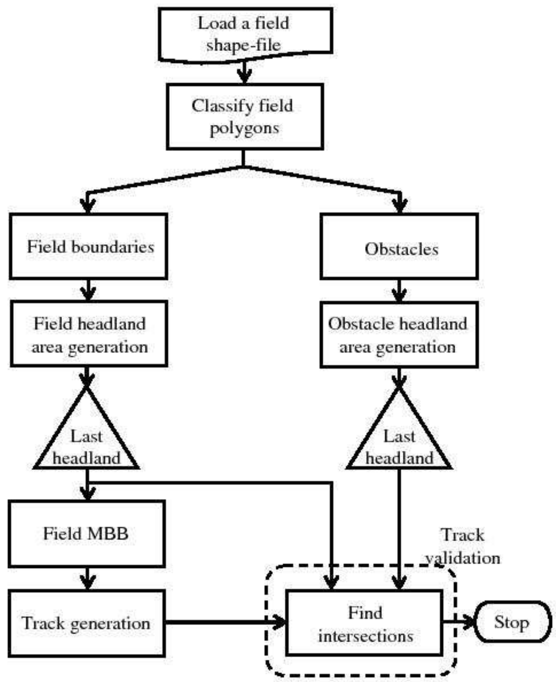

Fig. 3 – A flowchart of basic track generation.

$S_i = \left\{\mathbf{B}^{e_i}_{h+1}, \mathbf{B}^{e_i+1}_{h+1}, \ldots, \mathbf{B}^{e_i+|s_i|+2}_{h+1}\right\}$, where e_i is the index of the first point of the edge while the relation $\left|\Theta\left(\varepsilon_{\mathbf{B}^i_{h+1}\mathbf{B}^{i+1}_{h+1}}, \varepsilon_{\mathbf{B}^{i+1}_{h+1}\mathbf{B}^{i+2}_{h+1}}\right)\right| \le \vartheta, \forall i \in \{e_i, \ldots, |S_i|-2\}$ is satisfied, where $\Theta : \mathbb{R}^3 \times \mathbb{R}^3 \mapsto [0, 360)$ is an operator that returns the angle between two (oriented) line segments.

The length of curved edge is obtained using the relation

$$l_{s_i} = \sum_{k=e_i}^{k=e_i+s_i+1} \left\|\mathbf{B}^k_{h+1} - \mathbf{B}^{k+1}_{h+1}\right\|$$

The index of the longest edge, S_{i^*}, is obtained by the relation

$$i^* = \underset{i\in\{1,\ldots,|\mathcal{S}|\}}{\arg\max} \left(l_{s_i}\right)$$

In the case where $\vartheta = 0$ (straight edge), the index of the longest straight edge is given by:

$$i^* = \underset{i\in\{1,\ldots,|\mathbf{B}_{h+1}|\}}{\operatorname{argmax}} \left(\|\mathbf{B}^i_{h+1} - \mathbf{B}^{i+1}_{h+1}\|\right)$$

The selection of the longest edge of the virtual field depicted in Fig. 4a is considered. To obtain the longest curved edge of the field, the algorithm is applied to vertices 1 to 15 to return the vector [**1** **3** 4 5 **7** 8 9 **11** **13**] where the bold indices represent the first point of an edge or a connected curved edge satisfying the threshold criterion. Hence there are 5 connected curved edges: [**1** 2 3]; [**3** 4 5 6 7]; [**7** 8 9 10 11]; [**11** 12 13] and [**13** 14 15]. In the current field, the last curved edge starts at index number 13 which is the last index of the field boundary points and the first curved edge starts at index number 1 which is the first index of the field boundary points. Therefore the last and the first curved edges have to be combined into one edge, namely [**13** 1 2 3]. By computing the Euclidean length of each of the candidate edges, the longest edge is selected to determine the driving direction.

3.2.2. *Generation of parallel tracks to the longest "curved" edge*

After determining the S_{i^*} set, parallel curved tracks are generated. The distance between the selected driving edge or side and the first two generated tracks on both of its sides is $w/2$ while other tracks are separated by the same distance, w.

A parallel curved track is obtained by applying the parallel line operator, Π, to all the edges of the curved side and then the line intersection operator, Δ, is applied to the consequent pairs of the resultant parallel lines (Fig. 4b). The intersection operator is then applied to the obtained curve to get its intersections with the field headland or obstacles headlands.

To ensure that a field is fully covered with parallel tracks, a segment of length $2L$ perpendicular to the $\varepsilon_{\mathbf{B}^{e_{i*}}_{h+1}\mathbf{B}^{e_{i*}+1}_{h+1}}$ segment i with its centre at point $B^{e_{i*}}_{h+1}$ is created, where L is the length of the diagonal of the MBB including the field. After generating parallel tracks to the selected edge, the intersection points of these lines are obtained to construct the newly generated parallel track. This process continues for generating parallel tracks for each point and then only tracks which have direct intersection with field polygons are being maintained. Fig. 5 presents the method applied to two virtual fields for the cases of straight and curved track generation, respectively.

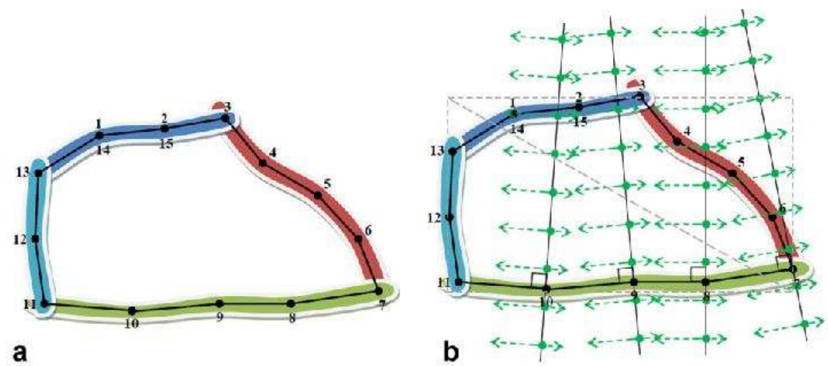

Fig. 4 – An example of selection of the longest edge and generation of parallel tracks to it.

The longest side of the field, S_{i^*}, has n_i indices where the first index is e_i. The parallel tracks are then generated using the relation:

$$t_j^k = \Delta(\Pi(\varepsilon_{\mathbf{B}_{h+1}^{e_{i^*}+k-1}\mathbf{B}_{h+1}^{e_{i^*}+k}}, d, \pm 1), \Pi(\varepsilon_{\mathbf{B}_{h+1}^{e_{i^*}+k}\mathbf{B}_{h+1}^{e_{i^*}+k+1}}, d, \pm 1)),$$
$$k \in S_{i^*}, j \in \{1, \ldots, m\}$$

where

$d = w/2 + w(j-1)$, $j \in \{1, \ldots, T\}$, $m = \lfloor 1 + (\ell - (w/2))1/w \rfloor$ and $\lfloor\rfloor$ denotes the floor function..

3.3. *Single-block field generation*

In this case, the whole field is considered as a block and the process of the field representation is terminated by the generation of the parallel tracks.

3.4. *Multiple-blocks field generation*

In this case, a complex-shaped field (described by a non-convex polygon) is divided into a number of simple-shape fields (described by convex polygons) using a recursive method. The field, in a first step, is considered as a single-block and parallel tracks are generated according to the method described above. In a second step, each generated track is tested if it intersects the internal field boundary ${}_1B_h$ in more than two points, namely the starting and ending point of the track. If a number n of intersection points are obtained, a track is divided into $n-1$ segments and the remaining field area (that is the area which includes the still un-tested tracks) is divided into $n-2$ blocks, in the case that n is an even number, and to $n-1$, in the case that n is an odd number (in order to include the trivial case of the intersection of the track with a vertex of the internal field boundary). The previous procedure is recursively repeated for each of the derived field blocks and terminates when there is no track in the remaining field area that intersects the internal boundary of this area in more than two points (there are no more possible divisions).

In general, for each block ${}_kB$, $k \in \{1, \ldots, b\}$, the number of intersection points between each track $i \in {}_kT$ and the headland boundary ${}_kB_{h+1}$ is obtained. This means that, for each segment

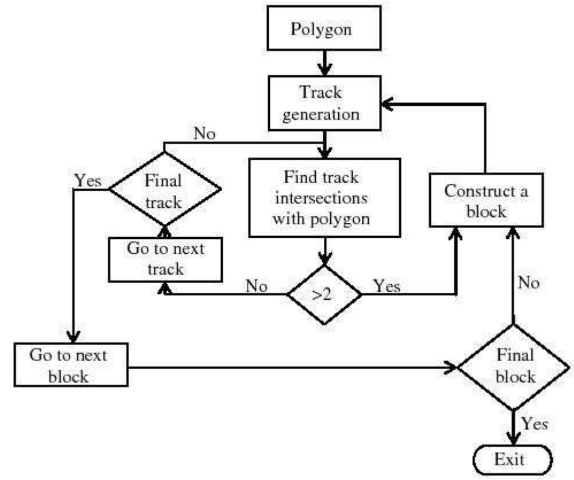

Fig. 6 – Flowchart of recursive approach.

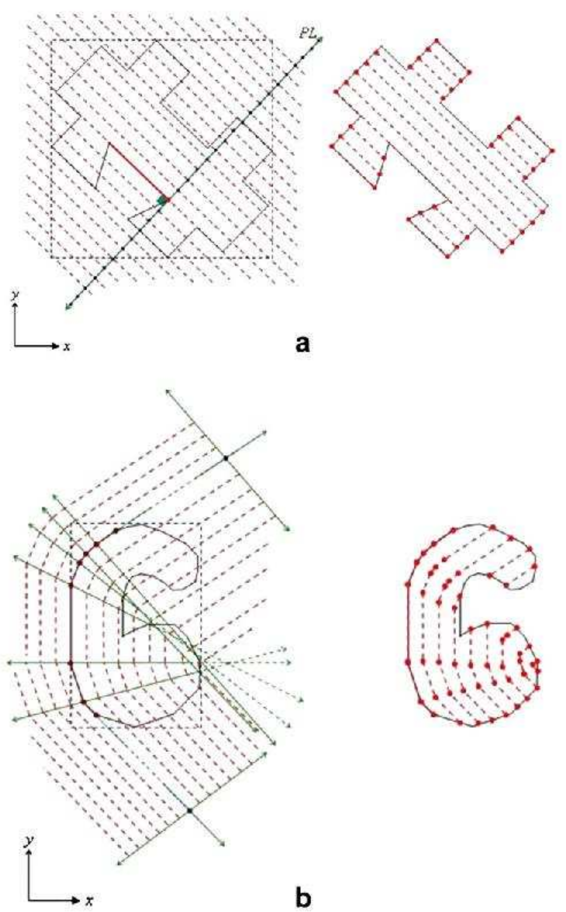

Fig. 5 – Straight (a) and curved (b) track generation for the complete coverage of the MBB of the field.

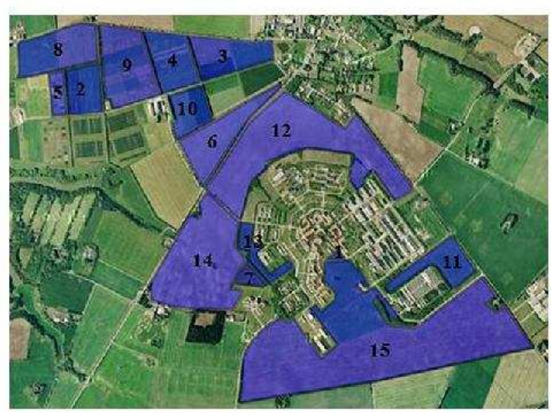

Fig. 7 – Satellite image of field boundaries of Foulum Research Centre, Denmark, 56° 30′ 0″ North, 9° 35′ 0″ East (a) and the location of the 15 fields presented in Table 1.

Table 1 – Processing time of different fields of different shapes and areas.

Field	Area (ha.)	Shape	Processing time (s)							
			$w = 2$ m				$w = 6$ m			
			S-BF			M-BF	S-BF			M-BF
			$\vartheta = 0$	$\vartheta = 15^\circ$	$\vartheta = 25^\circ$		$\vartheta = 0$	$\vartheta = 15^\circ$	$\vartheta = 25^\circ$	
1	0.21		0.28	0.28	0.28	–	0.11	0.11	0.11	–
2	4.08		0.64	2.55	2.55	–	0.41	0.81	0.81	–
3	6.06		1.16	11.63	11.63	–	0.73	3.78	3.78	–
4	5.70		1.31	3.72	3.72	–	0.72	1.38	1.38	–
5	1.47		0.33	0.63	0.63	–	0.23	0.33	0.33	–
6	7.52		1.45	9.20	9.20	–	0.66	2.47	2.47	–
7	1.17		0.31	0.31	0.31	–	0.14	0.19	0.19	–
8	7.27		1.36	1.36	2.35	–	0.81	2.06	2.06	–
9	8.94		1.42	11.06	11.06	–	0.86	3.31	3.31	–
10	3.76		1.09	6.59	6.59	–	0.64	1.91	1.91	–
11	4.50		1.25	4.81	4.81	–	0.66	1.95	1.95	–
12	21.82		3.56	22.42	31.14	82.73	1.80	7.08	9.69	26.13
13	2.40		1.16	2.45	2.45	5.03	0.50	0.50	0.50	2.24
14	16.72		2.97	21.00	21.00	–	1.56	6.67	6.67	–
15	44.93		9.14	239.73	239.73	402.59	4.23	66.75	66.75	123.66

in the set $\langle(\gamma^i_{1x},\gamma^i_{1y}),(\gamma^i_{2x},\gamma^i_{2y}),\ldots,(\gamma^i_{n_ix},\gamma^i_{n_iy})\rangle$ and each one of the $p = |_k B_{h+1}| - 1$ segments of the headland boundary, the result of the operator $\Delta[\varepsilon_{(\gamma^i_{jx},\gamma^i_{jy}),(\gamma^i_{(j+1)x},\gamma^i_{(j+1)y})}, \varepsilon_{{}_k\mathbf{B}^p_{h+1}}, {}_k\mathbf{B}^{p+1}_{h+1}]$ is being checked. The total number of divisions equals the number of times that the operator results in an output not equal to the empty set (Fig. 6).

If the driving direction in a generated block is parallel to the direction of the primary block, these two blocks are physically merged into one block. The driving direction in a block can be a result of the algorithm determined by the angle threshold value, or alternatively can be selected by the user (i.e., by defining an edge to which the generated tracks should be parallel).

4. Results

A number of examples are presented in order to demonstrate the above mentioned method. The geometrical representations of the tested fields were based on shape-files including all the necessary information pertaining to the field as a geographic feature. The shape-files were provided by the GIS database of the Danish Ministry of Food, Agriculture and Fisheries. The algorithm was implemented using MATLAB® technical programming language (The MathWorks Inc., Natwick, MA) on a computer with a CPU of 3.2 GHz speed and a 1 GB RAM. A satellite image of the fields of Research Centre Foulum (Denmark: [N 56° 29′ 21.55, E 009° 34′ 59.40]) is shown in Fig. 7a and a patch plot of 15 selected fields is shown in Fig. 7b. The 15 selected fields have different shapes with complexity varying from very simple to very complex, representing typical Danish fields.

The results regarding the computational time of the algorithm for two operating widths (namely: $w = 2$ and $w = 6$), three different threshold values (namely: $\vartheta = 0°$, $\vartheta = 15°$, and $\vartheta = 25°$) including the case of multiple-block generation for the fields that can divided to blocks (namely: fields 12, 13, and 15) are given in Table 1.

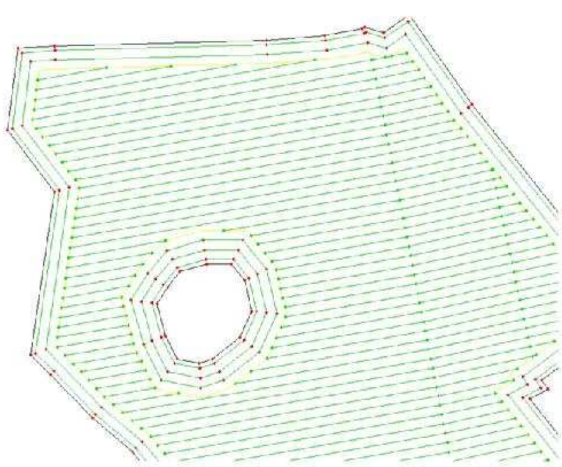

Fig. 8 – A close view of field 15 for 3 field headland passes and 3 obstacle-headland passes for a machine of 2 m operating.

5. Discussion

According to the experimental results, the computational time of the method was in the range 0.11–239.73 s for the case of single-block fields and in the range 2.24–402.59 s for the case of multiple-block fields. For the former case the average and the median were 10.31 s and 1.86 s, respectively, while for the latter the average and the median were 107.06 s and 54.53 s, respectively. The deviation between the median and the average was caused by the high computational time (compared to the rest of the examined fields) required for field 15 which has a very complex shape. If field 15 is excluded from the average and median calculations (providing a more homogenous sample of fields in terms of shapes) the resulting average and median values for the case of single-block fields are 3.59 s and 1.44 s, respectively, while the resulting average and median values for the case of multiple-block fields are 29.03 s and 54.43 s, respectively. The computational time in the case of field 15 is increased due to the presence of an obstacle (Fig. 8). The same field was tested assuming the absence of that obstacle and the resulted computational times were reduced by 4.52% (average). Regarding the in-field obstacles, it has to be noted that the proposed approach does not deal with small obstacles which cause temporary deviations from the calculated paths. These deviations are handled by the driver (only the first time that the operation is executed in the case of most auto-steering-systems) or by the obstacle avoidance sensor system in the case of an autonomous machine. However, the obstacles handled by the approach are those that can cause the division of the field into blocks (and a headland has to be created around them), such as the one presented in Fig. 8.

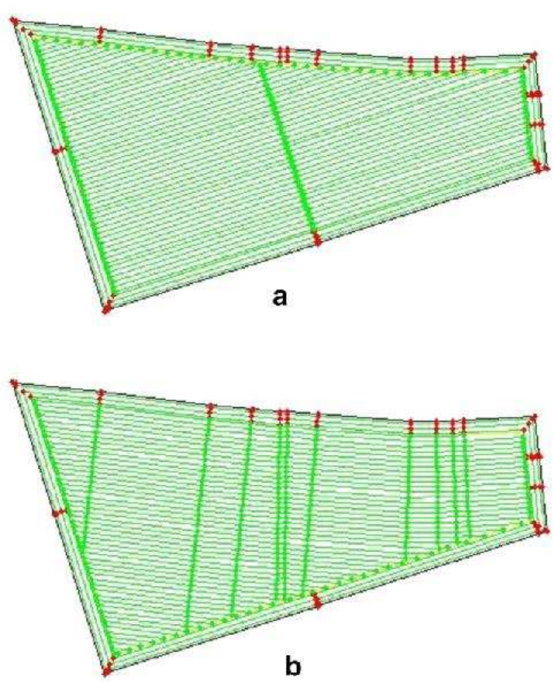

Fig. 9 – Field 3 covered by straight (a) and curved (b) tracks.

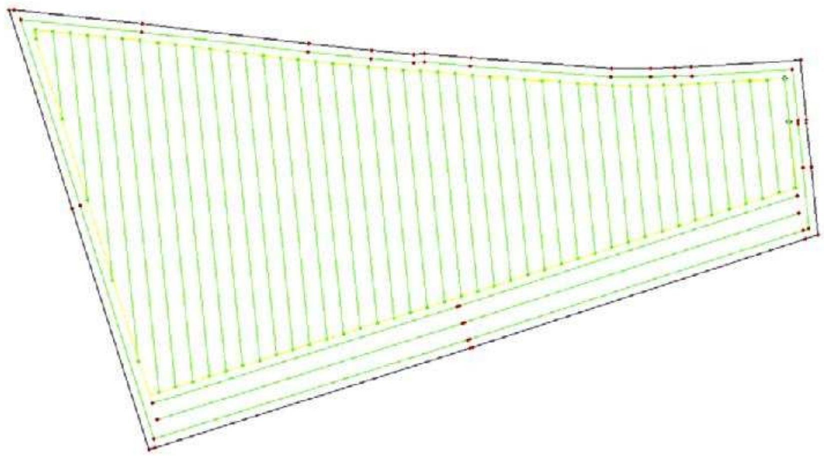

Fig. 10 – Headland areas with different numbers of passes; one headland pass in the north headland and three passes in the south.

In Table 1 there are equal processing times for more than one threshold value for some fields. Namely, all computational times are equal in the case of fields 1 and 7, computational times for $\vartheta = 0^\circ$ and $\vartheta = 15^\circ$ are equal in the case of field 8, and times for $\vartheta = 15^\circ$ and $\vartheta = 25^\circ$ are equal in the case of fields 2, 3, 4, 5, 6, 9 10, 11, 13, 14, 15. Equal computational times between two different threshold values occur when, for both threshold values, the same longest edge results. For example, in field 3 for threshold value $\vartheta = 0$ (straight tracks), the generated tracks are parallel to its south edge (Fig. 9b), while for threshold value $\vartheta = 15^\circ$ (curved racks) the generated tracks are parallel to its north edge (Fig. 9b).

In Fig. 10 the case of two different headland widths in the same field is presented. This can occur, e.g., when a field is tangential to a road which can be used as an extension of the headland area. For example, in the north headland of the field only one pass has been generated, while in the south, three headland passes have been generated.

Also, there are cases where more than two different directions can result. In field 12, by setting the threshold value $\vartheta = 0$ the resulting straight tracks are parallel to the longest straight edge of the field (Fig. 11). Nevertheless, it is clear from the picture that it leads to an inappropriate operating direction. Alternatively, by using a threshold value $\vartheta = 15^\circ$, parallel tracks to the slightly curved north-west edge of the field are generated (Fig. 12). Further increasing the threshold to $\vartheta = 25^\circ$, a new set of tracks is generated parallel to the north curved edge of the field (Fig. 13), resulting in longer tracks, fewer in number (and consequently requiring less machine turnings), yet more curved. The number of the resulting tracks and the average track length for these three cases for field 12 are given in Table 2.

Fig. 14 shows the sequence of dividing field 12 into 5 blocks through 4 recursive cycles of the algorithm. The main field polygon (Fig. 15a) (block 1) was first operated using the single-block field generation algorithm resulting in 244 parallel tracks. Track number 43 is divided into three segments and hence the rest of the field area is divided into two new blocks (2.2 and 2.3 in Fig. 15b). Each of these two blocks is then operated using the single-block field algorithm resulting in 13 and 197 tracks for each, respectively. Block 2.3 was not further divided while block 2.2 was divided since track number 35 is divided into three segments resulting in two new blocks, 3.2 and 3.4 (Fig. 15c). Finally, block 3.2 was divided into blocks 4.4 and 4.5 (32 and 149 tracks, respectively) in the fourth recursion (Fig. 15d).

The low computational requirements of the derived method, of the order of a few seconds (Table 1), make it

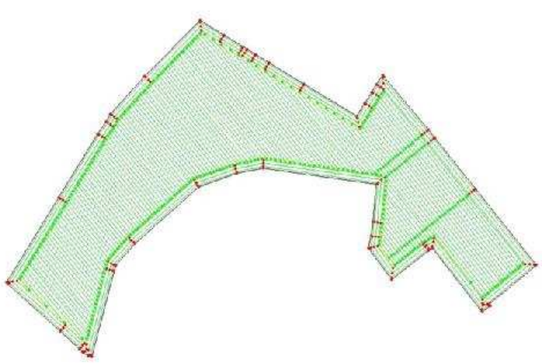

Fig. 11 – Field 12 for threshold $\vartheta = 0^\circ$.

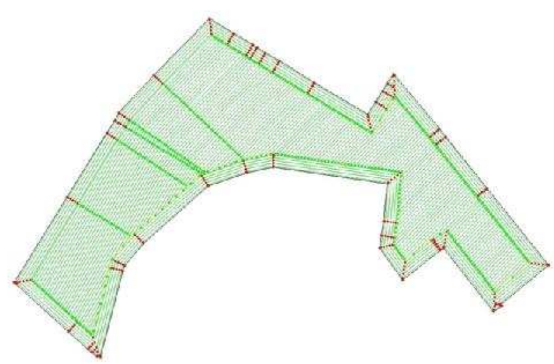

Fig. 12 – Field 12 for threshold $\vartheta = 20^\circ$.

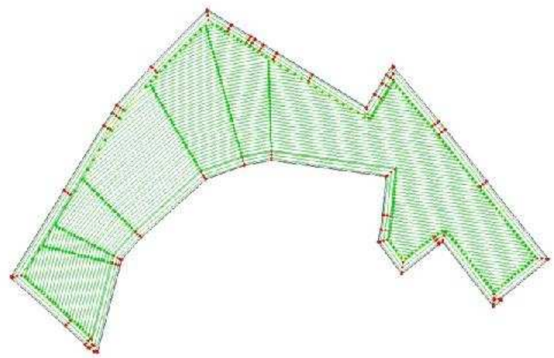

Fig. 13 – Field 12 for threshold $\vartheta = 25^\circ$.

In the case of fully automated agricultural machines, the path planning for a complete field area coverage operation presumes the connection of the presented method with a method for the generation of headland turning paths. For the latter, there is a large body of dedicated literature and a number of different approaches have been produced such as 2-dimestional geometrical models for Ackerman-steering vehicles/tractors (e.g., Bochtis, 2008), kinematics models (e.g., Kise, Noguchi, Ishii, & Terao, 2002) and dynamic models for different types of machine kinematics (e.g., Miller, Steward, & Westphalen, 2004) and tractor–trailer combinations (e.g., Oksanen & Visala, 2004).

As has been previous mentioned, the field geometrical representation is not a new idea in itself and has been used internally in the available commercial systems. Nevertheless, the information regarding the geometrical field representation (coordinates of the points that describe the tracks, headland passes, etc.) cannot be created before the actual operation and thus it is not possible to use these systems as part of a decision support system (i.e., to evaluate different driving directions, overlaps, different fieldwork patterns, etc.). Even after the actual operation has been executed, it is not possible to evaluate the operation as part of a decision support systems since the created information regarding the field geometry is not extractable. In contrast, the presented approach can be used as a basis for an off-line decision support system since the formalised mathematical description of the problem provides the required background for the formulation of optimisation problems related to operations management. For example, the overlapping area during the headland turnings can be easily formulated as:

Table 2 – Tracks configuration in field 12 for different threshold values.

Operating width (m)	$w = 2$			$w = 6$		
Threshold	$\vartheta = 0^\circ$	$\vartheta = 15^\circ$	$\vartheta = 25^\circ$	$\vartheta = 0^\circ$	$\vartheta = 15^\circ$	$\vartheta = 25^\circ$
Total number of tracks	490	412	318	154	132	99
Average track length (m)	204.74	244.21	286.97	180.22	211.79	292.40

feasibly for real-time use. Real-time generation of field tracks is very important for a number of reasons. Firstly, not all of the fields are included and represented in shape-file data bases, so on-site generation of the boundary polygon is required (i.e., driving the agricultural machine around the field boundary). Secondly, each operating width needs a different representation and furthermore, the representation should be based rather on the effective operating width as opposed to the designed operating width, as the effective operating width is influenced by a number of factors (e.g., the accuracy of the positioning system used). Finally, the headland area available for manoeuvring and, equivalently, the number of the headland passes, depends on the geometrical and kinematic features of the machine that carries out the operation. The use of different machines, even with the same operating width, needs a different field representation in the case where the headland area has to be modified.

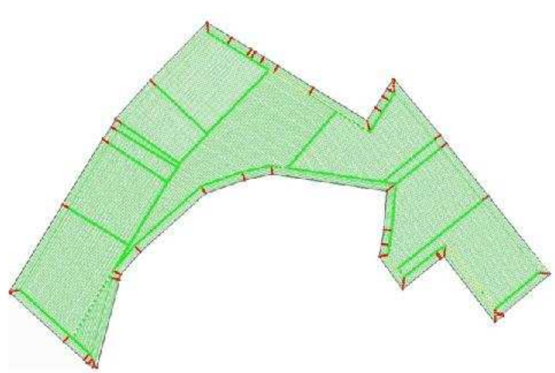

Fig. 14 – Field 12 operated using the recursive method.

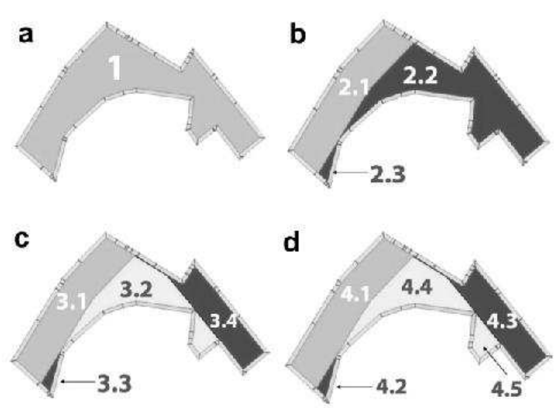

Fig. 15 – Sequence of blocks construction in field 12 using the recursive approach.

$$\frac{w^2}{2}\cdot\sum_{i=1}^{i=T}\left[\frac{1}{\tan\left(\Theta\left[\varepsilon_{\mathbf{\Gamma}_1^{i+1}\mathbf{\Gamma}_{n_{i+1}}^{i+1}},\varepsilon_{\mathbf{\Gamma}_{n_{i-1}}^{i-1}\mathbf{\Gamma}_{n_{i+1}}^{i+1}}\right]\right)}+\frac{1}{\tan\left(\Theta\left[\varepsilon_{\mathbf{\Gamma}_1^{i+1}\mathbf{\Gamma}_{n_{i+1}}^{i+1}},\varepsilon_{\mathbf{\Gamma}_1^{i+1}\mathbf{\Gamma}_1^{i-1}}\right]\right)}\right]$$

(tracks 0 and $|T|+1$, are "dummy" tracks created by the algorithm parallel to the first and last track of the field, respectively). As another example, the total non-working distance travelled during headland turnings while following the alternate fieldwork pattern can be formulated as:

$$\sum_{i=1}^{T-1}\left(\frac{1-(-1)^i}{2}\cdot\left[L_{\min}\left(r_{\min,}w,\Theta\left[\varepsilon_{\mathbf{\Gamma}_1^{i+1}\mathbf{\Gamma}_{n_{i+1}}^{i+1}},\varepsilon_{\mathbf{\Gamma}_1^{i+1}\mathbf{\Gamma}_1^{i-1}}\right]\right)\right]\right.$$
$$\left.+\frac{1-(-1)^{i+1}}{2}\cdot\left[L_{\min}\left(r_{\min,}w,\Theta\left[\varepsilon_{\mathbf{\Gamma}_1^{i+1}\mathbf{\Gamma}_{n_{i+1}}^{i+1}},\varepsilon_{\mathbf{\Gamma}_{n_{i-1}}^{i-1}\mathbf{\Gamma}_{n_{i+1}}^{i+1}}\right]\right)\right]\right)$$

where $r_{\min}$ is the minimum turning radius of the machine, and $L_{\min}$ is a function that allows the minimum length of headland turns executed by an Ackerman-steering agricultural machine to be computed by the kinematic model, based on equations of motion of a non-holonomic vehicle (Bochtis, 2008). Expressions such as the above can be used to find, for example, the driving direction that results in the least overlaps (i.e., during spraying), or the least total non-working distance, or can even be used for multiple-criteria optimisation problems.

The scope of this paper has been to provide a tool for the real-time generation of alternative geometrical representation of a field, leaving the problem of the selection of the optimal one to future work. It has to be mentioned that the problem of field representation and the problem of optimal field area coverage are two distinct and different tasks. This can be easily understood using the abstractive representation of the track generation and the field coverage using the tracks with the design of a road network and the optimal coverage with the optimal route planning within this network, respectively. In a field operation, optimal coverage refers to the sequence in which the agricultural machine visits the field blocks and the sequence that it traverses the tracks within each block (Bochtis & Sørensen, 2009; Bochtis & Vougioukas, 2008). Certainly, the design of the network affects the value of the objective function of the route optimisation problem. Nevertheless, in the case of the agricultural operations, the special features and the inherently agronomic constraints provide limited space for considerations of alternatives in the generation of the tracks "network". Furthermore, there are cropping systems that cannot be included in a general approach like this. For example, systems regarding row crops in ridges cannot be addressed by the proposed method in its current form and this is considered an important subject for future research.

6. Conclusions

In this paper, a method for the generation of a field geometrical representation has been presented. The geometrical representation of the field provides a map, on which the operational planning of field operations involving advanced optimisation methods for the route planning problem of agricultural machines can take place.

According to the experimental results, the computational time of the method was in the range of 0.11–239.73 s (average 32.39 s) for the case of single-block fields and in the range of 2.24–402.59 s (average 107.06 s) for multiple-blocks fields. The tested fields were of different shapes and the area ranged from 0.21 ha to 44.93 ha. The low computational requirements of the method make it feasible for real-time use involving cases such as fields that are included in shape-file data bases, for different accuracies of positioning systems, different machinery kinematics, and different number of required headland passes.

Appendices

Appendix I. Pseudo-code of filter 1

$B_j = \texttt{FILTER1}\ (B_j)$
FOR $m = 3 : |B_j| - 1$
  $i = 1$
  WHILE $i \le |B_j|$
    IF $\left\|\Delta\left(\varepsilon_{\mathbf{B}_j^i\mathbf{B}_j^{i+1}},\varepsilon_{\mathbf{B}_j^{i+m-1}\mathbf{B}_j^{i+m}}\right)-\mathbf{B}_j^i\right\|+\left\|\Delta\left(\varepsilon_{\mathbf{B}_j^i\mathbf{B}_j^{i+1}},\varepsilon_{\mathbf{B}_j^{i+m-1}\mathbf{B}_j^{i+m}}\right)-\mathbf{B}_j^{i+1}\right\|$
    $\le\left\|\mathbf{B}_j^i-\mathbf{B}_j^{i+1}\right\|$
      IF $\left\|\Delta\left(\varepsilon_{B_j^iB_j^{i+1}},\varepsilon_{B_j^{i+m-1}B_j^{i+m}}\right)-B_j^{i+m-1}\right\|+\left\|\Delta\left(\varepsilon_{B_j^iB_j^{i+1}},\varepsilon_{B_j^{i+m-1}B_j^{i+m}}\right)\right.$
      $\left.-B_j^{i+m}\right\|\ldots\ldots\le\left\|B_j^{i+m-1}-B_j^{i+m}\right\|$
        FOR $k = i + 1 : i + m - 1$
          $B_j^k\equiv\Delta\left(\varepsilon_{B_j^iB_j^{i+1}},\varepsilon_{B_j^{i+m-1}B_j^{i+m}}\right)$
        ENDFOR
      ENDIF
    ENDIF
    INCREMENT i
  ENDWHILE
ENDFOR

Appendix II. Pseudo-code of filter 2

$B_j = \texttt{FILTER2}\ (B_j,\ \kappa)$
FOR $m = 3 : |B_j| - 1$
  $i = 1$
  WHILE $i \le |B_j|$
    IF $\left\|\Delta\left(\varepsilon_{B_j^iB_j^{i+1}},\varepsilon_{B_j^{i+m-1}B_j^{i+m}}\right)-B_j^i\right\|\le\kappa$
      FOR $k = i + 1 : i + m - 1$
        $B_j^k\equiv\Delta\left(\varepsilon_{B_j^iB_j^{i+1}},\varepsilon_{B_j^{i+m-1}B_j^{i+m}}\right)$
      ENDFOR
    ENDIF
    INCREMENT i
  ENDWHILE
ENDFOR

REFERENCES

Alia, O., Verlindena, B., & Oudheusdena, D. V. (2009). Infield logistics planning for crop-harvesting operations. *Engineering Optimization, 41*(2), 183–197.

Anderson, N. W. (2004). Method and system for determining an energy-efficient path of a vehicle U.S. Patent No. 2004, 006, 8352. Washington, DC: U.S. Patent and Trademark Office.

Bak, T., & Jakobsen, H. (2004). Agricultural robotic platform with four wheel steering for weed detection. *Biosystems Engineering, 87*(2), 125–136.

Birnie, D. A. (2009). Method and system for planning the path of an agricultural vehicle. U.S. Patent No. 2009, 011, 8904. Washington, DC: U.S. Patent and Trademark Office.

Bochtis, D. (2008). *Planning and control of a fleet of agricultural machines for optimal management of field operations*. Ph.D. Thesis. AUTh, Faculty of Agriculture, Department of Agricultural Engineering, Greece.

Bochtis, D. D., & Oksanen, T. (2009). Combined coverage path planning for field operations. In E. J. Van Henten, D. Goense, & C. Lokhorst (Eds.), *Proc. Joint International Agricultural Conference, JIAC 2009, Precision Agriculture 09* (pp. 521–527). Netherlands: Wageningen.

Bochtis, D. D., & Sørensen, C. G. (2009). The vehicle routing problem in field logistics part I. *Biosystems Engineering, 104*(4), 447–457.

Bochtis, D. D., & Sørensen, C. G. (2010). The vehicle routing problem in field logistics: Part II. *Biosystems Engineering, 105*(2), 180–188.

Bochtis, D. D., & Vougioukas, S. G. (2008). Minimising the non-working distance travelled by machines operating in a headland field pattern. *Biosystems Engineering, 101*(1), 1–12.

Bochtis, D. D., Vougioukas, S. G., & Griepentrog, H. W. (2009). A mission planner for an autonomous tractor. *Transactions of the ASABE, 52*(5), 1429–1440.

Choset, H. (2001). Coverage for robotics - A survey of recent results. *Annals of Mathematics and Artificial Intelligence, 31*, 113–126.

de Bruin, S., Lerink, P., Klompe, A., van der Wal, T., & Heijting, S. (2009). Spatial optimisation of cropped swaths and field margins using GIS. *Computers and Electronics in Agriculture, 68*, 185–190.

Dudek, G., & Jenkin, M. (2000). *Computational principles of mobile robotics*. Cambridge University Press.

Earl, R., Thomas, G., & Blackmore, B. S. (2000). The potential role of GIS in autonomous field operations. *Computers and Electronics in Agriculture, 25*(1–2), 107–120.

Flann, N. S., Hansen, S. L., Gray, S. A. (2007). Path planner and method for planning a contour path of a vehicle. U.S. Patent No. 2007, 019, 2024. Washington, DC: U.S. Patent and Trademark Office.

Have, H., Nielsen, J., Blackmore, B. S., & Theilby, F. (2005). Development and test of an autonomous Christmas tree weeder. In J. V. Stafford (Ed.), *5th European conference on Precision Agriculture* (pp. 629–635). The Netherlands: Wageningen Academic Publishers.

Hofstee, J. W., Spätjens, L. E. E. M., & Ijken, H. (2009). Optimal path planning for field operations. In E. J. Van Henten, D. Goense, & C. Lokhorst (Eds.), *Proc. Joint International Agricultural Conference, JIAC 2009, Precision Agriculture 09* (pp. 521–529). Netherlands: Wageningen.

Keicher, R., & Seufert, H. (2000). Automatic guidance for agricultural vehicles in Europe. *Computers and Electronics in Agriculture, 25*(1–2), 169–194.

Kise, M., Noguchi, N., Ishii, K., & Terao, H. (2002). Enhancement of turning accuracy by path planning for robot tractor. In Qin Zhang (Ed.), *Automation Technology for Off-Road Equipment (ATOE) Proceedings* (pp. 398–404). Chicago, Illinois, USA: ASAE, Pub #701P0509.

Klee, U., Hofmann, L., & Pickle, P. (2003). Safety aspects for automatic guidance of agricultural machines and low-cost solutions. *Research in Agricultural Engineering, 49*(3), 103–109.

Miller, M. A., Steward, B. L., & Westphalen, M. L. (2004). Effects of multimode four-wheel steering on sprayer machine performance. *Transactions of the ASAE, 47*(2), 385–395.

Nørremark, M., Griepentrog, H. W., Nielsen, J., & Søgaard, H. T. (2008). The development and assessment of the accuracy of an autonomous GPS-based system for intra-row mechanical weed control in row crops. *Biosystems Engineering, 101*(4), 396–410.

Oksanen, T., & Visala, A. (2004). Optimal control of tractor-trailer system in headlands. In Q. Zhang, M. Iida, & A. Mizushima (Eds.), *Automation Technology for Off-Road Equipment: Proceedings of the 7–8 October 2004 Conference (Kyoto, Japan)*. ASAE Publication Number 701P1004.

Oksanen, T., & Visala, A. (2007). Path planning algorithms for agricultural machines. *Agricultural Engineering International: the CIGR Ejournal, vol. IX*. Manuscript ATOE 07 009.

O'Rourke, J. (1985). *Finding minimal enclosing boxes. Parallel Programming*. Netherlands: Springer.

Palmer, R. J., Wild, D., & Runtz, K. (2003). Improving the efficiency of field operations. *Biosystems Engineering, 84*(3), 283–288.

Pilarski, T., Happold, M., Pangels, H., Ollis, M., Fitzpatrick, K., & Stentz, A. (2002). The demeter system for automated harvesting. *Autonomous Robots, 13*(1), 9–20.

Sachs, J. L., Roszhart, T. J., Schleicher, T., Beck, A. D., Bezdek, M. A. (2009). System and method for generation of an inner boundary of a work area U.S. Patent No. 2009,024, 0430. Washington, DC: U.S. Patent and Trademark Office.

Senneff, A. M., Leiran, B. G., Roszhart, T. J. (2009). Method and system for generating end turns U.S. Patent No. 2009, 003, 7041. Washington, DC: U.S. Patent and Trademark Office.

Sørensen, C. G., & Bochtis, D. D. (2010). Conceptual model of fleet management in agriculture. *Biosystems Engineering, 105*(1), 41–50.

Sørensen, C. G., & Nielsen, V. (2005). Operational analyses and model comparison of machinery systems for reduced tillage. *Biosystems Engineering, 92*(2), 143–155.

Taix, M., Soueres, P., Frayssinet, H., & Cordesses, L. (2006). Path planning for complete coverage with agricultural machines. In S. Yuta, et al. (Eds.), *Field and service robotics. STAR, Vol. 24* (pp. 549–558).

Toth, P., & Vigo, D. (2002). *The vehicle routing problem*. SIAM Monographs on Discrete Mathematics and Applications 2002, ISBN 0-89871-498-2.

Chapter 3

Driving Angle and Track Sequence Optimization for Operational Path Planning using Genetic Algorithms

Hameed, I. A., Bochtis, D. D., & Sørensen, C. G.

Journal of Applied Engineering in Agriculture, ASABE, 2011, 27(6), 1077-1086.

Driving Angle and Track Sequence Optimization for Operational Path Planning Using Genetic Algorithms

I. A. Hameed, D. D. Bochtis, C. G. Sorensen

Abstract. *The objective of this article was to develop an initial approach for a method to combine two recently developed methods related to the field area coverage problem. The first stage generated a field geometrical representation and the second stage aimed to optimize the routing of agricultural vehicles within this geometrically defined world. In the first stage, using the former method the optimal driving direction is derived based on the minimization of the overlapped area. The second stage uses the later method, the optimal routing is determined for the derived driving direction and is based on the minimization of the non-working distance. In its current state, the developed approach can provide optimal solutions in terms of overlapped area and sub-optimal solutions in terms of total non-working travelled distance. Still, these sub-optimal solutions proved more efficient compared to the conventional field work patterns. Improving this sub-optimality as well as the reducing the computation times of the method in order to be feasible for real-time implementation, are considered issues of future researching.*

***Keywords.** Agricultural vehicles, Route planning, B-patterns.*

The coverage path in a field has a significant effect on the time lost in the field due to the non-working travelled distance and excessive maneuvering (Hunt, 2001). A determining portion of the non-working travelled distance and hence the non-working time occurs during turning on the headland area. The negative impact of turning time on field efficiency has been verified experimentally in grain harvesting (Taylor et al., 2002; Hansen et al., 2003) or tillage operations (Sørensen and Nielsen, 2005), as well by simulations (Benson et al., 2002). The time consumed for a headland turning depends on the distance travelled during the turning (i.e., the length of the maneuver) and the mean turning speed. Some maneuvering types are easy to execute at higher speeds, while other types require skillful driving or reversing of the motion direction causing a reduced mean turning speed, higher non-working distance, and a larger headland area. In addition, some maneuvering influences soil conditions unfavorably (Keller, 2005; Ansorge and Godwin, 2007). Perpendicular disturbance of the soil is caused by the weight of the machine, while parallel disturbance is caused by changes in motion direction. Consequently, the headland area constitutes a 'low productivity field area' (Witney, 1996). Additionally, the headland maneuvering affects the fuel consumption since complex maneuvering requires more driving and/or reverse motion.

Submitted for review in December 2010 as manuscript number IET 8951; approved for publication by the Information & Electrical Technologies Division of ASABE in September 2011.

The authors are **Ibrahim A. Hameed**, Ph.D., **Dionysis D. Bochtis**, Assistant Professor, and **Claus Grøn Sørensen, ASABE Member**, Senior Researcher, Aarhus University, Faculty of Science and Technology, Department of Engineering, Tjele, Denmark. **Corresponding author:** Ibrahim A. Hameed, Aarhus University, Faculty of Science and Technology, Department of Engineering, P.O. Box 50, Blichers Allé 20, 8830 Tjele, Denmark; phone: 045 2426 6883; e-mail: Ibrahim.abdel-hameed@agrsci.dk.

In contrast to a routing problem where a route is optimized on an existing network of paths (e.g. road network), the field area coverage path consists of the two distinct problems of field representation and the problem of routing within this representation. Clearly, the geometrical representation affects the value of the objective function of the route optimization problem and thus the total problem must be considered a coupled problem.

Regarding the field representation problem, a number of methods have recently been developed. Oksanen and Visala (2009) presented two greedy algorithms to solve the field coverage path planning, where the first one utilizes a trapezoidal decomposition algorithm for splitting a single field area into subfields that are simple to drive or operate using the best driving direction, while the second algorithm comprise a real-time planner based on the basis of the machine's current state and the search is directed toward the next swath instead of the next subfield. Jin and Tang (2010) developed a geometrical model combined with a path-planning algorithm for the optimal field decomposition into sub-regions and the determination of optimal coverage path direction in each sub-region. The method can be implemented in both convex and non-convex fields including the case of multiple obstacles present, and results show an up to 16% reduction in the number of turns and a 15% reduction in headland turning cost as compared with results from other researchers, as well as from conventional farming practices. Hameed et al. (2010) developed an approach to generate the geometrical representation of the field as a geometrical entity comprising discrete geometric primitives, such as points, lines, and polygons. The approach does not provide the optimal representation according to a selected criterion, but provides a fast representation solution according to user preferences (driving direction, curved or straight tracks, single- or multiple-block generations). According to the experimental results, the computational time of the method averaged 32.39 s for the case of single-block fields while the

  ISSN 0883-8542

computational time averaged 107.06 s for multiple-block fields with areas ranging from 0.21 to 44.93 ha.

It has to be noted that all of the above mentioned approaches refer to the case of the two-dimensional representations of the field geometry. Jin and Tang (2011) presented a single case of a three-dimensional geometrical representation of the field. According to the presented results, 3D coverage path planning saved 10.3% on headland turning cost, 24.7% on soil erosion cost, 81.2% on skipped area cost, and 22.0% on a selected weighted sum of these costs.

Regarding the routing within a given field area with defined geometrical representation, a new type of algorithmically-computed optimal fieldwork patterns (B-patterns) have recently been introduced (Bochtis, 2008). The method is based on an approach where the field coverage is expressed as the traversal of a weighted graph, and the problem of finding optimal traversal sequences is equivalent to finding the shortest tours in the graph. The weight of the graph arcs could be based on any relative optimization criterion, such as total or non-working travelling distance, total or non-productive operational time, a dedicated soil compaction measure, etc. Contrary to any traditional field-work pattern, B-patterns do not follow the repetition of standard motifs but they are the unique result of the optimization approach on the specific combination of the mobile unit kinematics and dimensions, the operating width, the field shape, and the optimization criterion. The implementation of the B-patterns for conventional agricultural machines with auto-steering systems was presented in Bochtis and Vougioukas (2008). The experimental results showed that by using B-patterns instead of traditional fieldwork patterns, the total non-working distance can be reduced by up to 50%. The same approach has been implemented for the mission planning of an autonomous tractor for area coverage operations such as grass mowing, seeding, and spraying (Bochtis et al., 2009). B-patterns can be implemented for a majority of field operations, involving different machinery systems (single or multiple-machinery system) and different operational characteristics (deterministic, stochastic, and dynamic). These patterns can be generated from the implementation of the well-known combinatorial optimization problem, the vehicle routing problem (VRP), after the appropriate abstractive representations of the corresponding routing problems (Bochtis and Sørensen, 2009). Research into the potential savings from the implementation of these patterns has shown that the savings in terms of operational time ranged from 8.4% to 17.0%, while the mean savings in terms of fuel consumption, and consequently the CO_2 emissions was in the order of 18% (Bochtis et al., 2010).

The objective of this article is to develop an initial approach for a method to combine two recently developed methods related to the field area coverage problem. The first one regards a method for generation of field geometrical representation (i.e. Hammed et al., 2010) and the second one regards a method or the optimization of the routing of agricultural vehicles within this geometrically defined world (i.e. Bochtis, 2008). In a first stage, using the former method the optimal driving direction is derived based on the minimization of the overlapped area, and in a second stage using the later method, the optimal routing (B-patterns) is determined for the derived driving direction and based on the minimization of the non-working distance.

System Description

Assumptions

The following assumptions have been made for the presented system:

- Fields are two-dimensional, meaning that elevation changes are ignored.
- The positions for entering and exiting the field are considered as pre-determined parameters of the problem and not a part of the solution.
- The field is obstacle free (physical obstacles or unreachable areas).
- In the case of the field being divided into sub-regions, the driving direction is the same for all sub-regions.

Structure

Overview

The proposed system consists of a three-stage configuration. In the first stage, based on an appropriate geometrical representation method, the optimal driving direction is determined in terms of minimized overlapping area. Next, the resulting tracks corresponding to the case of the optimized driving direction are clustered into blocks and the routing method is applied to each of these blocks. Finally, the sequence of these blocks is optimized in terms of minimized travelling distance. A flowchart of the proposed approach is shown in figure 1.

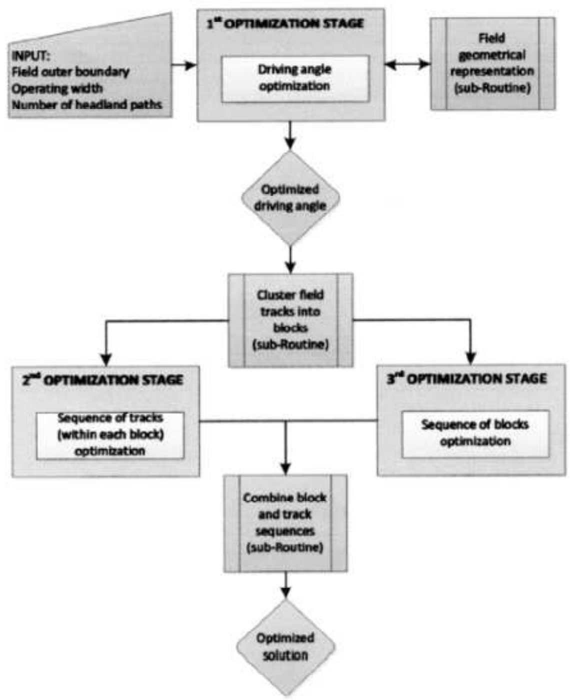

Figure 1. Flowchart of the field operational planning optimization process.

Driving Angle Optimization Stage

In order to optimize the driving direction of the field tracks, an appropriate geometrical representation for the field is needed. As mentioned in the introduction section, the approach of Hameed et al. (2010) was adopted. The inputs to the geometrical representation algorithm include the field outer boundary, the operating width of the implement, the iterative driving direction (each time the geometrical representation algorithm is called by the GA of this stage), and the number of headland passes. The vertices of the field boundary are given in the form of a shape/text file as a closed polygon in a UTM coordinate system. The approach is based on a minimum bounding box (MBB) principal which ensures that there will not be any skipped areas within the field area in the case of very complex fields. A flowchart showing the geometrical representation approach is shown in figure 2. Initially, based on the user pre-defined number of headland paths an inner field boundary is recursively generated. The distance between the first headland path and the field boundary is half of the implement width, $w/2$, and between subsequent headland passes is an implement width, w, where w denotes the (effective) operating width of the machine which carries out the operation. As part of the headland area generation, two filtering operations take place in order to avoid irregularities in the configuration of the generated boundaries. Tracks parallel to the designated driving direction are then generated to cover the remaining field area. The 2D coordinates of the resultant waypoints are stored into a standard KML file.

As a decision variable of the optimization problem in the first stage is considered the driving angle, which is defined as the angle between the driving direction and the horizontal axis of the MBB (fig. 3). The driving angle determines the size of the overlapped area (fig. 4), which is considered the optimization criterion for this stage.

Overlapped areas result from covering some area more than once resulting in excess use of fertilizers and chemicals and impacting economical and environmental aspects of the system. When a track is perpendicular to a headland path, the overlapped area equals zero. Otherwise, the overlapped area O_i (θ) for a given driving angle θ is computed using equation 1, as shown in figure 5, where $\phi_i(\theta)$ and $\beta_i(\theta)$ are the angles between the current track (i) and the upper and lower headland paths, respectively.

$$O_i(\theta) = w^2(\tan\phi_i(\theta) + \tan\beta_i(\theta))/2 \tag{1}$$

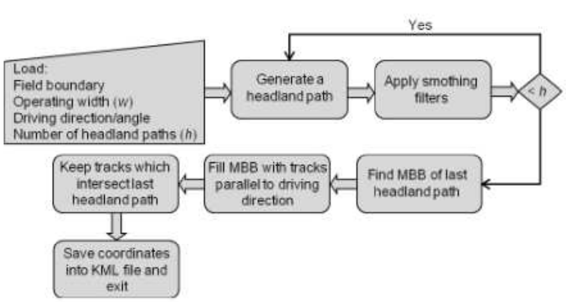

Figure 2. The architecture of the geometrical field representation approach.

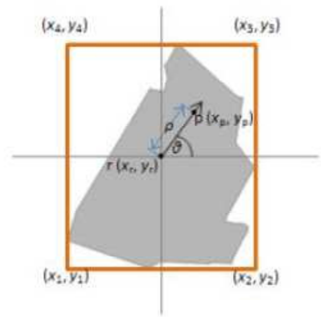

Figure 3. Driving direction defined by the field center point and an angle, θ, where 0 ≤ θ ≤ 180°.

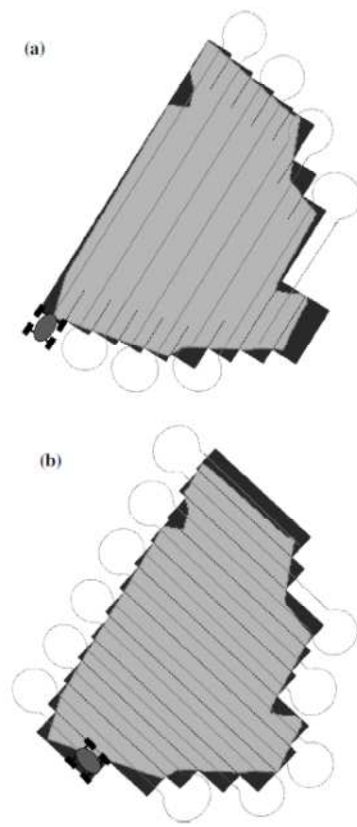

Figure 4. The influence of driving direction on the resulting overlapped area (shown in dark-gray).

For a driving angle the total cost equals:

$$O(\theta) = \sum_T O_i(\theta) \tag{2}$$

The objective of this first stage is to find the driving angle that minimizes the total overlapped area:

$$\vartheta^* \rightarrow \min \sum_T O_i \tag{3}$$

where T is the set of tracks required for a full field coverage as a result from the geometrical representation of the field for a given driving angle.

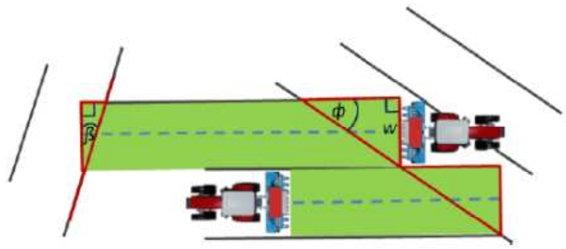

Figure 5. Overlapped area of a track (red triangles in the headland area).

Track Sequence Optimization Stage

The selection of a certain turn type is based on the kinematic restrictions of the machine, the skills of the operator or the driver, and the available space in the headland area (Bochtis and Vougioukas, 2008). Ω-turns and T-turns turns are adopted only when Π-turn cannot be performed (fig. 6). The governing equations for computing the non-working distance travelled by a vehicle for the Π and Ω-turns under the assumption that the driver can perform a turn ideally with no slipping are given in equation 4 where i is the number of the current track, j is the number of the next selected track by the algorithm, $r_{\min}$ is the minimum turning radius of a vehicle, and w is the operating width (Bochtis and Vougioukas, 2008).

$$\Pi\left(\left|i-j\right|\right) = (\pi-2)r_{\min} + w\left|i-j\right| \tag{4a}$$

$$\Omega\left(\left|i-j\right|\right) = r_{\min}\left(3\pi - 4\sin^{-1}\left(\left(2r_{\min} + w\left|i-j\right|\right)/4r_{\min}\right)\right) \tag{4b}$$

$$d_{turn}\left(\left|i-j\right|\right) = \begin{cases}\Omega\left(\left|i-j\right|\right) & \left|i-j\right| < 2r_{\min}/w \\ \Pi\left(\left|i-j\right|\right) & \left|i-j\right| \geq 2r_{\min}/w\end{cases} \tag{4c}$$

When tracks align with headland paths by an angle ϕ in radians (fig. 7b) an additional non-working distance called the alignment distance, d_{align}, has to be computed using equation 3 and be added to the turning distance, d_{turn}, where w is the operating width (m), and t_c and t_n are the number of the current and next track, respectively.

$$d_{nw} = d_{align} + d_{turn} = (t_n - t_c)w\cot(\varphi) + d_{turn} \tag{5}$$

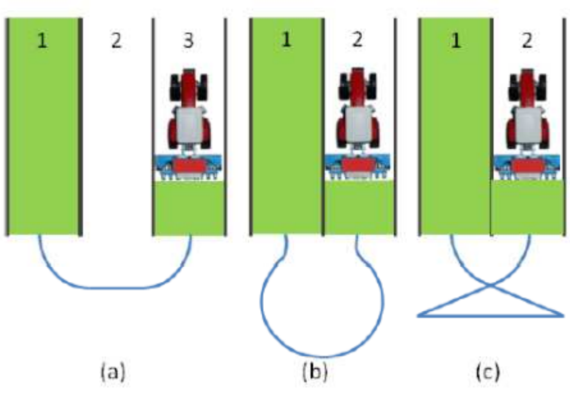

Figure 6. Examples of maneuvering types: (a) Π-turn, (b) Ω-turn, and (c) T-turn.

For the mathematical description of the objective function in this stage, a function introduced by Bochtis (2008) is implemented, namely the bijective (one-by-one and onto) function $p(\cdot): T \to T$, where $p(i)$ for any field track $i \in T$, returns the position of the i^{th} field track in the track traversal sequence in which the agricultural vehicle covers the field. The inverse function $p^{-1}(\cdot): T \to T$ gives the traversal sequence of the field tracks by the vehicle. Hence, the traversal sequence for the entire field is given by the permutation $\sigma = < p^{-1}(1), p^{-1}(2), ..., p^{-1}(|T|) >$ (detailed examples can be found in Bochtis and Vougioukas, 2008). Based on this description, the total distance travelled during the turnings at the headlands is given by:

$$J(\sigma) = \sum_{i=1}^{|T|-1} d_{turn}\left(\left|p^{-1}(i+1) - p^{-1}(i)\right|\right) \tag{6}$$

The B-pattern refers to the track sequence traversal that minimizes the total non-working travelled distance during turnings:

$$\sigma^* \to \min J \tag{7}$$

In the proposed method, as it will be explained in the following section, the set of tracks (T) is clustered into a number of n sub-sets which population $|T_k|, k = 1,...,n$ is

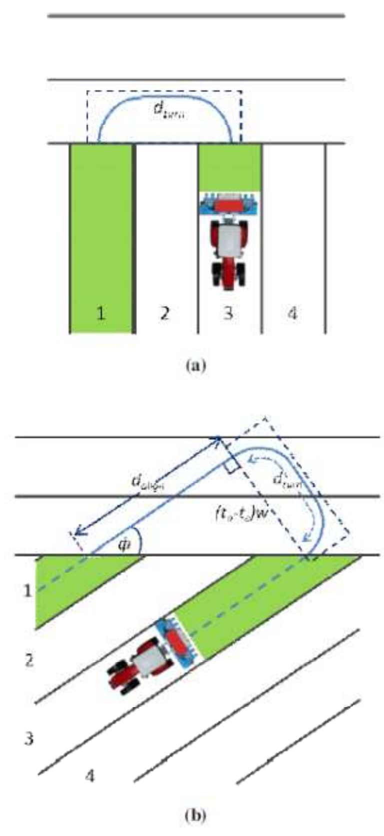

Figure 7. Non-working distance calculation for the case of Π-turn; (a) tracks are vertically aligned on the headland, and (b) tracks are aligned with an angle Φ with the headland.

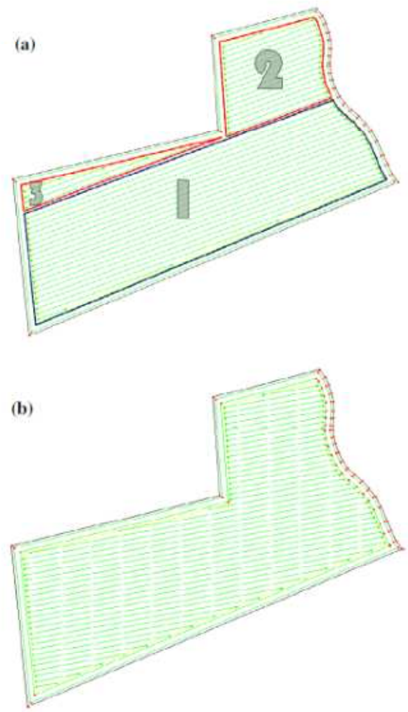

Figure 8. Track generation for a non-convex field where for the driving angle of 20° division into sub-regions is required (a) and for the driving angle of 10.14° field no division into sub-regions is required.

determined by algorithmic limitations. As a consequence, the B-pattern method is implemented in each block k separately providing the corresponding optimal track sequence within each block:

$$\sigma_k{}^* \rightarrow \min J_k, k = 1,...n \qquad (8)$$

Block Sequence Optimization Stage

From the optimization in the second stage for each block an entry and exit point are determined. Using the analogous bijective function for the description of the sequence of the sub-regions as in the case of tracks, $b(\cdot):\{1,...,n\} \rightarrow \{1,...,n\}$ and its inverse, the total distance for travelling between sub-regions can be written as:

$$B(\varepsilon) = \sum_{i=1}^{n-1} d_{trav}\left(\left| b^{-1}(i+1) - b^{-1}(i) \right| \right) \qquad (9)$$

where ε is the traversal sequence of the sub-regions and d_{trav} the distance for travelling from sub-region i to sub-region i+1.

The objective of the third stage is to find the optimal traversal sequence of the sub-regions:

$$\varepsilon^* \rightarrow \min B \qquad (10)$$

Solution Method

For the solution of the problem, a genetic algorithm was applied in order to combine these three stages without a global analytical description of the problem. According to the genetic algorithms principle, a population of solutions is maintained and a reproductive process allows parent solutions to be selected from the population. Offspring solutions which exhibit some of the characteristics of each parent are produced. The fitness of each solution can be related to the objective function value, analogously to biological processes where off-springs with relatively good fitness levels are more likely to survive and reproduce, with the expectation that the fitness levels throughout the population will improve as it evolves (Reeves, 1993; Baker and Ayechew, 2003).

The kickoff of any GA lies within the representation of each solution candidate or population member. Typically, this will be in the form of a string or chromosome. Individual positions within each chromosome are referred to as genes. Although binary strings have been favored by many researchers, some successful implementations of non-binary representations have been used (Bereta and Burczyński, 2007). In this article, both representations were used. For the driving angle optimization problem, an individual solution (i.e., chromosome) has one gene in the form of a binary string and each chromosome has values in the range [0° 180°]. In contrast, in the track sequencing optimization problem a non-binary representation was used, since an individual solution has the form of a string of the length $|T_k|, k = 1,..., n$ and each chromosome or solution candidate is a random permutation within $|T_k|$. Furthermore, computational requirements impose that the size of the clusters should not exceed a certain number of elements in order to assure that all the possible permutations within the cluster will be generated. This fact leads, in general, to sub-optimal solutions in the global problem of track sequencing, although the solution is optimal for each cluster.

Besides the algorithmic imposed clustering, there is also the case that the field geometry will require that the field be divided into blocks. For non-convex fields and for some driving angles tracks can potentially be divided or clustered into a number of blocks. As for an example, in figure 8a the driving angle requires the field to be divided into three sub-regions, while in figure 8b there are no sub-region divisions required.

The driving angle has been optimized by using the standard GA operators such as 'roulette wheel' selection, single point crossover, and mutation. In the second and third stages, new operators are used and will be discussed in the following sections. In the third stage, clusters are combined in the optimum order to obtain one sequence string. In this stage, a solution candidate is a string of length 2n. Bits 1, 3, …, 2n-1 have a value in the range of [1, n] representing the block sequence. Bits 2, 4, …, 2n are binary numbers of the values 1 for reversible blocks or 0 for non-reversible blocks. When a block is reversible, the sequence of tracks in this block is reversed

Selection Operator

Several selection operators were developed for numerical optimization in order to reduce the sampling error and improve calculation precision. In this article the roulette-wheel selection method was used in all of the optimization stages to select the fittest individuals from one generation to create the basis for the next generation (table 1).

Figure 9. The two test fields: (a) convex field and (b) non-convex field.

Crossover Operator

In the track sequencing problem, an invalid individual may be produced by using a single point consistent crossover, such that the single point crossover cannot be used directly (Bo et al., 2006). There are three crossover operators for a sequence representation: partially mapped crossover (PMX) (Gorges-Schleuter, 1985), order crossover (OX) (Davis, 1985), and cycle crossover (CX) (Oliver et al., 1987). PMX keeps the important similarities of parent and child generation. OX emphasizes the sequence order. CX reserves the absolute position of the elements in the parent generation. Oliver et al. (1987) indicated that OX is 11% better than PMX, and 15% better than CX. In track sequencing, the main problem is deciding the order of tracks in the solution string and specifically, avoiding duplication or missing of tracks. Therefore, the nonconforming sequential searching crossover, which is a version of OX, is used. The operator selects two parent chromosomes and a crossover position randomly. The codes of one individual before or after the randomly selected position are kept, and the total string of the other individual is being searched orderly, and those codes that do not exist in the reserved string are found. These codes are used to form a new individual for the next generation and have been successfully applied to the optimization of the process route sequencing problem (Bo et al., 2006). For the same reasons the nonconforming sequential searching crossover was also implemented in the third stage, while at the first stage a uniform crossover was used (table 1).

Mutation Operator

Flip bit mutation was adopted in the first stage, while inconsistent mutation was adopted in track sequencing and block sequencing problems (table 1). Some individuals of the next generation were selected randomly. Then, the positions of two codes in each individual were exchanged randomly to realize the mutation operation.

Termination Criterion

In the proposed approach, GAs terminate if any of the following criterion are fulfilled; when a pre-defined number of generations is reached or when the fitness value of the optimized solution generated after a pre-defined number of generations does not change.

Results

The applicability and effectiveness of the proposed approach is demonstrated by applying it in two field types, namely convex and non-convex fields. The convex field (i.e., field 1), shown in figure 9a is located at Foulum Research Centre, Denmark [56° 29' 28.29", 9° 34' 18.00"], and has an area of 7.93 ha. The second field, shown in figure 9b, is non-convex and is located in Northern part of Jutland, Denmark [56° 32' 45.94", 9° 30' 25.79"], and has an area of 17.2 ha.

The total time of a field operation was calculated based on the total effective travelled distance, which equals the total length of tracks and headland paths, assuming an average operating speed of 7.5 km/h and the total non-working travelled distance, assuming an average turning speed of 5 m/s for the case of Π-turns and of 2.5 m/s for the case of Ω-turns. The operating with was assumed to be equal to 9 m while the minimum turning radius of the vehicle was assumed to be equal to 6 m.

For the presented cases and in this article, a standard GA with population size 60, mutation and crossover probabilities 0.5 and 0.2, respectively, and a total number of generations 150 was used. The values of the probabilities have been determined based on the evaluation of the algorithmic performance in cases of intuitively-known solutions regarding simple-shaped fields, e.g. squared and rectangular.

Table 1. Operational parameters of each optimization stage.

Optimization Stage	Coding Type	Genetic Operators			Fitness Function
		Selection	Crossover	Mutation	
1st Stage Driving angle	Binary	Roulette-wheel	Uniform crossover	Flip bit mutation	Minimizing overlapped area
2nd Stage Track sequence	Real-valued	Roulette-wheel	Nonconforming sequential searching crossover	Inconsistent mutation	Minimizing total distance for headland turnings
3rd Stage Block sequence	Real-valued	Roulette-wheel	Nonconforming sequential searching crossover	Inconsistent mutation	Minimizing non-working travelled distance between blocks

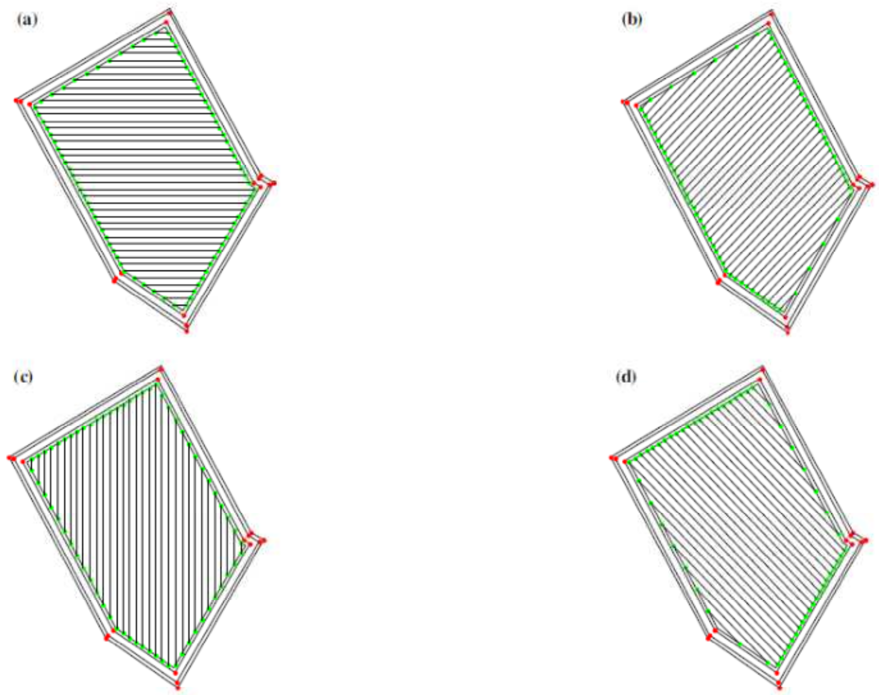

Figure 10. Field 1 geometrical representation for the selected driving angles of (a) 0°, (b) 45°, (c) 90°, and (d) 135°.

The algorithm run on a 2.4-GHz Intel Centrino Mobile Workstation with 2-GB RAM. The code was written on Matlab® 7.0 with Windows® XP. The use of the specific tools imposed the limitation of a maximum of 12 elements sets in the generation of permutations in the second stage, and thus the number of tracks per cluster was subsequently limited to 12.

Test Field 1

In order to show the impact of the driving angle on the operational parameters, the resulting parameters from the first stage (i.e., driving angle optimization stage) of the algorithm are given in table 2 (columns 2-6) for the selected driving angles of 0°, 45°, 90°, and 135° (using as reference direction the *x*-axis, fig. 10). Since these results are derived from the first stage of the algorithm they regard the conventional AB fieldwork pattern. The last row of table 1 gives the operational parameters for the optimized driving angle (with the minimized overlapped area) as it results from the first stage of the algorithm (fig. 11).

By applying the second and third stages (track sequence and block sequence optimization stages) of the algorithm, the operational time can be reduced from 1.25 h to 1.22 h. The field has been divided into four blocks, three each of 12 tracks and one block of one track. The B-patterns sequence within each block is given in table 3. The optimized sequence of the blocks is 1-2-3-4. The course of the total operation is schematically shown in figure 12.

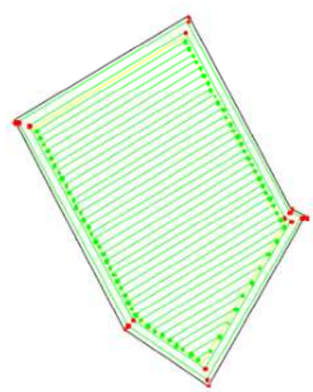

Figure 11. Field 1 geometrical representation for the optimized driving angle (29.98°).

Table 2. Operational parameters for selected and optimized driving angles for test field 1.

	Driving Angle (°)	No. of Tracks	Tracks Length (m)	Non-working Distance (m)	Overlapped Area (m^2)	Operational Time (h) Stage 1	Operational Time (h) Stage 2
Selected	0	41	6690	1514	2055	1.42	-
	45	37	6690	1347	1774	1.37	-
	90	33	6692	2904	3169	1.54	-
	135	29	6686	1159	2705	1.28	-
Optimized	29.98	37	6684	1218	902	1.35	1.25

Table 3. The produced optimized sequence of tracks within the four blocks.

Block	Optimized Track Sequence											
1	12	8	6	9	1	3	5	2	4	7	11	10
2	18	23	20	19	17	21	24	22	16	13	14	15
3	25	31	29	32	30	27	28	26	36	34	33	35
4	37	x	x	X	x	x	x	x	x	x	x	x

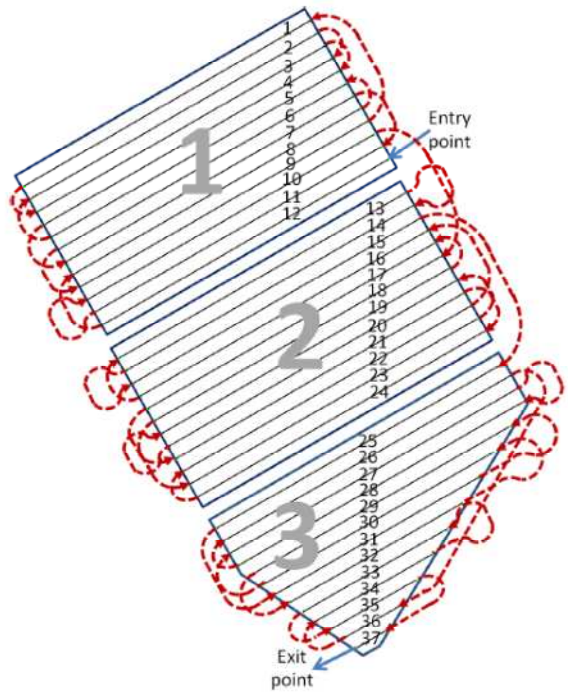

Figure 12. The course of the total operation in terms of tracks and blocks sequences in field 1.

The computational time was 7.36 min for the first stage, 11.02 min for the second stage, and 0.43 min for the third stage.

Test Field 2

The resulting parameters from the first-stage (i.e., driving angle optimization stage) of the algorithm are given in table 4 (columns 2-6) for the selected driving angles of 0°, 45°, 90°, and 135° (fig. 13). The last row of table 3 gives the operational parameters for the optimized driving angle (fig. 14).

By applying the second and third stages (i.e., track sequence and block sequence optimization stages) of the algorithm the operational time can be reduced from 2.82 to 2.66 h. The field has been divided into six blocks, five each of 12 tracks and one block of 11 tracks. The B-patterns sequence within each block is given in table 5. The computational time was 9.05 min for the first stage, 13.37 min for the second stage, and 1.30 min for the third stage.

Discussion

The solutions provided by the presented algorithmic approach are sub-optimal in terms of non-working travelled distance. This stems from the clustering of the field tracks into groups of limited number of population and also from the fact that the sequence of the clusters is viewed as a separate problem. Regarding the limitation in the population of the clustered sets, a relaxation can be applied by invoking heuristics or randomized methods for the selection of the candidate solutions. However, there is a trade-off between relaxation that results in larger search domains and the degree of the optimality of the final solution that has to be considered.

In contrast, the algorithmic approach for the generation of B-patterns view the tracks sequencing and clusters sequencing as a coupled optimization problem, and furthermore, the clusters are generated following only geometrical constraints (i.e. in the case of non-convex fields) and not computational constraints. It has to be noted that in the mentioned approach there are cases which involve solutions according to which one sub-region (corresponding to a cluster of tracks) might be partially covered before continuing to another sub-region, and the reaming part of the first mentioned sub-region will be covered at a later time following the optimal sequencing (see for example a case in Bochtis and Oksanen, 2009).

Using the algorithm developed in Bochtis (2008), a modified Clarke-Wright savings heuristic algorithm for the solution of binary optimization problems (implemented in C++), the generated optimal track sequences involve non-working distances of 1,017 and 1,938 m for fields 1 and 2, respectively, (this regards the driving directions that are the outputs of the first stage of the presented method) resulting in a reduction of the total operating time of 12.4% and 13.1% (1.09 h and 2.45 h) for fields 1 and 2, respectively, compared to the one derived from the implementation of the presented method (1.25 h and 2.82 h). It also has to be noted that the

Table 4. Operational parameters for selected and optimized driving angles for test field 2.

	Driving Angle (°)	Number of Rows	Rows Length (m)	Non-working Distance (m)	Overlapped/Missed Area (m^2)	Operational Time (h)	
						Stage 1	Stage 2
Standard	0	57	15204	1862	2361.84	2.80	–
	45	61	17286	1901	2320.72	3.00	–
	90	69	15653	2917	3523.43	3.12	–
	135	79	15212	2298	2993.45	3.07	–
Optimized	113.86	74	15475	1783	2407.14	2.96	2.82

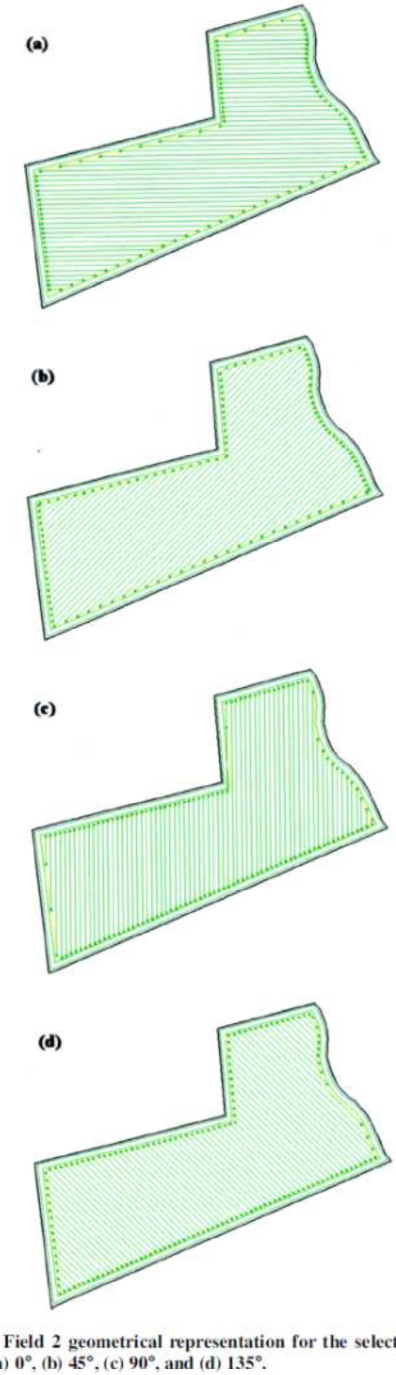

Figure 13. Field 2 geometrical representation for the selected driving angles of (a) 0°, (b) 45°, (c) 90°, and (d) 135°.

computational times of the heuristic algorithm were 0.22 and 3.8 s for fields 1 and 2, respectively. These times are significantly faster than the required computational times of the GA implemented in the presented method.

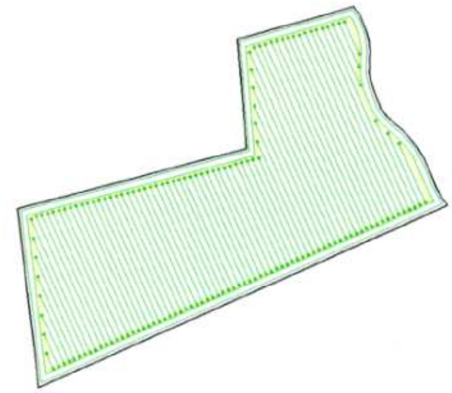

Figure 14. Field 2 geometrical representation for the optimized driving angle (113.86°).

Nevertheless, the disadvantages the presented algorithmic approach in terms of high computation times and sub-optimality are countered by the fact that it is an integrated approach combining three internally connected stages. The connection of the first stage of the algorithm (i.e. optimized driving angle generation) with a fast algorithmic approach providing optimal B-patterns, as well as the development of a multiple-criterion approach (both overlapped area and non-working distance) as a coupled optimization problem, are considered issues of future researching.

Additionally, an open issue for further research is the removal of the assumption regarding the adoption of the same driving direction within each sub-region of the field (as stated in the Assumptions section).

Conclusions

This article presented a three-stage GA-based approach that combines two recently developed methods related to the field area coverage problem, namely a method for generating a field geometrical representation and a method for the optimization of the routing of agricultural vehicles within this geometrically-defined world. The criterion for the first stage is the minimization of the overlapped area, while the criterion in the second and third stages is the minimization of the non-working distance.

In its current state, the developed approach can provide optimized solutions in terms of overlapped area as well as total non-working travelled distance. Still these sub-optimal solutions proved more efficient compared to the conventional field work patterns. Improving this sub-optimality, as well as reducing the computation times of the method in order to be feasible for real-time implantation, are considered issues of future researching.

Table 5. The produced optimized sequence of tracks within the six blocks.

Block	Optimized Track Sequence										
1	5	1	3	4	2	7	12	10	11	8	6	9
2	18	14	19	15	17	23	22	20	24	21	16	13
3	26	28	32	27	25	33	36	34	30	35	31	29
4	43	40	42	47	45	46	48	44	39	37	41	38
5	55	60	58	52	54	57	59	49	50	53	51	56
6	62	64	70	67	71	66	69	65	68	63	61	x

References

Ansorge, D., and R. J. Godwin. 2007. The effect of tyres and a rubber track at high axle loads on soil compaction: Part 1. Single axle studies. *Biosyst. Eng.* 98(1): 115-126.

Baker, B. M., and M. A. Ayechew. 2003. A genetic algorithm for the vehicle routing problem. *Comput. Oper. Res.* 30(5): 787-800.

Benson, E. R., A. C. Hansen, J. F. Reid, B. L. Warman, and M. A. Brand 2002. Development of an in-field grain handling simulation in ARENA. ASAE Paper No. 023104. St. Joseph, Mich.: ASAE.

Bereta, M., and T. Burczyński 2007. Comparing binary and real-valued coding in hybrid immune algorithm for feature selection of ECG signals. *Eng. Appl. Artif. Intel.* 20(5): 571-585.

Bo, Z. W., L. Z. Hua, and Z. G. Yu. 2006. Optimization of process route by genetic algorithms. *Robotics and Computer-Integrated Manufacturing* 22(2): 180-188.

Bochtis, D. 2008. Planning and control of a fleet of agricultural machines for optimal management of field operations. Ph.D. thesis. Thessaloniki, Greece: Faculty of Agriculture, Department of Agricultural Engineering, Aristotle University.

Bochtis, D. D., and S. G. Vougioukas. 2008. Minimizing the non-working distance travelled by machines operating in a headland field pattern. *Biosyst. Eng.* 101(1): 1-12.

Bochtis, D. D., and T. Oksanen. 2009. Combined coverage path planning for field operations. In *Proc. Joint Intl. Agric. Conf., JIAC 2009, Precision Agriculture 09*, 521-527. E. J. Van Henten, D. Goense, and C. Lokhorst, eds. Netherlands: Wageningen.

Bochtis, D. D., S. G. Vougioukas, and H. W. Griepentrog. 2009. A mission planner for an autonomous tractor. *Trans. ASABE* 52(5): 1429-1440.

Bochtis, D. D., and C. G. Sørensen. 2009. The vehicle routing problem in field logistics: Part I. *Biosyst. Eng* . 104(4): 447-457.

Bochtis, D. D., S. G. Vougioukas, C. G. Sørensen, I. A. Hammed, and T. Oksanen. 2010. Fleet Management: Assessment of Potential Savings. Report, EU project: Integration of Farm Management Information Systems to support real-time management decisions and compliance of management standards, WP 3: Analysis Influences of robotics and biofuels on economic and energetic efficiencies of farm production (retrived from http://www.futurefarm.eu/system/files/FFD6.3.2_Fleet_Management_Assessment_Final.pdf).

Davis, L. 1985. Applying adaptive algorithms to epistatic domains. In *Proc. of the Ninth Intl. Joint Conf. on Artificial Intelligence*, San Mateo, California, USA: Morgan Kaufmann Publishers Inc., 162-164.

Gorges-Schleuter, M. 1985. ASPARAGOS An asynchronous parallel genetic optimization strategy. In *Proc. of the 1st Intl. Conf. on Genetic Algorithms*, 422-427. Hillsadle, N.J.: Lawrence Erlbaum Associate.

Hameed, I. A., D. D. Bochtis, M. Nørremark, and C. G. Sørensen. 2010. Automated generation of guidance lines for operational field planning. *Biosyst. Eng* . 107(4): 294-306.

Hansen, A. C., R. H. Hornbaker, and Q. Zhang. 2003. Monitoring and analysis of in-field grain handling operations. ASAE Paper No 701P1103e. In *Proc. of Intl. Conf. on Crop Harvesting*. St. Joseph, Mich.: ASAE.

Hunt, D. 2001. *Farm Power and Machinery Management*. 10th ed. Ames, Iowa: Iowa State Press.

Jin, J., and L. Tang. 2010. Optimal coverage path planning for arable farming on 2D surfaces. *Trans. ASABE* 53(1): 283-295.

Jin, J., and L. Tang. 2011. Coverage path planning on three-dimensional terrain for arable farming. *J. Field Robot.* 28(3): 424–440.

Keller, T. 2005. A model for the prediction of the contact area and the distribution of perpendicular stress below agricultural tyres from readily available tyre parameters. *Biosyst. Eng.* 92(1): 85-96.

Oksanen, T., and A. Visala. 2009. Coverage path planning algorithms for agricultural field machines. *J. Field Robot*. 26(8): 651-668.

Oliver, I. M., D. J. Smith, and J. R. C. Holland. 1987. A study of permutation crossover operators on the travelling salesman problem. *Proc. of the 2nd Intl. Conf. on Genetic Algorithms*, 224-230. Hillsadle, N.J.: Lawrence Erlbaum Associate.

Reeves, C. R. 1993. *Modern Heuristic Techniques for Combinatorial Problems*. Oxford: Blackwell Scientific Press.

Sørensen, C. G., and V. Nielsen. 2005. Operational analyses and model comparison of machinery systems for reduced tillage. *Biosyst. Eng*. 92(2): 143-155.

Taylor, R. K., M. D. Schrock, and S. A. Staggenborg. 2002. Extracting machinery management information from GPS data. ASAE Paper No. 0210008. St. Joseph, Mich.: ASAE.

Witney, B. 1996. *Choosing and Using Farm Machines*. Edinburgh, Scotland, UK: Land Technology Ltd.

Chapter 4

An Object Oriented Model for Simulating Agricultural In-Field Machinery Activities

Hameed, I. A., Bochtis, D. D., Sørensen, C. G., & Vougioukas, S.

Computers and Electronics in Agriculture, 2012, 81(1), 24–32.

Computers and Electronics in Agriculture 81 (2012) 24–32

Contents lists available at SciVerse ScienceDirect

Computers and Electronics in Agriculture

journal homepage: www.elsevier.com/locate/compag

An object-oriented model for simulating agricultural in-field machinery activities

I.A. Hameed [a], D.D. Bochtis [a], C.G. Sørensen [a,*], S. Vougioukas [b]

[a] University of Aarhus, Faculty of Science and Technology, Dept. of Engineering, Blichers Allé 20, P.O. Box 50, 8830 Tjele, Denmark
[b] Aristotle University of Thessaloniki, Agricultural Engineering Laboratory, Dept. of Hydraulics, Soil Science and Agricultural Engineering, Egnatias 156, 54124 Thessaloniki, Greece

ARTICLE INFO

Article history:
Received 5 September 2011
Received in revised form 25 October 2011
Accepted 4 November 2011

Keywords:
DSS
Field efficiency
Machinery management

ABSTRACT

Field operations planning is essential for the operational efficiency in terms of time and cost, especially in complex operations involving capacity constraints and cooperating units. In order to deal with such type of planning problems an object-oriented simulation model which simulates in detail in-field machine activities during the execution phase, was developed and applied. The developed simulation model regards the material input operations with capacity constraints, where a quantity of a "commodity" is transported by the machine and is distributed in the field area. The case of the organic fertilizing application was used as the basis for the description of the object oriented model involving the description of all related programming entities (i.e., classes, attributes, and methods). Combined state and activity diagrams were provided as the basic elements of the simulation model. It was shown that the simulation model provides all the key operational parameters necessary for the evaluation of a selected scenario. This makes it feasible the use of the simulation model as an integral part of a decision support system for advising farmers about in-field operational decisions (e.g., traffic system, driving direction, refilling position) and machinery dimensioning (e.g., tank capacity, operating width, etc.).

1. Introduction

In last few decades, several computer simulation models have been developed that can be employed for analyzing complex agricultural processes and operations. These applications, like any simulation model, depict the state of the system over time by adhering to given assumptions and inputs providing the possibility to assess a number of selected scenarios across a large range of alternatives. Examples of developed agricultural simulation models include whole farm models (Sherlock et al., 1997; Shaffer et al., 2000; Post, 2002; Neal et al., 2005a,b; Blazy et al., 2010), dairy farm models (Vayssières et al., 2009a,b; García-Martínez et al., 2011) crop simulation models (Matthews et al., 2000; Graves et al., 2002), soil models (Kwon and Hudson, 2010; Keller et al., 2007), models for estimating greenhouse gas emissions from farm production (Crosson et al., 2011; Drouet et al., 2011), etc.

Regarding field operations a number of advanced simulation models have been introduced. Arjona et al. (2001) developed a discrete event simulation model of the harvesting and transportation systems for a sugarcane plantation. Benson et al. (2002) developed a model for the simulation of harvesting and in-field grain handling operations, built on a manufacturing simulation programming language. Dyer and Desjardins (2003) introduced a computer simulation of farm power requirements, machine hours and fuel consumption, while Sørensen (2003) developed a model for machinery performance and logistics in the case of manure application and Sørensen and Nielsen (2005) built task models predicting operational performance for tillage operations de Toro and Hansson (2004) developed a discrete event simulation model for field machinery operations able to analyze machinery performance based on daily status of soil workability. Busato et al. (2007) developed a discrete event simulation model for a wheat harvesting system able to determine the optimal field bin allocations. Guan et al. (2008) introduced hybrid Petri nets into modelling of farm work flow in agricultural production able to exactly describe the farming process and optimally reallocating resources in the presence of uncertainties. Kumar and Pandey (2009) developed a model Visual Basic programming language for the prediction of tractor performance of two-wheel-drive (2WD) tractors.

Nevertheless, in the above mentioned research efforts there is a lack in field operation models that simulates in detail in-field machine activities during the execution phase (for example the path followed by the machine during a specific headland turning) and/or taking into account geometrical attributes of the operations environment that significantly can affect the productivity of the selected operational system (for example the in-field driving direction, the exact field shape, etc.). The objective of this paper is to build a simulation model that accommodates the above mentioned requirements. Furthermore, the proposed simulation model will specifically be aimed at material input field operations with capacity constraints as the most complex field operations, where the

* Corresponding author. Tel.: +45 84157638.
E-mail address: Claus.Soerensen@agrsci.dk (C.G. Sørensen).

0168-1699/$ - see front matter © 2011 Elsevier B.V. All rights reserved.
doi:10.1016/j.compag.2011.11.003

Table 1
Definitions of the system states.

State	Definition
$\overline{Refilling}$	The AU enters a $\overline{Refilling}$ state when its tank is getting empty and exits it when the re-filling process is completed
$\overline{Application}$	The AU enters the $\overline{Application}$ state immediately after reaching the location where the application is resumed and exits it when its tank is getting empty
$\overline{Resuming}$	The AU enters the $\overline{Resuming}$ state immediately after the completion of the refilling process in the RU location and exits it when it reaches the location where the application is resumed

agricultural vehicle has to execute a number of routes in order to complete the operation (e.g., seeding, fertilizing, and spraying).

2. System description

The developed simulation model regards the material input operations with capacity constraints. The material input operations are defined as the operations where a quantity of a "commodity" is transported by the machine and is distributed in the field area (e.g., seed, spraying solution or fertilizer) (Bochtis and Sørensen, 2009). The case of the organic fertilizing will be used as the basis for the description of the model.

The developed simulation model is an object-oriented implementation of the distance-based mathematical model developed by Bochtis et al. (2009). The developed model was based on the mathematical formulation of the discrete events regarding the motion of the machines involved in a material handling field operation. The mathematical approach of the model covers operations involving in-field transports in controlled traffic farming[1] (CTF) system and in the conventional un-controlled traffic farming (UCTF) system by relaxing the traffic constraints in the model. The simulation model is developed in Matlab® programming environment.

The following symbols are used throughout the paper in order to distinguish different kind of entities:

- Input attributes as: *InputAttribute* → (e.g., *FieldOuterBoundary* →, *DrivingAngle* →, etc.).
- Output attributes as: *OutputAttribute* (e.g., → *FieldInnerBoundary*, etc.).
- Methods as: |*Method*| (e.g., |*CreateField*|, etc.).
- Classes as $Class^{CL}$ (e.g., $ApplicationUnit^{CL}$, etc.).
- States as: $\overline{State}$ (e.g., $\overline{Application}$, etc.).
- Events as $\breve{Event}$ (e.g., $\breve{Apply}$, etc.).

2.1. States and events in the system

As the most cases of material input operations, in organic fertilizing a number of routes are required since a full load carried by the application unit (AU) is generally not sufficient for full area coverage of a normal-sized field. A "route" is designated as an operational cycle consisting of the following part operations carried out by the AU: (a) filling the tanker at the location of the refilling unit (RU) and driving from that location to the position where the application is commenced or resumed, (b) applying the carried material to the field, and (c) driving back to the location of the RU for a new tanker re-filling. In order to describe in the system these physical processes and operations a set of states and events are identified in Tables 1 and 2. Transitions of an object from a current state to a new state are caused by events. For example, $\breve{EmptyTank}$ is an event which triggers the transition from $\overline{Application}$ state into $\overline{Refilling}$ state.

[1] The CTF system is a specialised in-field traffic system where, according to its principles, permanent parallel wheel tracks are created within the field area, eliminating completely soil compaction from the wheels within the cropped area (Tullberg et al., 2007). The term UCTF refers to the traditional in-field traffic system where field machines work in parallel field-work tracks which are not pre-determined.

Table 2
Definitions of the system events.

Event	Definition
$\breve{Apply}$	It triggers the transition from $\overline{Resuming}$ state to $\overline{Application}$ state
$\breve{Refill}$	It triggers the transition from $\overline{Application}$ state to $\overline{Refilling}$ state
$\breve{Resume}$	It triggers the transition from $\overline{Refilling}$ state to $\overline{Resuming}$ state
$\breve{EmptyTank}$	It triggers the transition from $\overline{Application}$ state to $\overline{Refilling}$ state
$\breve{EndOfTrack}$	It triggers the completion of a current track
$\breve{NextTrack}$	It triggers turning from a current to a next track

2.2. The object-oriented program entities

The benefits realized from using object-oriented programming approach include simplifying system complexity and increasing flexibility of the simulation model. In object-oriented programming, the world of interest is described as a collection of object-classes each with a set of attributes and items, with a mechanism by which they can communicate with each other and generate new objects (Register, 2007). This representation technique facilitates development, utilization and maintenance of the system.

2.2.1. Basic classes

The developed object oriented model consists of four basic classes;

- the field class ($Field^{CL}$),
- the application unit class ($ApplicationUnit^{CL}$),
- the refilling unit class ($RefillingUnit^{CL}$) and
- the simulator engine class ($SimulatorEngine^{CL}$).

Each class is characterized by a set of properties, attributes, and methods. Methods are developed to construct and deconstruct an instance of a class, and to provide an interface with the object to initialize, update, access, print or visualize specific attributes. Other methods are used to instruct and control a class to behave as it is required. When the simulation stops, some methods will be called to destroy or deconstruct the objects in order to free memory for other computing operations. A detailed description of each class will be given in the following.

2.2.1.1. Field class. An object of the $Field^{CL}$ is used to represent geometrically a field in the 2D plane. Some predefined sub-classes are used, such as polygon sub-class $Polygon^{CL}$ which is used to represent a closed set of points in the UTM coordinate system and the line segment sub-class $lineSegment^{CL}$ which is used to represent a line segment connecting two points (Hameed et al., 2010). In $Field^{CL}$, headland paths are represented using an array of $Polygon^{CL}$ objects and the field tracks are defined using an array of $lineSegment^{CL}$ objects.

$Field^{CL}$ is characterized by the following input and output attributes, and methods:

Input attributes:

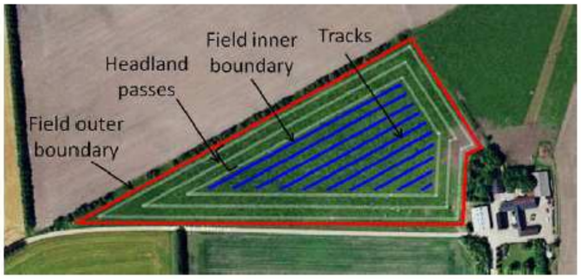

Fig. 1. A typical field representation.

(1) Field outer boundary, *FieldOuterBoundary* →, represented as an object of *Polygon*^{CL} and consists of a set of 2D points arranged in clock-wise direction (see the red polygon in Fig. 1).
(2) Driving angle, *DrivingAngle* →, is defined as the angle between the driving direction and *x*-axis of the 2D coordination system used.
(3) Track sequence, *TrackSequence* →, is the sequence of traversing the tracks representing the field-work pattern.
(4) Number of headland passes, *NumberOfHeadlandPasses* →, is the required number of headland passes executed by the AU after completing the operation in the main field area.
(5) Operating width, *OperatingWidth* →, of the applicator.

Output attributes:

(1) → *FieldInnerBoundary*, is an object of '*Polygon*^{CL}' consisting of a set of 2D points arranged in clock-wise direction which encloses the main field area (corresponding to the net area to be covered by the field tracks, as shown in Fig. 1).
(2) → *HeadlandPasses*, are defined as an array of objects of polygon sub-class '*Polygon*^{CL}'.
(3) → *Tracks*, are defined as an array of objects of the line segment sub-class *lineSegment*^{CL}. Field tracks are generated parallel to the driving direction.
(4) → *FieldArea* is the area enclosed by the field outer boundary (*FieldOuterBoundary* →).
(5) → *LengthOfFieldTracks*, is the total length of the field tracks.
(6) → *HeadlandLength*, is the total length of the headland passes.
(7) → *TrackInnerPoint*, is used to mark the last covered point in a track. A track has a → *TrackInnerPoint* if it is partially covered.
(8) → *ResumeTrack*, is the last non-fully covered track in a AU route.

Methods:

(1) |*CreateField*|, which constructs an instance of the field class *Field*^{CL} initializing the object attributes and calling methods to load the geometrical field data, generate headland passes and field tracks, visualize them, and saving the relevant waypoints into specific files.
(2) |*LoadField*|, which imports field description from a shape file.
(3) |*GenerateHeadlnad*|, which generates headland passes based on the *OperatingWidth* →, *NumberOfHeadlandPaths* →, *FieldOuterBoundary* →, *BoundaryOfInFieldObstacle* →, and *NumberOfHeadlandPaths* → attributes. The output is an array of objects of type polygon *Polygon*^{CL} representing headland paths.
(4) |*GenerateTracks*|, which generates equidistant lines, according to the *OperatingWidth* →, parallel to the selected driving direction.
(5) |*SharpEdgeFilter*|, which removes potential sharp edges from the generated headland pass (Hameed et al., 2010).
(6) |*LoopFilter*|, which removes potential loops from the generated headland pass (Hameed et al., 2010).
(7) |*CaculateFieldArea*|, which calculates the field area.
(8) |*CreateTrackInnerPoint*|, which is used to create a → *TrackInnerPoint*. An AU calls this method when its tank becomes empty to mark the last covered point in that track.
(9) |*CheckTrackInnerPoint*|, which is used to check whether a track has a → *TrackInnerPoint* or not.
(10) |*EndOfTrack*|, which identifies the end point of the current track in order for the AU to exit a track and enter the next one.
(11) |*SaveResumeTrack*|, which saves a → *ResumeTrack*.
(12) |*ShowField*|, which provides a visual map of the field in 2D plot diagram.
(13) |*SaveField*|, which exports field headland passes and tracks into a text, shape, or xml file.
(14) |*DestructField*|, which destroys Field objects to free memory space.

A typical field representation is shown in Fig. 1. Three headland paths and tracks parallel to the longest edge of the field are generated for 10 m operating width.

2.2.1.2. Application unit class.
Input attributes:

(1) Driving speed: there are three different speeds in regular farming practices defined as follows:
 (a) *FullTankSpeed* →, when the AU is in transport mode and when the tank is full.
 (b) *EmptyTankSpeed* →, when the AU is in a transport mode and when its tank is empty.
 (c) *ApplicationSpeed* →, when the AU is in a application mode.
(2) $r_{\min}$ → . which is the minimum turning radius of AU.
(3) *TankCapacity* →, which is the total tank capacity of the AU.
(4) *ApplicationRate* →, which is the application rate of the AU.

Output attributes:

(1) → *OperationState*, which describes the operational states of the vehicle. A flag is used to differentiate between each different state ($\overline{\textit{Application}}$ state (−1), $\overline{\textit{Resume}}$ state (0) and $\overline{\textit{Refilling}}$ state (+1), where states are defined in the next section).
(2) → *EffectiveTraveledDistance*, which is the total distance covered by the AU during the application (i.e., $\overline{\textit{Application}}$ state).
(3) → *HeadlandTravelledDistance*, which is the total distance that AU travels in the headland area for reaching the RU and returning back to the resume track (i.e., → *ResumeTrack*).
(4) → *TransportDistance*, which is the transport distance travelled in a track without application.
(5) → *TurningDistance*, which is the distance travelled while turning.

Methods:

(1) |*CreateVehicle*|, which creates an instance of the AU class and calls necessary methods to initialize and update its attributes.

(2) |*Refill*|, which refills AU's tank to the tank capacity, *TankCapacity* →.
(3) |*Apply*|, which is called by an AU object when it applies.
(4) |*TravelInTrack*|, which updates the AU's position as it moves from its current location to a certain destination on the same track and also updates attributes such as → *EffectiveTraveledDistance*.
(5) |*TravelInHeadland*|, which updates the AU's position as it moves over headland passes. It is called when an AU is in the transport mode or in the application mode when covering the headland area. It updates distances such as → *HeadlandTravelledDistance*.
(6) |*Turn2EnterTrack*|, which updates the position of an AU when attempting to enter a track from a headland or from a previous track. It updates the → *TurningDistance*.
(7) |*Turn2EnterHeadland*|, which enables an AU to make a turn to leave its current headland pass and enter to the next uncovered headland pass.
(8) |*AtRUHeadland*|, which checks if the AU reached the RU's location.
(9) |*AtTrackInnerPoint*|, which checks if the AU reaches a → *TrackInnerPoint*.
(10) |*EmptyTank*|, which checks if the AU's tank becomes empty.
(11) |*NextTrack*|, which checks if there is a next track in the *TrackSequence* →.
(12) |*DestructVehicle*|, which eliminates the AU object when its job is accomplished.

2.2.1.3. Refilling unit class. The RU can be located at a fixed location or can move over the headland area in order to reach the AU near the track being operated. RU class contains the following attributes and methods:

Input attributes:

(1) *DrivingSpeedOfRU* →, which is the in-field driving speed of the RU.
(2) *LocationOfRU* →, which is an array of 2D points which represent the potential refilling points, all located in the headland area.
(3) *RefillType* →, 0 for static refilling and 1 for dynamic refilling.

Output attribute:

(1) → *RUHeadlandTravelledDistance*, which is the accumulated distance travelled in the headland area.

Method:

(1) |*CreateVehicle*|, which creates an instance of the RU class and calls necessary methods to initialize and update its attributes.
(2) |*TravelInHeadland*|, which updates the RU position over headland.
(3) |*DestructVehicle*|, which is a method used to eliminate the RU object when its job is accomplished in order to free memory space for other computational tasks.

2.2.1.4. Simulator engine class. The $SimulatorEngine^{CL}$ is the core of the simulation model which controls and coordinates the behaviour of the different objects in order to carry out the operational tasks. Moreover, it is responsible for recording and updating all relevant data. It also contains the functionality which supports either CTF or UCTF system. $SimulatorEngine^{CL}$ contains the following attributes and methods:

Output attributes:

(1) → *TotalOperationalTime*, which is the total time of the field operation.
(2) → *FieldEfficency*, which is the ratio of the in-field effective travelled distance to the total travelled distance.

Methods:

(1) |*Sim*|, which creates the $SimulatorEngine^{CL}$ by calling necessary methods to initialize its attributes. It also calls constructors of other objects and destructors when the operation is accomplished.
(2) |*Init*|, which initializes the attributes of the $SimulatorEngine^{CL}$.
(3) |*FindShortestPathToRU*|, which finds the shortest path between the AU's location to the RU's location. It returns a sequence of points in 2D coordinates representing that path.
(4) |*HeadingToRU*|, which checks if the AU is heading towards the RU.
(5) |*Run*|, which initiates the execution of the $SimulatorEngine^{CL}$. Its execution terminates when all field tracks and headland passes are fully covered.
(6) '|*DestructSE*| ': is a method used to eliminate the SE when its job is accomplished.

2.3. Strategy of field coverage

The developed simulation model covers a field in two stages. In the first stage, field tracks are covered and in the second stage headland passes are covered. State diagrams combined with activity diagrams are used to describe the behaviour of the system by describing all of the possible states of an object as events occur.

2.3.1. Traversing the field tracks

It is assumed that when the operation commences, the AU enters the $\overline{Resuming}$ state. In $\overline{Resuming}$ state the AU moves in a headland pass and turns to enter the first track according to the *TrackSequence* →. Once an AU enters a track, it by default searches for the → *TrackInnerPoint*. If there is no → *TrackInnerPoint*, it leaves the $\overline{Resuming}$ state and enters the $\overline{Application}$ state; otherwise, it starts moving in this track until it reaches the → *TrackInnerPoint* of the current track and then enters the $\overline{Application}$ state. In $\overline{Application}$ state, an AU executes two methods simultaneously, namely, the |*TravelInTrack*| and the |*Apply*| methods. An AU continues executing these methods until it reaches the end of this track (|*EndOfTrack*|). If the tank becomes empty before reaching the |*EndOfTrack*|, an AU calls the |*CreateTrackInnerPoint*| method to mark how far it went in covering this track. AU then saves this track as a resume track (i.e., → *ResumeTrack*) and exits the $\overline{Application}$ state and enters the $\overline{Refilling}$ state. If the AU can reach |*EndOfTrack*| method, it checks its tank capacity and if it is not empty it will check if there are more uncovered tracks in the sequence vector (i.e., *TrackSequence* →) and then turns to enter a new track to continue in $\overline{Application}$ state; otherwise, it exits traversing field tracks and starts in traversing headland passes. An AU continuously alternates between these states until the all field tracks are being traversed. A combined state and activity diagram for traversing the field tracks is shown in Fig. 2.

2.3.2. Traversing headland passes

This process starts immediately after finishing the traversing of the field tracks. If the AU tank is empty after traversing all field tracks, the AU goes immediately to $\overline{Refilling}$ state in order to refill its tank; otherwise, it starts application. A headland pass is treated as a normal field track. At any point of the current headland pass, if the AU's tank becomes empty, the AU creates a → *TrackInnerPoint*

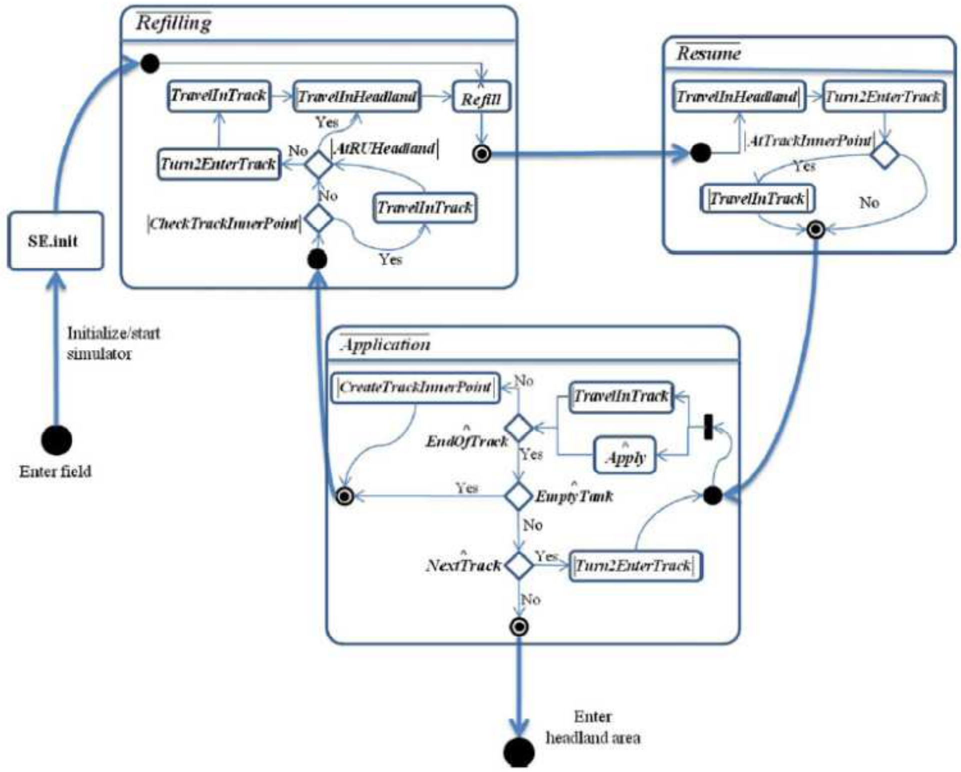

Fig. 2. Combined state and activity diagram of the AU class for covering field tracks.

in order to mark to how far the current headland pass has been covered and then exits the $\overline{\textit{Application}}$ state into a $\overline{\textit{Refilling}}$ state creating a middle point. In $\overline{\textit{Resuming}}$ state, the AU returns to the created → *TrackInnerPoint* to ensure that a headland pass is fully covered. If the AU reaches the end of a headland pass with nonempty tank, it turns to enter the next headland pass using |*Turn2EnterHeadland*| and resumes application. When AU's tank becomes empty, it enters the $\overline{\textit{Refilling}}$ state and calls the |*FindShortestPathToRU*| method. If the AU is heading towards the RU (i.e., |*HeadingToRU*|), it keeps moving in the same direction until reaching the RU's location, otherwise, it turns in the current headland path using the |*Turn2EnterHeadland*| method in order to move in the opposite direction. Upon reaching the RU's location, an AU refills/unload its tank and calls the |*Turn2EnterHeadland*| method in order to change its heading angle towards the → *TrackInnerPoint* again and then starts moving in that headland pass to reach it. Upon reaching the → *TrackInnerPoint*, the AU resumes application and this cycle of operations is continuously repeated until there are no more headland passes to cover. A combined state and activity diagram of this process is shown in Fig. 3.

3. Simulation result and discussion

In Section 3.1, the functionality of the simulation model will be demonstrated by applying it to a selected field. In Section 3.2, in order to demonstrate how the simulation model can be used as a decision support system it will be applied to the same field using different combinations of input parameters.

3.1. Demonstration example

The simulation model is applied to a selected field of 6.57 ha area shown in Fig. 4 (N 55° 32′ 10.00″, E 10° 4′ 1.96″). The geometrical representation of the field for an operating width of 9 m, a driving angle of −12.5°, and a single headland pass is shown in Fig. 5. The specific driving angle has been selected to produce tracks similar to what operators usually chose in this field. In this demonstration example, the RU is located stationary at the left top corner of the field. The input parameters are given in Table 3. The values of these parameters are based on recordings of related field operations. It is assumed that wheat is grown in the field. The threshold for Nitrogen application in wheat field is 170 kg N/ha per year (Danish Food Industry Agency, 2011), which is translated into a 0.0043 m^3/m^2 application rate (assuming 4 kg N/m^3 of applied material).

The course of the tanker volume is shown in Fig. 6 where the AU is loaded 9 times in total; 7 times to traverse field tracks and 2 times to traverse headland area. A selected route of the total operation, namely the route corresponding to the second refill of the AU is used to cover tracks 7, 8 and 9 and is shown in Fig. 7(a). The route of the AU corresponding to refill number 4 is shown in Fig. 7(b). The route of the AU corresponding to refill number 8 where a headland pass is being covered is shown in Fig. 7(c). The output information produced by the simulator model for the specific input values defined in Table 3 is given in Table 4. Field efficiency in this paper is defined as the ratio of the effective travelled distance to the total travelled distance in the field.

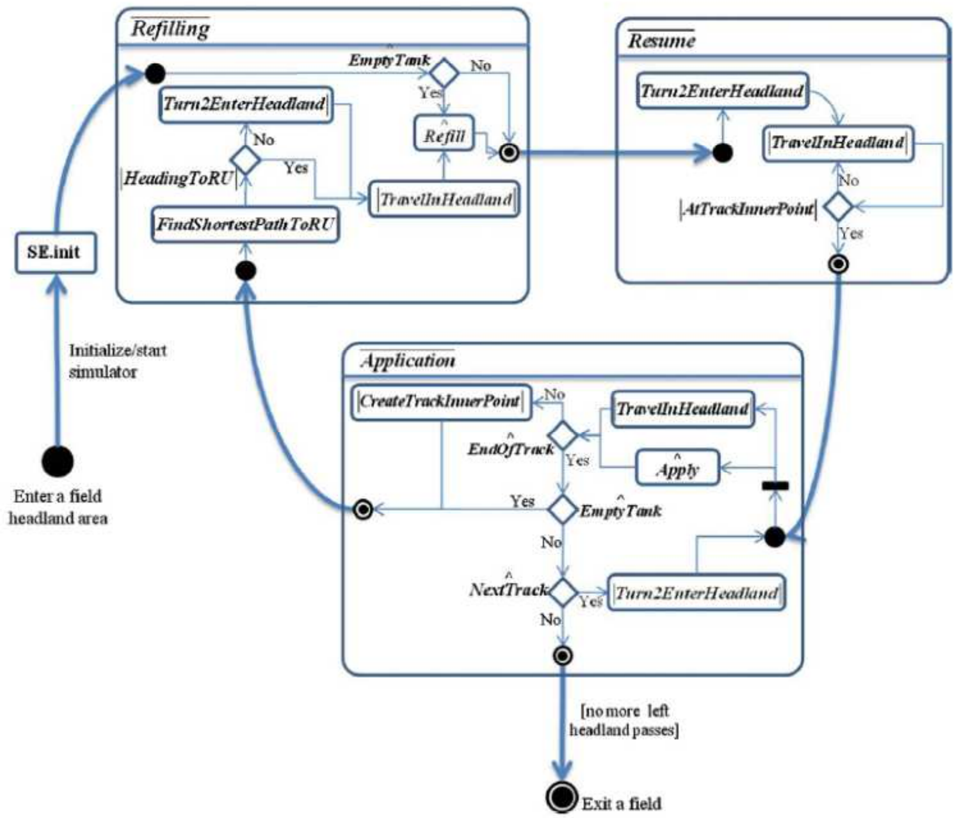

Fig. 3. Combined state and activity diagram of the AU class for covering field headland area.

Fig. 4. The experimental field (55° 32′ 10.00″ N, 10° 4′ 1.96″ E).

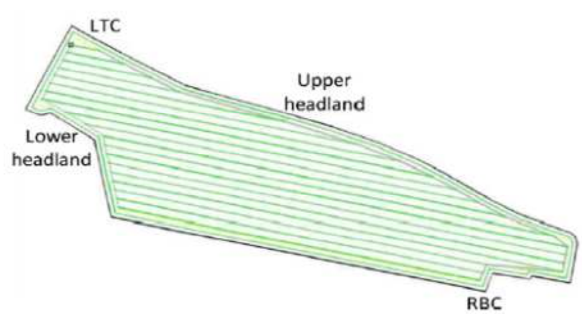

Fig. 5. Geometrical representation of the experimental field (LTC stands for left top corner of the field and RBC stands for right bottom corner of the field).

3.2. The simulation model as a decision support system

In this section, the potential use of the developed simulation model as a decision support system (DSS) is outlined. Operational scenarios are evaluated corresponding to selected combinations of:

- two traffic systems; CTF against UCTF,
- two tramlines directions for the specific field; −12.5° and its perpendicular, counterpart (i.e., 87.5°),
- two tank capacities; 25 and 35 m^3,
- two operating widths; 9 and 18 m.
- three RU's locations; left top corner (LTC), centre of top headland path (CTH) and right bottom corner (RBC), and
- two organic fertiliser dosages of 130 kg N/ha and 170.

The setup settings using these test variables are composed and shown in the upper section of Table 5. The output information produced by the simulation model for each setup is given in the lower section of Table 5.

Table 3
Values of input parameters.

Loading time	300 s
Application speed	3.0 m/s
Turning speed	2.0 m/s
Empty transport speed	3.5 m/s
Partially-loaded transport	2.0 m/s
Fully loaded transport speed	1.5 m/s
Application rate	0.0043 m^3/m^2
Tank capacity	35 m^3
Operating width	9 m
Minimum turning radius	6 m
Driving angle	−12.5°

By using the simulation approach as a decision support system, the following parameters can be evaluated:

- *Traffic system.* Setups 1 and 9 and setups 2 and 10, respectively, have been selected to be identical to all examined parameters except for the traffic system (e.g., setup 1 adopts CTF while setup 9 adopts UCTF). In this way the effect of the traffic system on the field efficiency or on the total operational time can be quantified. As it can be seen, for example, from the table the adoption of the CTF system increases the operational time by 5.01% when going from setup 9 to setup 1 and by 4.98% when going from setup 10 to setup 2. At the same time, the field efficiency decreases by 11.52% when going from setup 9 to setup 1 and by 8.25% when going from setup 10 to setup 2.
- *Driving direction.* It is worth noting that selection of the driving direction is very important in the case of the CTF. As it has been proven in Bochtis et al. (2010), the rule that driving parallel to the longest edge of the field is the most efficient does not hold in the case of the CTF. As it can be seen by comparing setups 1 and 2, which have been selected to have the same prerequisites (including the adoption of the CTF system) except for the driving direction, by selecting the driving direction to be 87.5°, which in this specific case is the perpendicular to the longest edge of the field, the operational time is decreased (by 4.5%) and the field efficiency is increased (by 6.6%). The same result can be extracted from comparing setups 5 and 6.
- *Tank capacity and operating width.* Although it is a general rule that by increasing the tank capacity or the operating width the field efficiency is subsequently increased (compare for example setups 3 and 4 for the case of different tank capacities and setups 1 and 3 for the case of different operating widths), the simulation can quantify this level of this increase and thus providing an evaluation measure for the manager for balancing the reduction of the operational cost by implementing a larger capacity alongside with the increased fixed cost (ownership or hiring cost).
- *RU's location.* For the specific case study (comparing setups 4 and 7) the selection of the RU's location had not any effect on operational time and field efficiency.
- *Fertilizer dosages.* As it is expected, changing dosages has the opposite effect to changing tank capacity (for example, this fact can be deduced by comparing setups 4 and 5). Although the limitations in dosage are imposed be legislation rules, usually the farmer operates with dosages bellow the upper threshold and thus it is still a variable that he can use for optimizing the field machine configuration.

From the previous analyses of the effect of each operational parameter on field efficiency it can be deduced that the developed

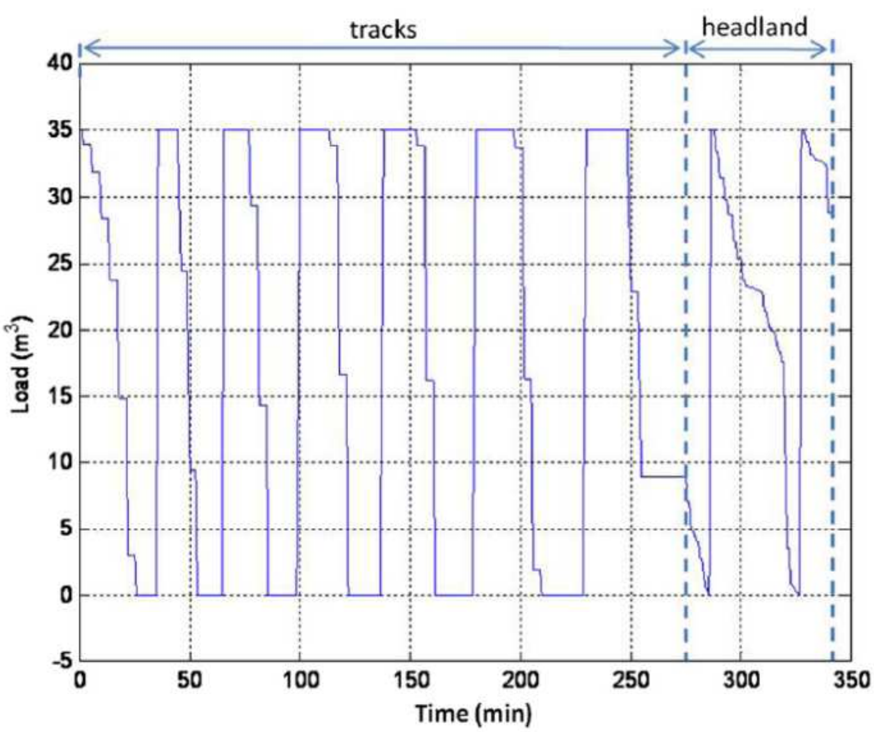

Fig. 6. Load activity plot (in a refill, load amount increases abruptly from 0 to 14.6 m^3 then decrease in application).

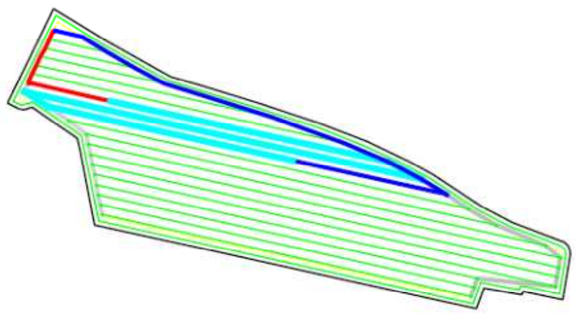
(a)

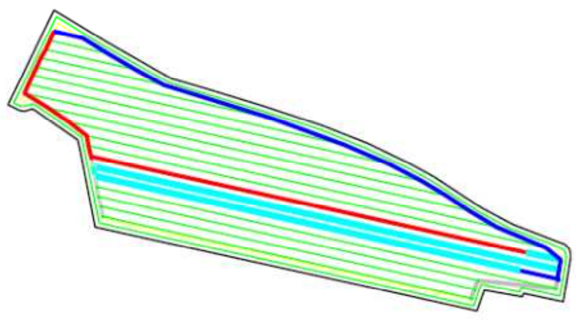
(b)

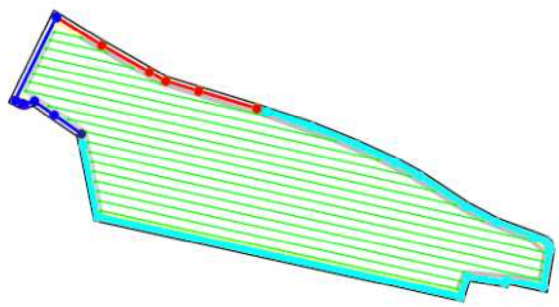
(c)

Fig. 7. AU routes in a complete operation cycle, (a) route number 2 (b) route number 4 (c) route number 8 (route of $\overline{Resuming}$ in red, route of $\overline{Application}$ in cyan and route of $\overline{Refilling}$ in blue). (For interpretation of the references to colour in this figure legend, the reader is referred to the web version of this article.)

simulation model can be used as a DSS to provide a farm manager with the necessary information to evaluate alternative scenarios and to assist in providing the appropriate solution which satisfies manager preferences in terms of operation time, and subsequently, all related operational parameters, such as fuel consumption, and labour cost. Especially, in the case of selecting in-field traffic system, the DSS can provide valuable information regarding the overall efficiency of the system. In addition, the output information can help in selecting the technical specifications related to machinery features, such as tank capacity and operating width, and how these features relate to operational constraints, such as driving direction (or permanent tramlines in the case of the CTF) and RU's positioning. In general, testing and verifying a specific

Table 4
Values of output parameters.

Length of field tracks (m)	6101
Length of headland paths (m)	1296
Effective travelled distance (m)	7397
Full tank transport distance (m)	3229
Empty tank transport distance (m)	3953
Turning distance (m)	888
Field area (m^2)	65,686
overlapped/missed covered area (m^2)	887
Amount of organic fertilizer applied in tracks (m^3)	236
Amount of organic fertilizer applied in headland area (m^3)	50
Number of refills	9
Effective time (h)	1.03
Non-effective time (plus reloading time) (h)	1.78
Total operational time (h)	2.81
Field efficiency (%)	47.83

operational setting before going to the field can have a significant impact on operational cost.

The current model has a number of limitations which are the objectives of further research. First of all, it applies only to free of obstacles fields. In the case of in-field obstacles, an extended approach involving sub-field division must be invoked where each sub-field area will be treated as an individual field. Second, it does not apply to concave fields automatically. In the current version concave fields require a manual intervention for the sub-division of the field area into convex polygons which are subsequently are treated as separate fields. Finally, the RU is assumed solely to move in the headland area and no movement is allowed in the main field area, and thus refilling can take place only in the headland area. As a future perspective, relaxing this limitation on the RU motion will allow the implementation of the simulation also in the case of grain harvesting since the principles for the main unit are the same in both fertilising and harvesting operations except in the case of the sequence that the unit operates firstly in the headland area and secondly in the main field area. Covering the main field area and covering the headland area are two distinct processes in the simulation model, and as such, the sequence of these two processes can be selected by the user. The only difference between the two different sequences is the initial load of the tanker (or the grain hopper in the case of harvesting) in the second process which is the remaining load of the first process and this is talking account by the system automatically.

4. Conclusions

Planning of field operations is essential for the operational efficiency in terms of time and cost, especially in complex operations involving capacity constraints and cooperating units. In order to deal with such type of planning problems an object oriented simulation which simulates in detail in-field machine activities during the execution phase, was developed and applied. It was shown that the simulation model provides all the key operational parameters necessary for the evaluation of a selected operational scenario. This makes it feasible the use of the simulation model as an integral part of a decision support system for advising farmers about in-field operational decisions (e.g., traffic system, driving direction, refilling position) and machinery dimensioning (e.g., tank capacity, operating width, etc.). For example, the simulation model showed that the adoption of the CTF system increases the operational time approximately 5% while at the same time decreases the field efficiency in the range of 11.52–8.25%, based on selected field scenarios involving organic fertilising. Another example, regarded the selection of the driving direction, where the results showed a

Table 5
Input/output parameters for some tested setups.

	Setup 1	Setup 2	Setup 3	Setup 4	Setup 5	Setup 6	Setup 7	Setup 8	Setup 9	Setup 10
Input parameters										
Operating width (m)	9	9	18	18	18	18	18	9	9	9
Driving direction (°)	−12.5	87.5	−12.5	−12.5	−12.5	87.5	−12.5	−12.5	−12.5	87.5
Tank capacity (m^3)	25	25	25	35	35	35	35	35	25	25
Dosage (kg N/ha)	170	170	170	170	130	130	170	130	170	170
Standing pos. of RU	LTC	LTC	LTC	LTC	LTC	LTC	RBC	CTH	LTC	LTC
Traffic farming system	CTF	CTF	CTF	CTF	CTF	CTF	CTF	CTF	UCTF	UCTF
Output parameters										
Effective dist. (m)	7397	7290	3659	3640	3640	3644	3640	3644	7397	7290
Turning dist. (m)	898	2028	612	548	495	882	548	882	891	2023
Transport dist. (m)	11,165	8680	9638	7011	4405	3776	7011	3776	8930	7203
Total traveled dist. (m)	19,460	17,998	11,496	11,199	8540	8302	11,199	8302	17,218	16,515
Mis./overlapped area (m^2)	887	−76	179	−157	−157	−101	−157	−101	887	−76
Number of refills	12	12	12	9	6	6	9	6	12	12
Effective time (h)	1.03	1.01	0.51	0.51	0.51	0.51	0.51	0.51	1.03	1.01
Total operational time (h)	3.56	3.40	2.87	2.26	1.64	1.61	2.26	1.61	3.39	3.24
Field efficiency (%)	38.01	40.50	26.31	32.51	42.63	43.89	32.51	43.89	42.96	44.14

decrease in operational time by 4.5% and an increase in the field efficiency by 6.6% when comparing selected scenarios with different driving directions.

References

Arjona, E., Bueno, G., Salazar, L., 2001. An activity simulation model for the analysis of the harvesting and transportation systems of a sugarcane plantation. Computers and Electronics in Agriculture 32 (x), 247–264.

Benson, E.R., Hansen, A.C., Reid, J.F., Warman, B.L., Brand, M.A., 2002. Development of an in-field grain handling simulation in ARENA. ASAE international Meeting, July 28–31, 2002, Chicago, IL, USA, Paper No. 023104.

Blazy, J.-M., Tixier, P., Thomas, A., Ozier-Lafontaine, H., Salmon, F., Wery, J., 2010. BANAD: a farm model for ex ante assessment of agro-ecological innovations and its applications to banana farms in Guadeloupe. Agricultural Systems 103 (4), 221–232.

Bochtis, D.D., Sørensen, C.G., 2009. The vehicle routing problem in field logistics. Part I. Biosystems Engineering 104 (4), 447–457.

Bochtis, D.D., Sørensen, C.G., Jørgensen, R.N., Green, O., 2009. Modelling of material handling operations using controlled traffic. Biosystems Engineering 103, 397–408.

Bochtis, D.D., Sørensen, C.G., Busato, P., Hameed, I.A., Rodias, E., Green, O., Papadakis, G., 2010. Tramlines establishment in controlled traffic farming based on operational machinery cost. Biosystems Engineering 107, 221–231.

Busato, P., Berruto, R., Saunders, C., 2007. Modeling of grain harvesting: interaction between working pattern and field bin locations. Agricultural Engineering International: The CIGR Ejournal IX (Manuscript CIOSTA 07 001).

Crosson, P., Shalloo, L., O'Brien, D., Lanigan, G.J., Foley, P.A., Boland, T.M., Kenny, D.A., 2011. A review of whole farm systems models of greenhouse gas emissions from beef and dairy cattle production systems. Animal Feed Science and Technology 166–167, 29–45.

Danish Food Industry Agency, 2011. Fertilizer planning – Guidelines 2011. Ministry of Food, Agriculture and Fishery, ISBN 978-87-7120-039-3, pp. 139.

de Toro, A., Hansson, P.-A., 2004. Analysis of field machinery performance based on daily soil workability status using discrete event simulation or on average workday probability. Agricultural Systems 79, 109–129.

Drouet, J.-L., Capian, N., Fiorelli, J.-L., Blanfort, V., Capitaine, M., Duretz, S., Gabrielle, B., Martin, R., Lardy, R., Cellier, P., Soussana, J.-F., 2011. Sensitivity analysis for models of greenhouse gas emissions at farm level: case study of N_2O emissions simulated by the CERES-EGC model. Environmental Pollution 159 (11), 3156–3161.

Dyer, J.A., Desjardins, R.L., 2003. Simulated farm fieldwork, energy consumption and related greenhouse gas emissions in Canada. Biosystems Engineering 85 (4), 503–513.

García-Martínez, A., Bernués, A., Olaizola, A.M., 2011. Simulation of mountain cattle farming system changes under diverse agricultural policies and off-farm labour scenarios. Livestock Science 137 (1–3), 73–86.

Graves, A.R., Hess, T., Matthews, R.B., Stephens, W., Middleton, T., 2002. Crop simulation models as tools in computer laboratory and classroom-based education. Journal of Natural Resources and Life Sciences Education 54, 31–48.

Guan, S., Nakamura, M., Shikanai, T., Okazaki, T., 2008. Hybrid Petri nets modeling for farm work flow. Computers and Electronics in Agriculture 62 (2), 149–158.

Hameed, I.A., Bochtis, D.D., Sørensen, C.G., Nøremark, M., 2010. Automated generation of guidance lines for operational field planning. Biosystems Engineering 107 (4), 294–306.

Keller, T., Defossez, P., Weisskopf, P., Arvidsson, J., Richard, G., 2007. SoilFlex: a model for prediction of soil stresses and soil compaction due to agricultural field traffic including a synthesis of analytical approaches. Soil and Tillage Research 93 (2), 391–411.

Kumar, R., Pandey, K.P., 2009. A program in Visual Basic for predicting haulage and field performance of 2WD tractors. Computers and Electronics in Agriculture 67 (1–2), 18–26.

Kwon, H.-Y., Hudson, R.J.M., 2010. Quantifying management-driven changes in organic matter turnover in an agricultural soil: an inverse modeling approach using historical data and a surrogate CENTURY-type model. Soil Biology and Biochemistry 42 (12), 2241–2253.

Matthews, R.B., Stephens, W., Hess, T., Mason, T., Graves, A.R., 2000. Applications of Crop/soil Simulation Models in Developing Countries. Cranfield Univ. at Silsoe, Silsoe, UK (Final Rep. PD 82).

Neal, M., Drynana, R., Fulkerson, W., Levy, G., Wastney, M.E., Post, E., 2005a. Optimisation of a whole farm model. In: Proceedings of the Australian Agricultural and Resource Economics Society (AARES) Conference. Coffs Harbour, NSW, Australia.

Neal, M., Wastney, M., Levy, G., Drynan, R., Fulkerson, W., Post, E., Thorrold, B., Palliser, C., Beukes, P., Folkers, C., 2005b. Applying Differential Evolution to a Whole-Farm Model to Assist Optimal Strategic Decision Making. In: Zerger, A., Argent, R.M., (Eds.), MODSIM 2005 International Congress on Modelling and Simulation. Modelling and Simulation Society of Australia and New Zealand, December 2005, pp. 245–252. ISBN: 0-9758400-2-9.

Post, E., 2002. Adventures with portability. In: Third LCI International Conference on Linux Clusters: The HPC Revolution 2002, Florida, USA.

Register, A.H., 2007. A Guide to Matlab Object-Oriented Programming. SciTech Publishing, FL.

Shaffer, M.J., Bartling, P.N.S., Ascough II, J.C., 2000. Object-oriented simulation of integrated whole farms: GPFRAM framework. Computers and Electronics in Agriculture 28 (1), 29–49.

Sherlock, R.A., Bright, K.P., Neil, P.G., 1997. An object-oriented simulation model of a complete pastoral dairy farm. In: Proceeding of the International Conference on Modelling and Simulation. Modelling and Simulation Society of Australia, Hobart, pp. 1154–1159.

Sørensen, C.G., 2003. A model of field machinery capability and logistics: the case of manure application. Agricultural Engineering International: The CIGR Journal of AE Scientific Research and Development, 5, ISSN 1682-1130.

Sørensen, C.G., Nielsen, V., 2005. Operational analyses and model comparison of machinery systems for reduced tillage. Biosystems Engineering 92 (2), 143–155.

Tullberg, J.N., Yule, D.F., McGarry, D., 2007. Controlled traffic farming – from research to adoption in Australia. Soil and Tillage Research 97 (2), 272–281.

Vayssières, J., Bocquier, F., Lecomte, P., 2009a. GAMEDE: a global activity model for evaluating the sustainability of dairy enterprises Part II – Interactive simulation of various management strategies with diverse stakeholders. Agricultural Systems 101 (3), 139–151.

Vayssières, J., Guerrin, F., Paillat, J.-M., Lecomte, P., 2009b. GAMEDE: a global activity model for evaluating the sustainability of dairy enterprises Part I – whole-farm dynamic model. Agricultural Systems 101 (3), 128–138.

Chapter 5

Off-Line Area Coverage Planning for Field Robots Involving Obstacle Areas

Hameed, I. A., Bochtis, D. D., & Sørensen, C. G.

(Submitted to international journal of Advanced Robotic Systems)

Off-line area coverage planning for field robots involving obstacle areas

Ibrahim A. Hameed[1,*], Dionysis D. Bochtis[1], Claus G. Sørensen[1]

1 University of Aarhus, Faculty of Science and Technology, Dept. of Engineering, Blichers Allé 20, P.O box 50, 8830 Tjele, Denmark

* Corresponding author E-mail: ibrahimabdelhameed@yahoo.com

Abstract Technological advances combined with the demand of cost efficiency and environmental considerations lead farmers to review their practices towards the adoption of new managerial approaches including enhanced automation. The application of field robots is one of the most promising advances among automation technologies. Since the primary goal of an agricultural vehicle is the complete coverage of the cropped area within the field, an essential prerequisite is the capability of the mobile unit to cover the field area parts autonomously. In this paper, the main objective is to develop an approach for coverage planning for agricultural operations involving the presence of obstacle areas within the field area. The developed approach involves a series of stages including the generation of field-work tracks in the field polygon, the clustering of the tracks into blocks taking into account the in-field obstacle areas, the headland paths generation for the field and each obstacle area, the implementation of a genetic algorithm to optimize the sequence that the field robot vehicle visit the blocks, and an algorithmically generation of the task sequences derived from the farmer practices. This approach has proven that it is possible to capture the practices of farmers and embed these practices in an algorithmic description providing a complete field area coverage plan in a form prepared for execution by the navigation system of a field robot.

Keywords: autonomous agricultural vehicles, mission planning, genetic algorithms.

1. Introduction

Technological advances combined with the demand of cost efficiency and environmental considerations require farmers to reconsider their practices and adopt new managerial approaches including enhanced automation [1]. The application of new technologies which is able to maximize the operational efficiency of the system in a way that optimizes the use of scarcely resources and minimizes the environmental impact is needed [2]. The application of field robots is one of the most promising applications of these automation technologies.

Emerging field robots require to operate with minimum human intervention but also in an efficient way. Since the primary goal of an agricultural vehicle is the complete coverage of the cropped area of the field, an essential prerequisite is the capability of the mobile unit to cover the field area parts autonomously. An automated machine needs a planed path directing the execution of the operation. The boundaries of a field and its obstacle areas are usually fixed from year to year, providing a pre-determined environment where the resultant paths could be deterministic and known in advance.

Coverage planning for field operations is a special case of the general problem of path planning for outdoor environments (e.g., [3]). Due to the semi-structural environment both on-line planning based on sensor fusion (e.g., [4,5]) and off-line planning can be applied. Regarding the off-line planning for field area coverage, a number of approaches have been presented. The first step for a complete off-line planning is the solution of the problem of the geometrical representation of the field as an operational environment. In [6] the developed a field geometrical representation algorithm is presented which can generate straight and curved tracks and treating a field as a single region or dividing it into sub-regions and generate field work tracks parallel to the longest edge of the field/sub-region. This method has also been applied in a non-agricultural domain like the case of the grass cutting planning in stadiums [7]. Pursued methods have also taking into consideration biodiversity issues, as for example in [8]. Regarding the specific coverage planning procedure pertained to such generated operational environments, a number of method have been introduced. In [9] a grid representation for the field and a genetic algorithm were used to find the optimal path travelling through all the grids and hence covering the whole entire field area. Nevertheless, the method does not provide paths that are feasible for all fields operations, e.g. in the case of row crops. In [10] and [11] the algorithmically-computed optimal fieldwork patterns, the *B-patterns*, are presented, which provide the optimal field-work track sequencing according to the criterion of minimizing the non-working travelled distance of an agricultural vehicle. In [12] a genetic algorithms based approach for the simultaneous selection of the driving line direction and *B-patterns* generation that minimizes operational time and overlapped area was derived. In the case of field operations, also the terrain characteristics have a significant influence on the design and optimization of the coverage path planning. In [13] was presented the developed a route planning method for agricultural vehicles carrying time-depended loads with the objective of reducing the risk of soil compaction.

In this paper, the main objective is to develop an approach for coverage planning for agricultural operations involving the presence of obstacle areas within the field area. The aim of the approach is to capture the prevailing practices of farmers, and if possible to optimize such practices, and provide a complete field area coverage plan that is executable by the navigation system of a field robot.

2. Methodological approach

2.1 Geometrical representation

The developed approach includes three stages. In the first stage, the field polygon is filled with field tracks parallel to a user defined angle. In the second stage, the generated tracks are arranged and clustered into sub-fields (referred to as blocks) taking into account the in-field obstacles. In the third stage, headland paths are generated at the upper and lower sides of the tracks in each block. Each stage will be explained in details in the next sections.

2.1.1 First stage: track generation

In this stage, the field boundary and the boundaries of the in-field obstacle areas are firstly inputted using a user-provided source shape/text file. The minimum bounding box (MBB) of the field boundary is then generated and filled with with straight lines parallel to a user-defined driving angle, θ, spaced by distance equal to a user-defined operating width, w. The driving angle is defined as the angle between the driving direction and a horizontal reference x-axis (e.g. the UTM Easting axis). The intersection between each track line and the field outer boundary or the boundaries of the obstacle areas are then obtained. The parts of the tracks contained within the field boundary are maintained while the rest parts are eliminated. More details of this process can be found in [6].

As an example, the blue line of the field shown in Fig. 1a, represents the field outer boundary while the red line represents the boundary of an obstacle area. Generated field tracks for two selected driving angles are shown in Fig. 1b and Fig. 1c.

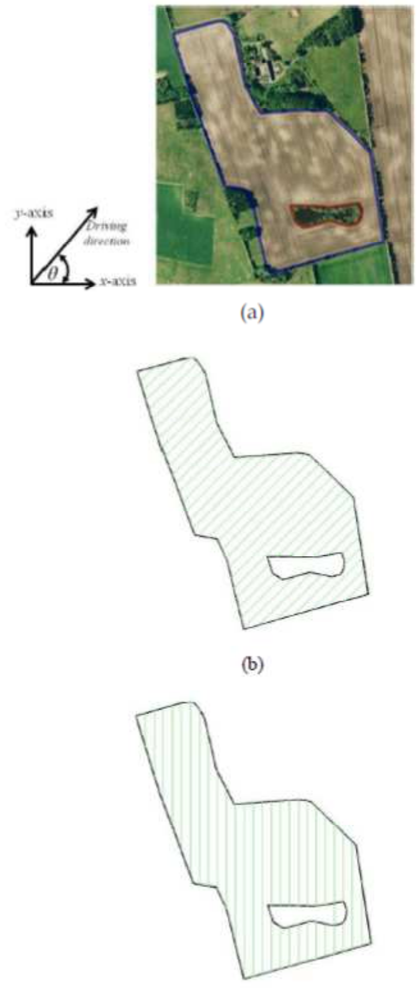

Figure 1. The outer boundary of a field (blue polygon), and the boundary of an in-field obstacle (red polygon) [+56° 29' 14.01", +9° 32' 33.33"] (a) and examples of generated field tracks for two selected driving angles: (b) $\theta = 45°$, and (c) $\theta = 90°$

2.1.2 Second stage: clustering of field tracks

A track generated in the first stage, is defined as a line segment which intersects with the field outer boundary in the form of two end points. Let $T_0 = \{1,2,3,...\}$ denote the set of these initial tracks. If a track intersects with an in-field obstacle area, then it can be divided into two independent tracks, each track having two end points with one end point located on the field outer boundary and the other end point located on the boundary of the intersecting obstacle boundary. In the general case, if a track $i \in T_0$ has n_i intersections, then it crosses $n_i/2-1$ obstacle area parts and can be subdivided into $m_i = n_i/2$ parts which makes up the new tracks. For $n=2$ the track intersects with no obstacles and therefore it is not sub-divided. The total number of tracks summarised as $\sum_{i=1}^{|T_0|} m_i$, and let $T = \{1,2,3,...\}$ denote the set of these tracks.

The next step involves the clustering of the generated tracks into blocks. The clustering process starts by checking the possible subdivision of a specific sequenced track. If the current track can be divided into m_i tracks, then m_i empty blocks are created and the generated tracks are allocated to these blocks in sequence. If the next track in the sequence expressed as $m_{i+1} = m_i$, the new m_{i+1} tracks are saved in the current m_i blocks. In contrast, if $m_{i+1} \neq m_i$ then m_{i+1} new empty blocks are created and the new generated tracks are saved in the new blocks in sequence. A pseudo-code of the clustering process is listed in Table 1.

```
trackNumber = 1
numberOfNewTracks=
numberOfPointsMakingATrack(trackNumber)/2
oldNumberOfNewTracks = numberOfNewTracks + 1
A:
IF numberOfNewTracks ≠ oldNumberOfNewTracks
   blocks = createEmptyBlocks(numberOfNewTracks)
END
FOR i = 1 TO numberOfNewTracks
   SAVE Track(trackNumber, i) INTO blocks(i)
END
oldNumberOfNewTracks = numberOfNewTracks
INCREAMENT trackNumber BY 1
currentTrack =Track(trackNumber)
numberOfNewTracks                                      =
numberOfPointsMakingATrack(trackNumber)/2
GOTO A
```

Table 1. The pseudo-code of the track clustering process

It has to be noted that the number of the generated blocks depends on the selected driving angle and consequently on the driving direction. As for example, Fig. 2 presents a virtual field with two obstacles and different number of resulting blocks for two different driving direction.

2.1.3 Third stage: headland polygons generation

In a field operation, headlands are created by the sequential passes that the agricultural machine has to perform peripheral to the main field area and around of each obstacle area (Fig. 2). A headland area consists of a sequence of internal (or external in the case of an obstacle area) boundaries corresponding to headland passes. The headland area width results from the multiplication of the effective operating width of the machine by the number of the peripheral passes. Let h denote the number of the headland passes. The distance between the first headland pass and the field boundary is the half of the implement width, $w/2$, while the distance between subsequent headland passes equals an implement width, w, where w denotes the (effective) operating width of operating implement. A headland path is obtained by acquiring the intersection points between segments of lines parallel to the segments of lines of the previous headland pass at distance d to the interior of the field area or the exterior area in the case of an obstacle. The distance d for the first headland pass is set to $w/2$, while for the rest of the passes it is set to w. An additional (virtual) headland pass is generated at distance $w/2$ from the last headland pass to be used as the internal boundary of the main field area.

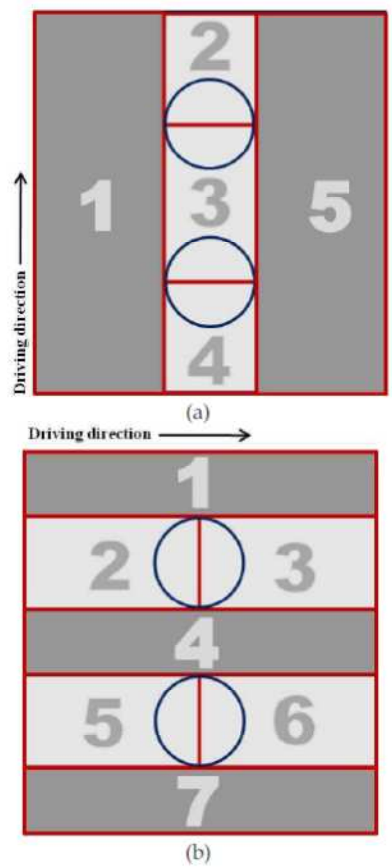

Figure 2. The effect of driving direction on the number of field blocks for a field with two obstacles

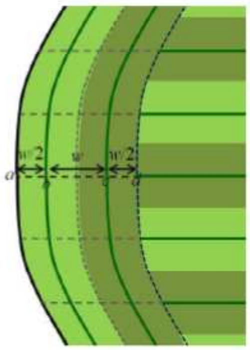

Figure 3. Creation of headland passes polygons: point a is the intersection of the track with the field outer boundary (black line), point b is at half operating width from the field outer boundary, point c is at full operating width from previous headland pass, and point d at half operating width from the last headland pass

2.2 Block sequence optimization

For a field robot to carry out an agricultural operation without crossing any of the field obstacles it should cover each block of tracks and therefore it is required to find the covering order of the generated blocks. This problem can be formulated as an optimization problem where the decision variable is the order of blocks and the objective function to be minimized is the connection distance between blocks.

Let $B=\{1,2,3,...\}$ denote the set of generated blocks and let $x_{ij}, i, j \in B / i \neq j$ denote the decision variables of the problem where $x_{ij}=1$ if the vehicle after block i transfers to block j and $x_{ij}=0$ otherwise. The objective function of the problem is $\sum_{\substack{i \in B \\ i \neq j}} \sum_{j \in B} x_{ij} c_{ij}$ that has to be minimizes, where c_{ij} the cost for transferring from block i to block j. The cost c_{ij} has not a uniquely specified value but it depends on the exit point from block i and the entry point of block j, and thus the problem can not be considered as a pure assignment problem. Four connection points or arguments can be defined for each block, as it is shown in Fig. 6. The exit point of a block is a function of the entrance point as derived by the configuration of the field tracks. Let $f(\cdot):\{1,...,4\} \rightarrow \{1,...,4\}$ express the function that a specific entrance connection point results in a specific connection point. In the case of odd number of field track in a block $f(1)=3$, $f(2)=4$, $f(3)=1$, and $f(4)=2$, while in the case of even number of tracks in the block then $f(1)=4$, $f(2)=3$, $f(3)=2$, and $f(4)=1$.

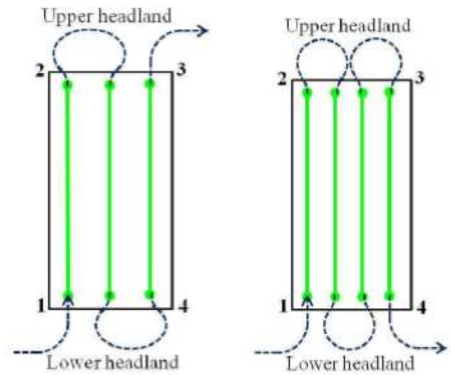

Figure 4. Entrance points are arranged in clock-wise direction: (a) a block with odd number of tracks, and (b) a block with even number of tracks

2.2.1 Small scale problems (SSP)

In this context, SSP are defined as the problem which has a number of blocks $|B| \leq 4$. For 4 blocks, there are up to 24 (i.e., $|B|!$) candidate solutions with repetitions or 12 candidate solutions without repetitions. In this type of problems, all possible sequences are obtained using random permutation within B. An Real valued genetic algorithm (RGA) is applied to find the optimum entrance points for each respective block in each sequence of blocks. A chromosome constitutes of $|B|$ genes where each gene has an integer value in the range of [1 4], as it is shown in Fig. 5a. The connection distance for each solution is saved and the one with minimum connection distance is returned. The advantage of this type of problems is that a global optimum solution is guaranteed, however, it is time consuming and not practical for more than 4 blocks

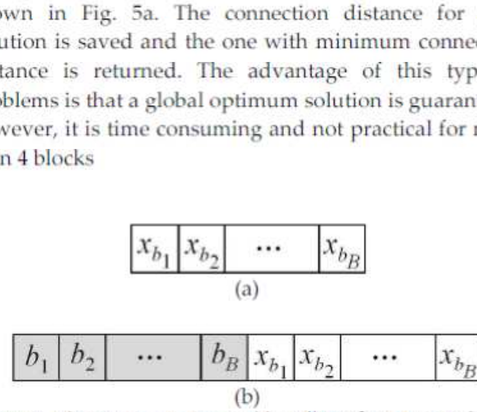

Figure 5. Chromosome structure: (a) coding of entrance points of blocks optimizing entrance points of field blocks, and (b) coding of block sequence in the first half and entrance points in the second half of the chromosome

2.2.1 Large scale problems (LSP)

For more than 4 blocks, an RGA is used to find the optimal sequence of blocks and at the same time finding the optimum entrance point of each respective block. The sequence of blocks is encoded in permutation and constitutes the first half of the chromosome while the entrance points of respective blocks constitutes the second half of the chromosome. The chromosome structure for solving this type of problems is shown in

4

Fig. 5b. The advantage of these types of problems is its quick convergence but the disadvantage is that there is no guarantee that the obtained solution is global optimum.

2.2.3 Real valued genetic algorithm (RGA)

The input to the block sequencing problem is two sequenced set of integers, where the first set of integers represents different blocks together with the order representing the time at which a block must be visited and a second set of integers where each integer represents a block entrance point. The output of the problem is the connection distance between blocks. The decision variables are represented by the sequences of blocks which are permutation encoded and entrance points which are real-valued encoded. Real-valued encoding not only reduces the computational efforts but also speeds up convergence. The performance of GA depends on the crossover and the mutation operators of GA [14]. The type and the implementation of operators depend on the encoding and also on the underlying problem. In real-valued encoding, every chromosome is a string of some values. Values can be anything connected to the underlying problem, from numbers, real numbers or chars to some complicated objects. In real-valued encoding, crossover operators used in binary encoding are applicable where parts of the strings from two parent chromosomes are swapped in order to produce two new offsprings [15]. Mutation is carried out by adding or subtracting a small value to a selected gene value. In case of integer values, this value is rounded to the nearest integer after the addition or subtraction.

In permutation encoding, every chromosome is a string or a sequence of integers, where each integer represents a different block and the order represents the time at which a block is visited. Permutation encoding can be used in ordering problems, such as the travelling salesman problem (TSP) or task ordering problems. In this case, each block has to be visited once and no blocks can be discarded. Also, a scheme analogous to simple crossover is required, but one which preserves the solution viability while allowing the exchange of ordering information. One such scheme, among others, is partially matched crossover (PMX). In this scheme, a crossing region is chosen by selecting two crossing sites at random. Crossover is performed in the centre region. Replicated alleles in the crossing region are replaced by cross-referencing with the parent of the alternate chromosome [16]. Mutation is often used in GAs as a way of adding random variation to the evolving population, preventing a total loss of diversity. To avoid a resulting non-viable block order, inversion mutation is used in which a randomized exchange of alleles in a randomized chosen chromosome is applied. This can be accomplished by applying a given (usually small) probability, much like mutation.

2.3 Generation of the final path

The sequence of the visited blocks and the sequence of traversing the tracks within each block cannot provide by themselves an executable and complete coverage of the field area. The reason for this is that in field operations, as mentioned earlier, auxiliary paths in terms of headland passes are needed in order to complete the operation. The execution time for these paths, i.e. prior or after finishing the main area coverage, depends on the type of operation. In the case of a material input operation (e.g. seeding), the headland passes are executed after the completion of the operation in the main area. In the case of output material operations (e.g. harvesting), the headland passes are executed prior to the operation in the main area.

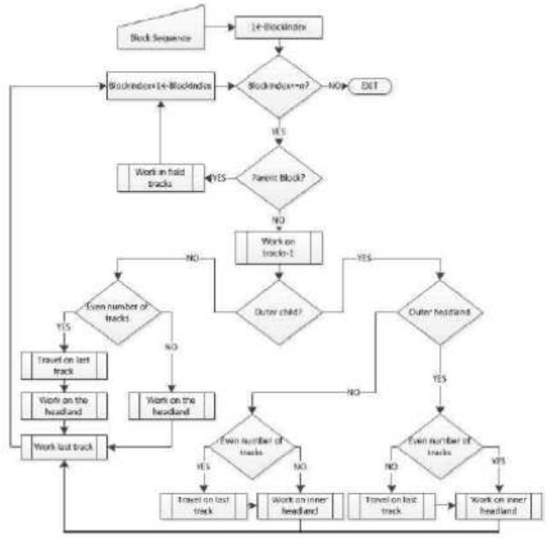

Figure 6. The flow diagram for the generation of the final path in the case of input material flow operations

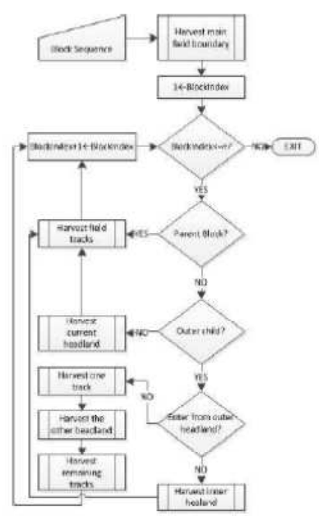

Figure 7. The flow diagram for the generation of the final path in the case of output material flow operations

In order to produce a complete coverage plan that includes both the traversal sequence between the tracks as well as the headland passes, two algorithms were developed, one for input material flow operations and one for output material flow operations, incorporating the task execution practices that have to be followed in agricultural operations. Fig. 6 and Fig. 7 represent the flow diagrams depicting the two algorithms representing input material flow operations (having as example the seeding operation), material output operations (having as example the harvesting operation), respectively.

(a)

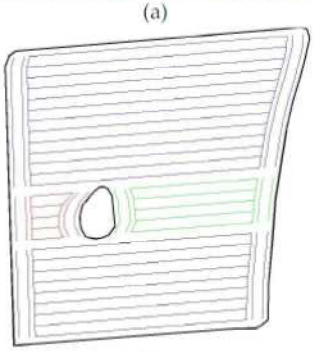

(b)

Figure 8. The field of example 1 with an obstacle area (a) and the block generation for a selected driving angle of 45°, working width of 9m and two headland passes (b)

3. Results

3.1 SSP example

The first demonstration field [+54° 57' 8.28" E, +9° 46' 49.31"N], shown in Fig. 8, has an area of 5.54 (ha) or 55375.38 (m2) and has one obstacle area. The coverage planning is generated for a driving angle of 4.5° and an operating width of 9 m and two headland passes. The application of the developed coverage planning method, in terms of the block generation, is shown in Fig. 9(a) where the field work tracks are clustered into 4 blocks. The computational time for this problem T was 0.18 s as an average of 10 running times.

The field has four blocks so it could be classified as a SSP and therefore the general GA was used to find the optimum entrance point for all possible permutations of block sequences (i.e., for 4! = 24 block sequences). The sequences of tracks in each block are given in Table 1.

The sequence of the blocks and the corresponding entrance and exit connection points are presented in Fig. 9. There are two optimal solutions which are given in Table 2. It is worth noting that the two solutions are identical but one is the reverse of the other. The two solutions are graphically shown in Fig.9. The solution is obtained in 0.47 min using a RGA of a population size of 100, 50 generations, 0.8 and 0.01 crossover and mutation probability, respectively.

Block number	Sequence of tracks
1	[1 2 3 4 5 6 7 8 9 10 11 12 13]
2	[14 16 18 20 22]
3	[15 17 19 21 23]
4	[24 25 26 27 28 29 30 31 32]

Table 1. Indexes of after division tracks in each block

Solutions	Best Block sequence	Enter points	Exit points	Connection distance
1	[1 3 2 4]	[1 2 2 1]	[3 4 4 3]	77.01 (m)
2	[4 2 3 1]	[3 4 4 3]	[1 2 2 1]	

Table 2. Optimal block sequence

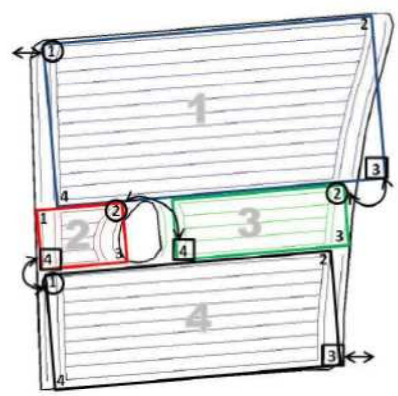

Figure 9. Illustration of the two optimum solutions: circles and squares could be either entrance or exit points and vice versa

3.2 LSP example

The second experimental field [+56° 30' 26.79", +9° 36' 54.35"], shown in Fig. 10, has an area of 94.03 (ha) (i.e., 940,309.60 m²) and two obstacle areas. An operating width of 18 m and two headland passes were assumed together with a driving angle of 84°. The field representation after been clustered into 7 blocks is shown in Fig. 11(a). The block generation was obtained in an average time of 0.28 s (i.e., average of 10 running times).

The field has 67 tracks classified in 7 blocks, as it is shown in Fig. 11(a). For 7 blocks, there are 5040 different sequence permutations. The RGA was used to find the best sequence of blocks. The solution was obtained in

14.41 min and a minimum connection distance of 610.04 m was achieved. The default sequence of tracks in each block is given in Table 3 while the resultant optimized solution is given in Table 4. In this problem, a mixed permutation and real-valued encoded GA of a population size of 100, a maximum generation number of 100, a crossover probability of 0.8 and a mutation probability of 0.01 were used.

(a)

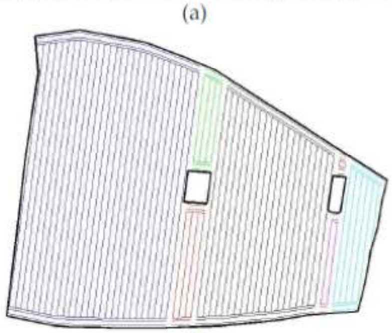

(b)

Figure 10. The field of example 2 with two obstacle areas (a) and the block generation for a selected driving angle of 84°, working width of 9m and two headland passes (b)

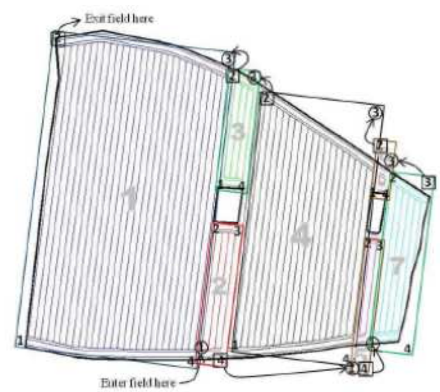

Figure 11. Illustration of the obtained optimized solutions: circles and squares represent entrance and exit points to and from a block respectively

3. Conclusions

The developed approach for coverage planning for agricultural operations involving the presence of obstacle areas within the field area provides the necessary information required for aiding and supporting navigation of field robots. The performance of the optimization algorithms used to optimize the coverage planning requires relatively low computational times as compared to an off-line planning system.

This approach has proven that is possible to capture the practices of farmers and embed these practices in an algorithmic description providing a complete field area coverage plan in a form prepared for execution by the navigation system of a field robot. Moreover, in the case of complex fields in terms of the number of obstacle areas, the approach can provide an optimized plan that enhances the farmer's practice.

Block number	Track sequence
1	[1 2 3 4 5 6 7 8 9 10 11 12 13 14 15 16 17 18 19 20 21 22 23 24 25 26 27 28]
2	[29 31 33 35]
3	[30 32 34 36]
4	[37 38 39 40 41 42 43 44 45 46 47 48 49 50 51 52 53 54 55 56]
5	[57 59]
6	[58 60]
7	[61 62 63 64 65 66 67]

Table 3. Indexes of after division tracks in each block

Solutions	Best Block sequence	Enter points	Exit points	Connection distance
1	[2 5 7 6 4 3 1]	[1 1 1 3 3 3 3]	[4 4 3 2 2 2 2]	610.04 (m)

Table 4. Optimal block sequence

9. References

[1] C.G. Sørensen, D.D. Bochtis. "Conceptual model of fleet management in agriculture, " *Biosystems Engineering*, vol. 105, pp. 41-50, 2010.

[2] C.G. Sørensen, V Nielsen. "Operational analyses and model comparison of machinery systems for reduced tillage, " *Biosystems Engineering*, vol. 92, pp. 143–155, 2005.

[3] Y. Guo, M. Yang, J. Cheng, "Knowledge-inducing Global Path Planning for Robots in Environment with Hybrid Terrain, ", *International Journal of Advanced Robotic Systems*, Vol. 7, No. 3, pp. 239-248, 2010.

[4] C. Deelertpaiboon, M. Parnichkun. "Fusion of GPS, Compass, and Camera for Localization of an Intelligent Vehicle", *International Journal of Advanced Robotic Systems*, Vol. 5, No. 4, pp. 315-326, 2008.

[5] Y. Kim, J. An, J. Kim. "A Fuzzy Obstacle Avoidance Controller Using a Lookup-Table Sharing Method and Its Applications for Mobile Robots", *International Journal of Advanced Robotic Systems*, Vol. 8, No. 5, pp. 39-48, 2011.

[6] I.A. Hameed, D.D. Bochtis, C.G. Sørensen, M. Nøremark. " Automated generation of guidance lines

for operational field planning, " *Biosystems Engineering*, vol. 107, pp. 294-306, 2010.

[7] I.A. Hameed, C.G. Sørensen, D.D. Bochtis, O. Green. "Field robotics in sports: automatic generation of guidance lines for automatic grass cutting, striping and pitch marking of football playing fields, " *International Journal of Advanced Robotic Systems,* vol. 8, pp. 113-121, 2011.

[8] S. de Bruin, P. Lerink, A., Klompe, T. van der Wal, S. Heijting. "Spatial optimisation of cropped swaths and field margins using GIS, " *Computers and Electronics in Agriculture*, vol. 68, pp. 185-190, 2009.

[9] Ryerson, A. E. F., & Zhang, Q. (2007). Vehicle path planning for complete field coverage using genetic algorithms. *Agricultural Engineering International: the CIGR Ejournal*, Manuscript ATOE 07 014(*IX*), 1-11.

[10] Bochtis D D; Vougioukas S (2008). Minimising the Non-working Distance Travelled by Machines Operating in a Headland Field Pattern. Biosystems Engineering, 101 (1), 1-12.

[11] Bochtis D D; Sørensen C G (2009). The Vehicle Routing Problem in Field Logistics Part I. Biosystems Engineering, 104(4), 447-457.

[12] Hameed I A; Bochtis D D; Sørensen C G. (2011). Driving angle and track sequence optimization for the operational path planning using genetic algorithms. Applied Agricultural Engineering, 27(6): 1077-1086.

[13] Bochtis D D; Sørensen C G; Green O (In press). A DSS for planning of soil-sensitive field operations. Decision Support Systems, Accepted Dec 2011, DOI: 10.1016/j.dss.2011.12.005.

[14] Whitley, D. (1994). A genetic algorithm tutorial. *Statistics and Computing*, 4(2), 65-85.

[15] Goldberg, D. E. (1989). *Genetic Algorithms in Search, Optimization & Machine Learning*. Addison-Wesley, MA.

[16] Goldberg, D. E., & Lingle, R. (1985). Alleles, Loci, and the Traveling Salesman Problem. Proceedings of the First International Conference on Genetic Algorithms and Their Application, edited by Grefenstette J., Lawrence Erlbaum Associates, Hillsdale, NJ, 154-159.

Chapter 6

Optimized Driving Direction Based on Three-Dimensional Field Representation

Hameed, I. A., Bochtis, D. D., Sørensen, C. G., Jensen, A. L. & Larsen, R.

(Submitted)

Optimized driving direction based on three-dimensional field representation

I A Hameed[a,*]; D D Bochtis[a]; C G Sørensen[a]; A L Jensen[a]; R Larsen[b]

a University of Aarhus, Faculty of Science and Technology, Dept. of Engineering Blichers Allé 20, P.O box 50, 8830 Tjele, Denmark

b University of Aarhus, Dept. of Agroecology and Environment, Blichers Allé 20, P.O box 50, 8830 Tjele, Denmark

* Corresponding author: IbrahimAbdelHameed@yahoo.com

Article Information

Keywords:
route planning
DEM
Optimization

Abstract

The agricultural vehicles used in various field work activities emit significant levels of atmospheric pollutant, e.g. CO2 and NO, which are of major concern due to their contribution to the greenhouse effect. Energy requirements and consequently emissions may be reduced by developing optimised in-field coverage planning systems for agricultural machines. The objective of this paper was to develop and implement a 3D coverage planning approach for material input operations that minimizes the energy requirements. The basic components of the consisted of a 3D geometrical representation of the field characteristics and a simulation tool for field operations under capacity constraints. Supplementary to that, energy consumption models was invoked taking into account terrain inclinations in order to provide the optimal driving line direction for traversing the parallel field-work tracks under the criterion of minimised direct energy requirements. Based on the results from two case study fields, it was shown that the reduction in the energy requirements when the driving angle is optimized by taking into account the 3D configuration of the field area was 6.5% in average for all the examined scenarios compared to the case when the applied driving angle is optimized assuming even field areas.

1. INTRODUCTION

The agricultural vehicles used in various field work activities emit significant levels atmospheric pollutant emissions, which include carbon dioxide (CO_2) and nitrogen oxide (NO), both of which are of major concern due to their contribution to the greenhouse effect. Reducing pollutant outputs through reduced fuel consumption therefore yield both environmental and financial benefits (Tavares et al., 2009). Fuel consumption may be reduced by developing optimised in-field coverage planning for agricultural machines. Recently, a number of automated coverage planning algorithms have been developed for the optimization and automation of autonomous field operations. For example, Oksanen and Visala (2009) and Jin and Tang (2010) developed algorithmic approaches to find efficient 2D coverage paths involving field area decomposition in sub-regions and optimal driving line direction. Bochtis and Vougioukas (2008) and Bochtis and Sørensen (2010) presented the algorithmically-computed optimal fieldwork patterns, the B-patterns, which provide the optimal field-work track sequencing according to the criterion of the minimization of the non-working travelled distance of an agricultural vehicle. Hameed et al.

(2011) derived a genetic algorithms based approach for the simultaneous selection of the driving line direction and B-patterns generation that minimizes operational time and overlapped area. A critical factor, however, that has not been taken into account in the above mentioned field area coverage approaches is the effect from varying terrain conditions. Only limited research on developing area coverage planning for 3D terrain has been reported. For example, Jin and Tang (2011) developed an optimized 3D terrain field coverage path planning algorithm that classifies the field terrain into flat and sloppy areas and then applies the most appropriate path planning strategy to each region in terms of minimised headland turning cost, soil erosion cost, and skipped/overlapped area cost, while Bochtis et al. (2012) developed a route planning method for agricultural vehicles carrying time-depended loads with the objective of reducing the risk of soil compaction. The terrain characteristics are expected to have significant influence on the design and optimization of the coverage path planning. Especially in terms of elevation variations, elevation changes or slopes have considerable influence on soil erosion, skips and overlaps between furrows, and vehicle's fuel consumption (Jin and Tang, 2011).

Material handling operations with time-depending loads carried by the agricultural vehicles specifically presents a potential for saving direct energy consumption in elevated terrains by optimising the relation between the inclination of a specific part of the area, the driving direction, and the load carried by the vehicle while operating on this part. These operations involve traversing the field with varying loads depending on the emptying or state of the carrying unit. The capacity constraints require that the vehicle has to execute a number of routes with varying loads in order to complete the operation (e.g., harvesting and fertilizing).

The objective of this paper is to develop and implement a 3D coverage planning approach for material input operations that minimizes the energy requirements. The approach will be based on developed tools for 2D geometrical representation and expanded to a 3D representation, and a simulation tool for field operations under capacity constraints. The approach will be supplemented with energy consumption models taking into account terrain inclinations in order to provide the optimal driving line direction for traversing the parallel field-work tracks under the criterion of minimised direct energy requirements.

2. METHODOLOGY

2.1 GENERAL

The approach provides, for a given field and given machinery characteristics, the optimal driving line direction for traversing the parallel field-work tracks in terms of minimised direct energy requirements. As a decision variable of the optimization problem is considered the driving angle, which is defined as the angle between the driving line direction and the horizontal axis of the applied Euclidean coordinates system. The method is based on an exhaustive search among all possible integer values of driving angles between 1° and 180°. The stages involved in the search are described in Fig. 1. In the first stage an existing 2D field representation generation tool (described in Section 2.2) is applied. In a next stage (described in Section 2.3), by combining the generated 2D representation and the information provided by the digital elevation model (DEM) of the field, a 3D representation is generated. Then an existing simulation tool for input material handling operations with capacity constraints is applied (described in Section 2.4).

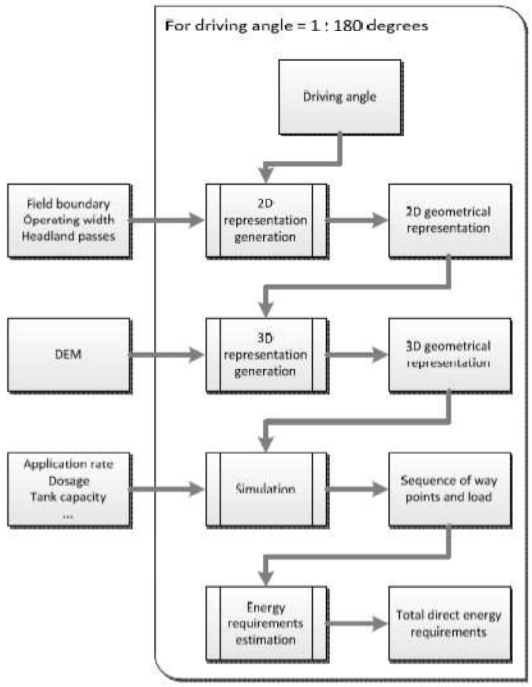

Fig. 1 – Flowchart of the 3D terrain optimized field coverage approach

The simulation provides the path followed by the agricultural vehicle for a complete field coverage and the corresponding carried load in each way-point. In the last stage, using fuel consumption models (described in Section 2.5) the total direct energy requirements for the execution of the operation using the tested driving angle are estimated. The tested driving angle with the minimum estimated direct energy requirements is selected as the optimal one.

2.2 2D FIELD REPRESENTATION

For the 2D geometrical representation of the field, a tool developed by Hameed et al., (2010) was used. The 2D geometrical representation of a field involves the generation of a geometrical map which is made up by discrete geometric primitives, such as points, lines, and polygons, providing a concise representation of the environmental data that can be readily used for operational planning. The input consists of the set of coordinates of the points on the field boundary, the operating width of the implement, the number of headland passes, and the tested driving direction. The tool generates the set of the parallel field-work tracks for the complete field area coverage and gives as an output the coordinates of the points representing the starting and the ending point of each track, and of the points representing the headland passes (Fig. 2). The tool was implemented using the MATLAB® technical programming language.

2.3 3D TERRAIN REPRESENTATION

In this stage, the 2D field representation is converted into a 3D field representation. The

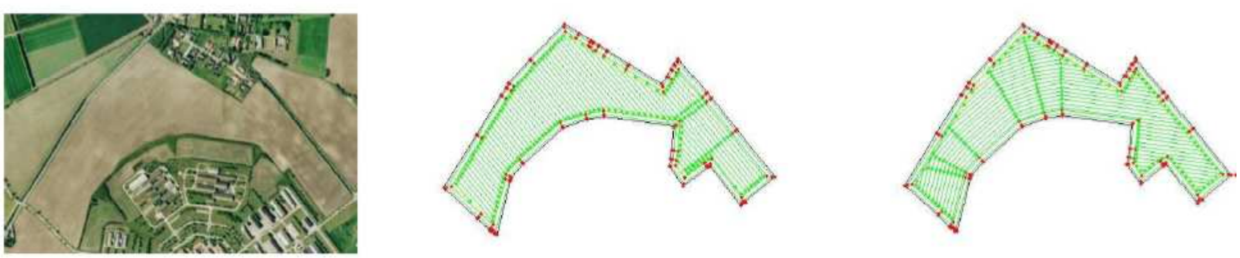

(a) (b) (c)

Fig 2 – Example implementation of the 2D geometrical field representation for the generation of straight (b) or curved (c) field-work tracks

information regarding the field topography needed for the generation of a 3D representation of the field terrain is provided by a digital file, called digital elevation model (DEM), consisting of terrain elevation for ground positions at regularly spaced horizontal intervals. DEM's data are structured as a grid of squares or cells (Sulebak, 2000). The cell length (m) represents the accuracy of the terrain representation in 3D space and this value is defined in the DEM file. A DEM file is arranged as an ASCI grid file containing in its header the file id, cell length, number of grid lines along x-axis, number of grid lines along y-axis, minimum and maximum x values of the grid in UTM, minimum and maximum y value of the grid in UTM, and minimum and maximum elevation values of the grid in UTM. Then elevation values of the grid cells (i.e., z values) are ordered in rows in the rest of the file representing the elevation matrix. The cell length of the field examples used in this paper is 1.6 m.

The 3D representation of the field is obtained by dividing each line segment of the 2D field representation into small segments each of length less than or equal to the cell length of the elevation model (i.e., DEM file) of the field area. After division, each resultant segment has two waypoints, namely, starting and ending points in 2D space. A unique cell from the DEM file is then allocated to each resultant waypoint and the elevation of each matched cell is assigned to its relevant waypoint of the 2D representation. A search sub-routine is used to allocate each waypoint of the 2D representation to a DEM cell. A pseudo-code of the developed search sub-routine is given in Table 1 for converting a 2D field-work track into the corresponding 3D representation.

Table 1 – Elevation search pseudo-code

```
READ elevationMatrix, xmax, xmin, ymax, ymin, cellLength FROM DEM
x =[xmax : -cellLength : xmin]
y =[ymax : -cellLength : ymin]
FOR each track (or headland path) segment
       READ segmentStarPoint, segmentEndPoint
       DEFINE stepSize = cellLength
       segmentLine = CREATELINE(segmentStarPoint,  segmentEndPoint)
       segmentLength = LENGTH(segmentLine)
       numberOfCells = ROUND(segmentLength/cellLength)
       WHILE numberOfCells > 0
          [xp, yp] = POINTONLINE(segmentLine, stepSize)
          xIndex = FIND( x > xp )
          yIndex = FIND( y > yp )
          z = elevationMatrix(LAST(xIndex), LAST(yIndex))
          SAVE  xp, yp, z
          DECREAMENT numberOfCells BY 1
          INCREAMENT stepSize BY cellLength
       END
END
EXIT
```

2.4 Material input operations simulation tool

In this stage, the execution of the operation following the tested driving angle is simulated using a developed model by Hameed et al., (2012). The object oriented simulation model regards the material input operations with capacity constraints, where a quantity of a ''commodity'' is transported by the machine and is distributed in the field area (e.g. the case of the organic fertilizing application). In the case of material input operations, a number of routes are required since a full load carried by the application unit is generally not sufficient for full area coverage of the field. A ''route'' consists of part operations including filling the tanker at a location out of the field and driving from that location to the position where the application is resumed, applying the carried material to the field, and driving back to the re-filling location. These activities involves a number of non-productive in-field transports with either full (in the case of travelling form refilling location back to the resuming position) or empty (in the opposite travelling) tanker. All these in-field transports are directly affected by the driving angle and have to be included in the estimation of the total energy requirements. The input to the simulation tool includes the 2D geometrical representation of the field (provided by the tool described in Section 2.2), a number of operation-specific information, i.e. application rate, dosage of the material, average speeds (working speed, turning speed, and in-field transport speed), and machinery-specific information, i.e. minimum turning radius, working width, and tank capacity. The output of the simulation model provides the sequence that the vehicle traverses the waypoints which has been defined in the 3D representation stage and the load carried by the vehicle at the individual waypoints in both the case of applying the material and the case of the associated in-field transports.

2.5 Energy requirements estimation model

In order to model the agricultural vehicle energy consumption as a function of the inclination of the field terrain, the case of the injector system for organic fertilizer was used. Specifically, the estimation of the required power was based on the following parametric equation introduced by Fröba and Funk, (1995):

$$\begin{aligned} P = & \left(p_1 + v \cdot w \cdot p_2\right) + \left(p_3 + d \cdot v^2 \cdot p_4\right) w + \\ & \left(0.115 M \cdot v \cdot a / 3600\right) + P_{air} + \\ & \left(g \cdot m \cdot v \cdot r_{rc} / 1800\right) \end{aligned} \quad (1)$$

where P is the required power (kW), v is the vehicle speed (km/h), w is the working width of the injector (m), d is the working depth (cm), M is the total vehicle and implement mass including the tank load, m is the vehicle and implement mass, (kg), a is the inclination of the terrain (%), g is the gravitational acceleration ($9.81 \mathrm{m/s^2}$), P_{air} is the total power account for air conditioner and compressors (kW), r_{rc} is the rolling resistance coefficient (r_{rc} equals 0.06 for good surface conditions, 0.12 for medium surface conditions, and 0.25 for bad surface conditions), p_1 and p_2 are pump constants (p_1=-0.2683 and p_2=0.06775), and p_3 and p_4 are injector factors (i.e., p_3= 4.55752 and p_4=0.03141). Eq. (1) is used to estimate the power required by a tractive unit pulling an injector traversing each segment of the generated 3D representation of the field according to the following process.

Let $T = \{1, 2, 3, \ldots\}$ be the set of the field-work tracks generated by the 2D representation process. Each track is divided into a number of segments $n_i, i \in T$ according to the 3D representation process. In each of the above mentioned segments, an inclination $a^i_j, i \in T, j = 1,\ldots n_i$ is allocated (in the 3D representation process). To calculate the inclination in a specific segment of a track, the change in elevation between two sequential cells in the direction of the track is divided by the length of the cell edge. In the case of time-depended loads in each segment, a mass value $M^i_j = m + l^i_j, i \in T, j = 1,\ldots,n_i$ is allocated and this equals the summation of the machinery (tractor + implement) mass, m (kg), and the load mass ($l^i_j, i \in T, j = 1,\ldots,n_i$) (this value is provided by the simulation tool output). Consequently, the required power for driving over each individual segment can be obtained using the following equation:

$$P^i_j = \begin{cases} (p_1 + v.w.p_2) + (i_1 + d.v^2.i_2)w + \left(0.115.\left[m + l^i_j\right].v.\theta^i_j/3600\right) + P_{air} + \left(g.\left[m + l^i_j\right].v.r_{rc}/1800\right), & \text{if } \theta^i_j > 0 \\ (p_1 + v.w.p_2) + (i_1 + d.v^2.i_2)w + P_{air} + \left(g.\left[m + l^i_j\right].v.r_{rc}/1800\right), & \text{otherwise} \end{cases} \quad (2)$$

The tank load for each segment is obtained using the equation:

$$l^i_j = C - r.w.d^i_j, where\, l^i_j \geq 0, i \in T, j = 1,\ldots,n_i \quad (3)$$

where r is application rate in (kg/m^2), and C is the tank capacity (kg).

The energy required for traversing each individual segment is obtained using:

$$E^i_j = 3.6\frac{P^i_j \cdot d^i_j}{v} \quad (4)$$

The total energy required for covering the main field body is then estimated as:

$$E = \sum_{i=1}^{|T|}\left(\sum_{j=1}^{n_i} E^i_j\right) \quad (5)$$

As mentioned, in each route executed by the vehicle an empty tanker in-field transport and a full-tanker in-field transport are involved. For each of these in-field transports, the simulation tool provides the sequence of the way points. The energy requirements for each individual segment traversed by the vehicle in an in-field transport is estimated using Eq.(2) where for the case of empty tanker the total vehicle mass equals m, while in the case of full-load tanker equals $m + c$, where c is the tanker capacity. The total energy requirements for the in-field transports equals:

$$E_{tr} = \sum_{i=1}^{k}\left(E^e_i + E^f_i\right) \quad (6)$$

where k denotes the number of routes and E^e_i and E^f_i are the total direct energy requirements for empty tanker and full-loaded tanker, respectively, in-field transports during route $i \in \{1,\ldots k\}$.

In the optimization problem, the driving angle which minimizes the total energy consumed in covering field area and in the associated in-field transportations is found. The objective function is given as follows:

$$\min_{\vartheta \to \vartheta^*}(E + E_{tr}) \quad (7)$$

where $\vartheta \in \left[0^o, 180^o\right]$ is the driving angle and ϑ^* is the optimum driving angle which minimizes the total energy consumption. The model has been implemented in the MATLAB® programming environment.

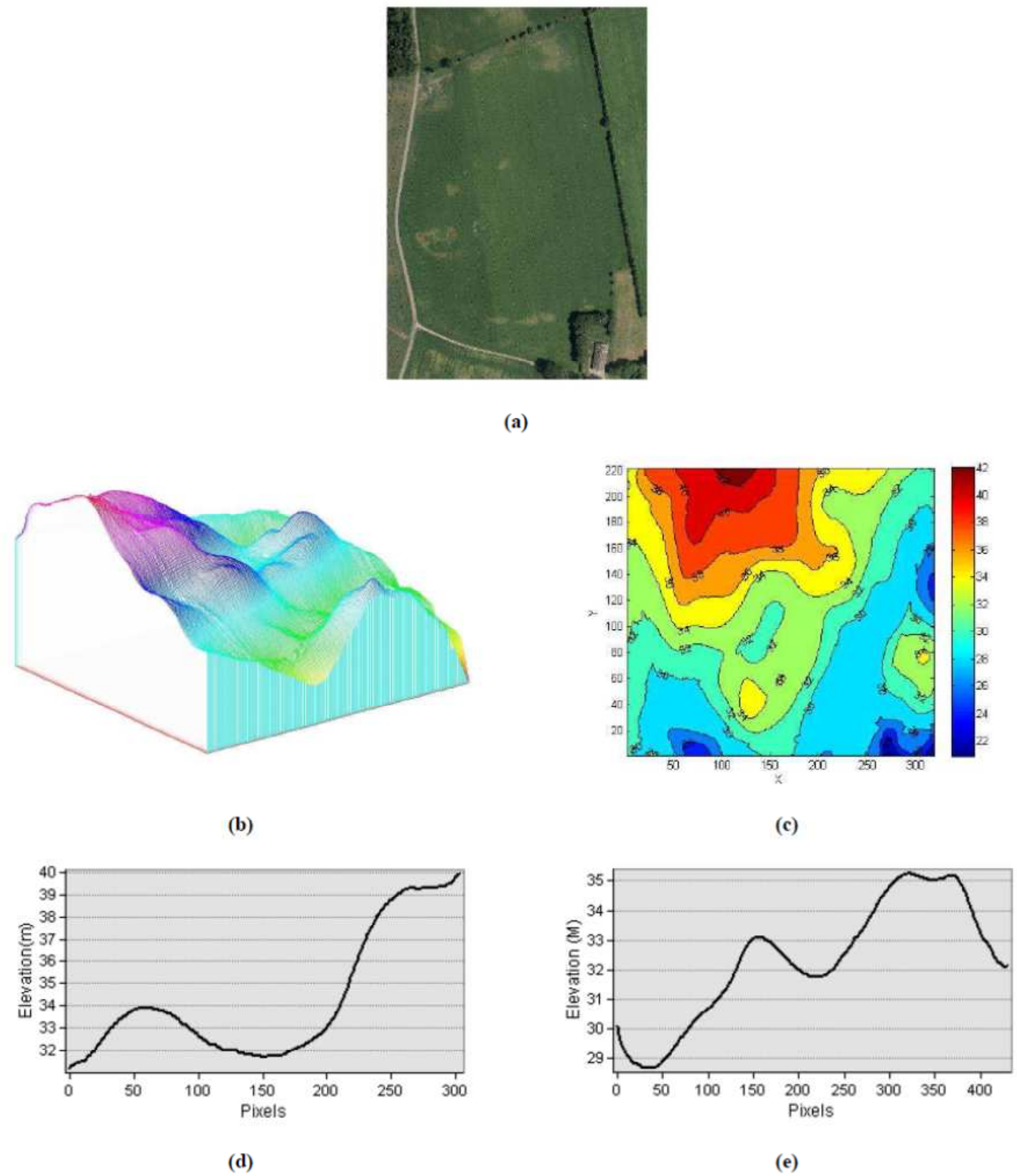

Fig. 3 – Experimental Field A: Satellite image (a), 3D surface view (b), contour view based on the DEM information (c), elevation profile from west (W) towards east (E) (d), and elevation profile from north (N) towards south (S) (e)

3. CASE STUDIES

3.1 THE EXPERIMENTAL FIELDS

Two experimental fields, referred to as field A and field B, were used for demonstrating the functionality of the developed approach. Fig. 3(a) shows the satellite image of the experimental field A (+56° 30' 25.64" N, +9° 35' 11.45" E) which has an area of 11.24 ha (112,416.45 m^2). The minimum, maximum and average elevations on this field are 20.89 m, 42.96 m, and 32.88 m, respectively. The 3D surface of field A, the contour view of the field's elevation model (i.e., DEM) and two elevation profiles of Field A are shown also in Fig. 3. Fig. 4 shows the satellite image of the experimental field B (+56° 30' 48.10" N, +9° 34' 15.61" E) which has an area of 21.22 ha (212,168.67 m^2). The minimum, maximum and average elevations on this field are 18.68 m, 42.96 m, and 35.77 m respectively. The 3D surface of field B, the

(a)

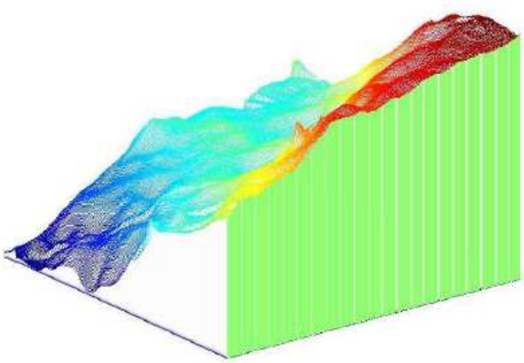

(b)

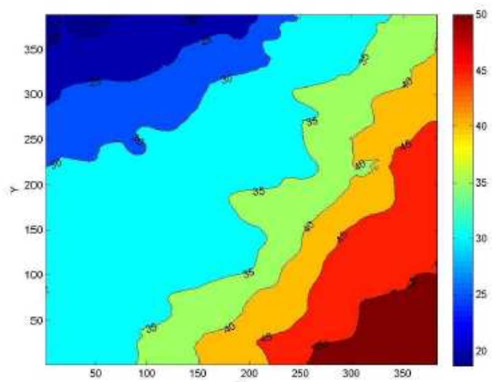

(c)

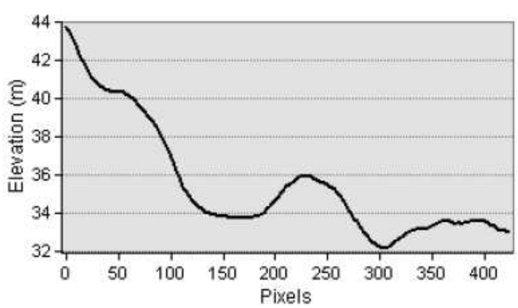

(d)

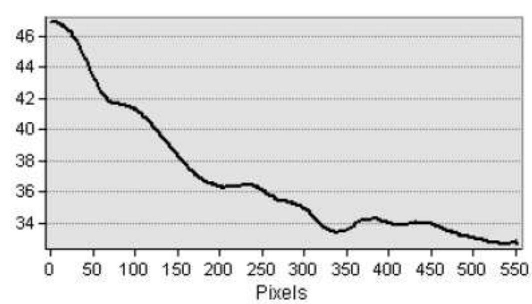

(f)

Fig. 4 – Experimental Field B: Satellite image (a), 3D surface view (b), contour view based on the DEM information (c), elevation profile from west (W) towards east (E) (d), and elevation profile from north (N) towards south (S) (e)

contour view of the field's elevation model (i.e., DEM) and two elevation profiles of field B are shown also in Fig. 4.

time was 10 min, and good surface conditions (i.e., r_{rc}=0.06) were assumed.

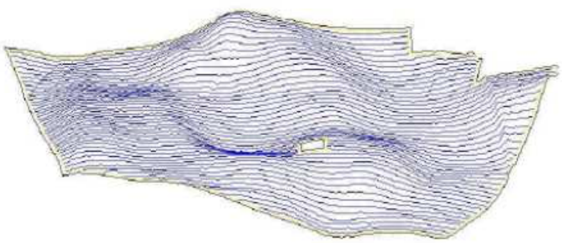

(a)

(b)

Fig. 5 – Field-work tracks configuration for experimental field A for the optimized driving direction for S1 and S3 (a) 100^0, and for S2 and S4 (b) 165^0

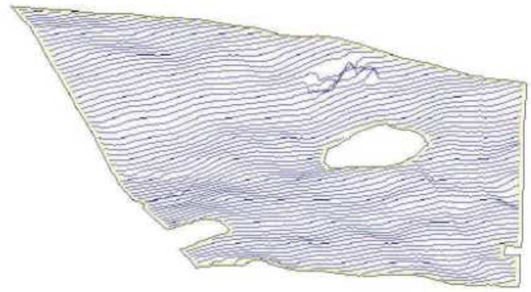

(a)

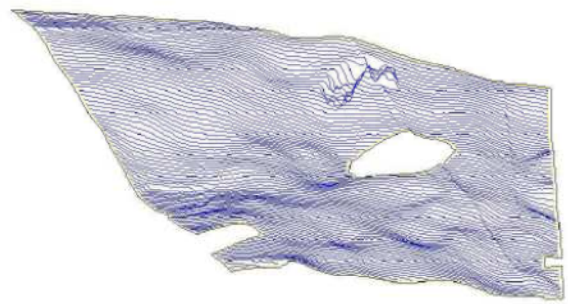

(b)

Fig. 7 – Field-work tracks configuration for experimental field B for the optimized driving direction for S1 and S2 (a) 172^0, and for S2 and S4 (b) 36^0

3.2 RESULTS AND DISCUSSION

The inputs for the simulated operations for both field A and field B included a machinery system involving a tractor and an organic fertilizer injector of a weight of 10.5 t. Four scenarios, in terms of different working width and tanker capacity combinations, were simulated, namely, scenario 1 (S1): 6 m working with and 15 t tanker capacity, scenario 2 (S2): 6 m working width and 25 t tanker capacity, scenario 3 (S3): 9 m working width and 25 tanker capacity, scenario 4 (S4): 9 m working width and 35 t tanker capacity., a tank of maximum capacity of 14.6 t. The assessed working speed was 8 km/h, and the turning speed was 5 km/h. Finally the application rate was assessed 50 t/ha, refilling

The results of the method applied in the experimental fields are listed in Table 2. For field A, the optimized driving angles were found to be 100^o for scenarios S1 and S3 and 165^0 for scenarios S2 and S4. The 3D configuration of the field work tracks for these two driving angles are presented in Fig. 5. Fig 6 presents the energy requirements for the different in-field part operations (i.e. full tanker transport, empty tanker transport, and travelled distance during the application phase) as a function of the tested driving angles. Respectively, in the case of field B, the optimized angles were found to be 172^0 for the scenarios S1 and S2, and 36^0 for scenarios S3 and S4. The 3D configuration of the field work tracks on field B for these two driving angles are presented in Fig. 7, and the

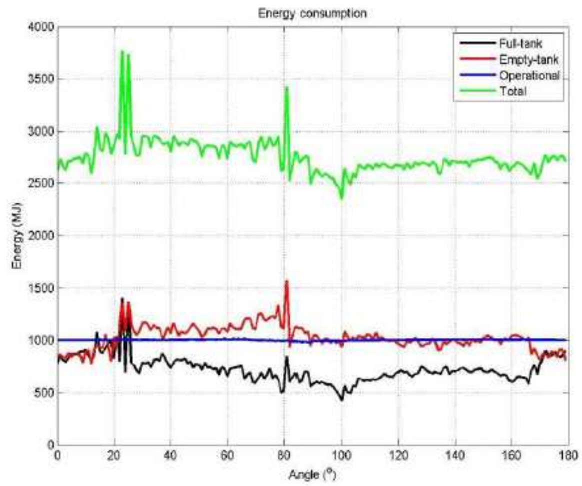

(a) S1 / optimal driving angle: 100°

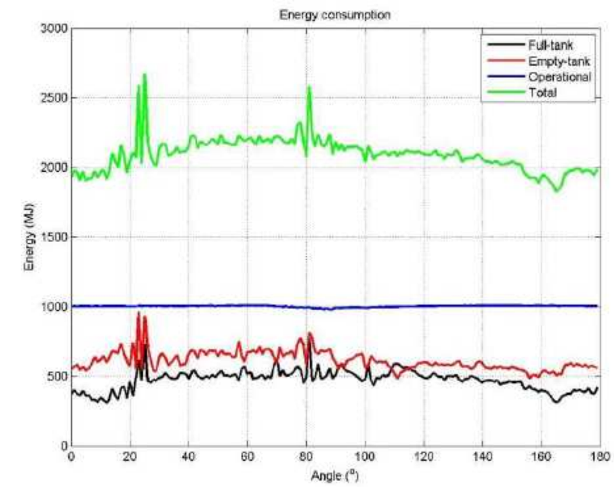

(b) S2 / optimal driving angle: 165°

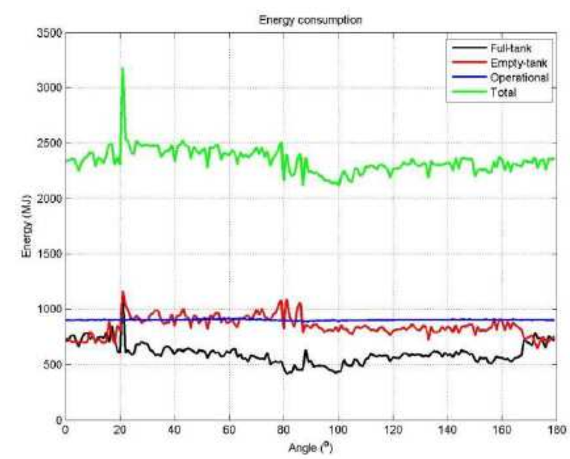

(c) S3 / optimal driving angle: 100°

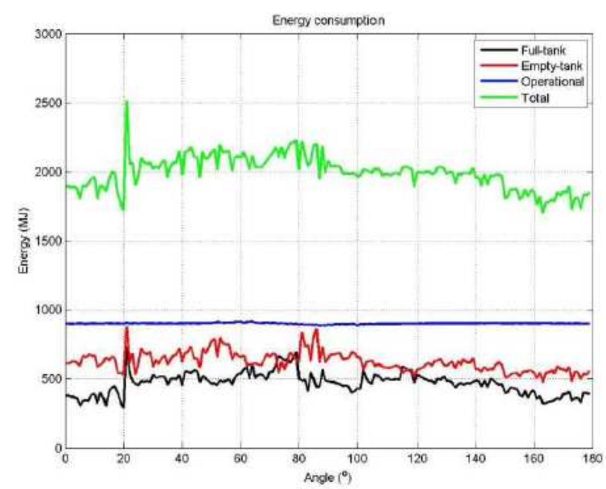

(d) S4 / optimal driving angle: 165°

Fig. 6 – Energy consumed in in-field activities for the different driving angles for the experimental field A

energy requirements as a function of the driving angle are presented in Fig. 8.

The computational time for the four scenarios S1, S2, S3, and S4 were 130.2 min, 127.3, min, 66.0 min, and 60.7 min, respectively, for field A, and 380.1 min, 274.7 min, 184.7 min, and 189.4 min, respectively, for field B. The high computational requirements is caused by the exhaustive search among all possible integer values of driving angles between 1° and 180° which result in 179 executions of the object oriented simulation for the operation. It is obvious that the computational time increases with the number of the travelled distance of the machine for covering the field area which is a function of the field area (for all scenarios the computational time for field B is higher than the corresponding computational time for field A) and of the working width (for both field A and field B the computational times for scenarios S1 and S2 are higher than the computational times for scenarios S3 and S4, since longer working width results to less field work tracks or equivalently to shorter travelled distance). In any case, the high computational requirements of the

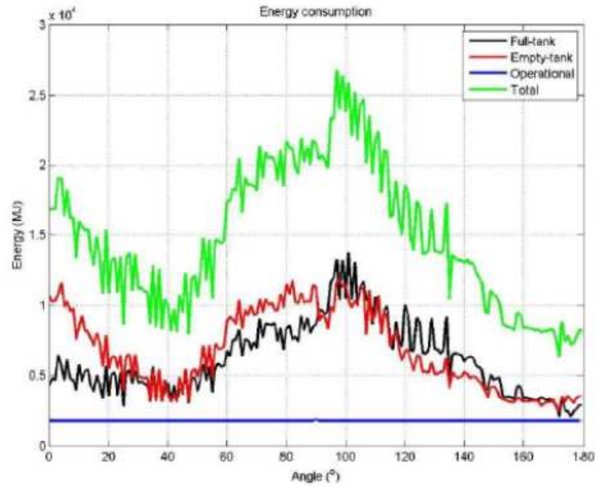

(a) 6.0 m operating width and 15.0 tons tanker (172°)

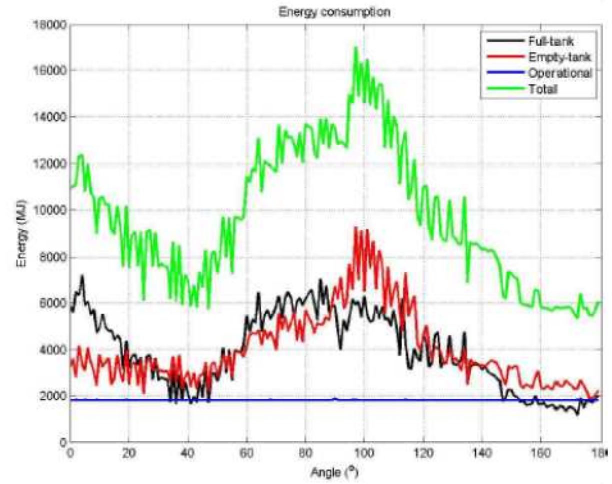

(b) 6.0 m operating width and 25.0 tons tanker (172°)

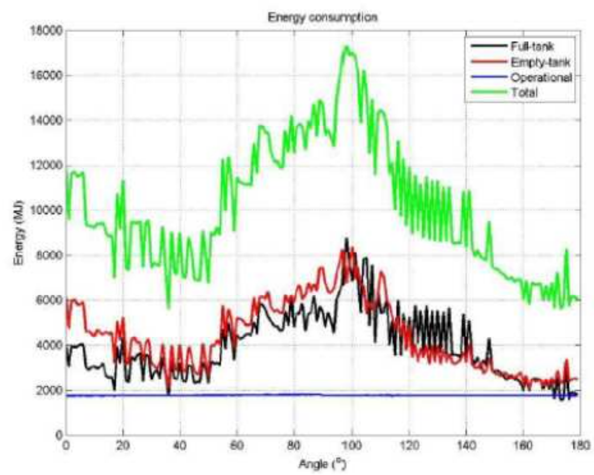

(c) 9.0 m operating width and 25.0 tons tanker (36°)

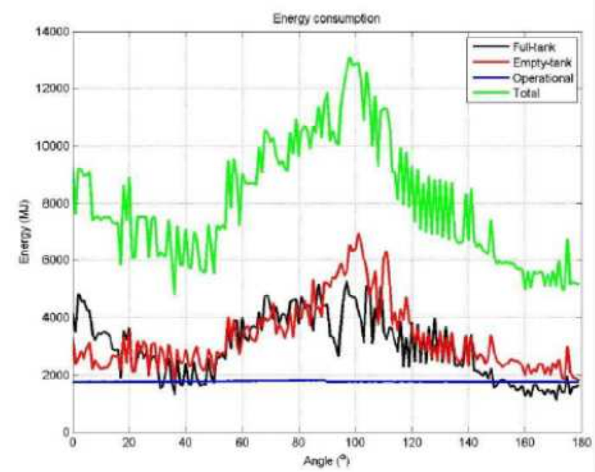

(d) 9.0 m operating width and 35.0 tons tanker (36°)

Fig. 8 – Energy consumed in in-field activities for the different driving angles for the experimental field B

presented system prohibits its application as an on-line (e.g. on-board) tool and its utility is restricted to an off-line decision making tool.

In order to examine the importance of the optimizing the driving angle in the 3D space instead of in the 2D space, all the simulation experiments were also executed assuming plane field area (the z-coordinates values in DEM files were replaced by zero). The resulted optimized driving angles for optimizing in the 2D space were 100^0 for all scenarios in field A, and 4^0 for S1 and S2, and 114^0 for S3 and S4 in field B. There is a coincidence in the solution in both 2D and 3D spaces in the case of S1 and S3, field A. Table 3 lists the energy and operational time requirements for the execution of the operation (in the 3D space) following the driving angle that results from the optimization in 2D space and 3D space. The reduction in the energy requirements when the driving angle is optimized by taking into account the 3D configuration of the field area is 6.4% for field A (ranged between 0 in S1 and 13.6 in S2) and

Table 2- Output operational parameters for the optimized driving angle for the experimental fields

	Field A				Field B			
Scenario	S1	S2	S3	S4	S1	S2	S3	S4
Operating width (m)	6	6	9	9	6	6	9	9
Tank capacity (t)	15	25	25	35	15	25	25	35
Optimal angle (^{0})	100	165	100	165	172	172	36	36
Number of tracks	49	79	32	52	94	94	78	78
Refills	36.0	22.0	22.0	15.0	72.0	43.0	43.0	31.0
Energy requirements for application (MJ)	23,555	19,916	14,812	12,403	52,998	38,749	29,834	24,986
Energy requirements for full tanker transport (MJ)	7,994	5,889	5,938	4,407	39,115	22,373	23,836	17,737
Energy requirements for empty tanker transport (MJ)	17,630	9,561	10,799	6,447	46,608	44,113	28,441	23,496

6.7% for field B (ranged between 6.0% in S1 and 6.8% in S2) resulting in a total average 6.5% for all cases.

Regarding the operational time, as it can be seen in Table 3, the optimization under the criterion of minimizing the energy requirements can have a negative impact. In the case of field A, there is an increase in the operational time of 8.7% in S2 and of 6.7% in S2 (3.8% increase in average for all scenarios in field A), while in the case of field B there is an increase of 10% in S1 and of 2.1% in S2 (3.9% reduction in average for all scenarios in field B).

Based on the previous, the implementation of a multiple-criteria optimization is an objective for future research where the energy requirements and operational time requirements will be both taking into consideration. Another future research objective is a two step optimization approach where beyond the driving angle, the traversal sequence of the tracks (B-patterns) will be a second decision variable.

4. Conclusions

The combination of a modelling approach for the 3D geometrical representation of the field area and an object oriented simulation tool for field operations under capacity constraints can provide the optimized driving angle direction for traversing the parallel field-work tracks for an agricultural vehicle caring out this type of operations, under the criterion of minimised direct energy requirements. The problem presents itself like a typical decision making under uncertainty problem and the results show that the inclusion of additional information, here in the form of field inclinations, improves the utility of the process. Specifically and based on the results from two case study fields, it was shown that the reduction in the energy requirements when the driving angle is optimized by taking into account the 3D configuration of the field area was 6.5% in average for all the examined scenarios, compared to the case when the applied driving

Table 3 - Comparison of energy and operational time requirements between the simulated operations when optimizing under 2D and 3D conditions

		Field A				Field B			
		S1	S2	S3	S4	S1	S2	S3	S4
Total energy requirements (MJ)	2D	2354	2113	2086	1937	6941	5898	5998	5129
	3D		1827		1701	6493	5471	5610	4798
	Discrepancy* (%)	**0**	**13.6**	**0**	**12.2**	**6.0**	**6.8**	**6.5**	**6.5**
Operational time (h)	2D	2.9	2.3	1.9	1.5	6.0	4.7	4.3	3.6
	3D		2.5		1.6	6.6	4.8	3.7	3.1
	Discrepancy* (%)	**0**	**-8.7**	**0**	**-6.7**	**-10.0**	**-2.1**	**14.0**	**13.9**

* (2D value– 3D value)/2D value) x 100%

angle is optimized assuming even field areas. Reduced total energy requirements are subsequently equivalent to reduced fuel consumption and direct CO_2 emissions. Nevertheless, the objective of minimizing energy requirements could result in coverage plans that requires increased operational time and potentially to increased cost. A further consideration of a multiple-objective optimal coverage planning approach for field operations under capacity constraints is needed and this is an objective for future research.

REFERENCES

Bochtis, D. D. & Vougioukas, S. (2008). Minimising the Non-working Distance Travelled by Machines Operating in a Headland Field Pattern. *Biosystems Engineering*, 101 (1), 1-12.

Bochtis, D. D. & Sørensen, C. G (2009). The Vehicle Routing Problem in Field Logistics Part I. *Biosystems Engineering*, 104(4), 447-457.

Bochtis, D. D., Sørensen, C. G. & Green, O. (2012). A DSS for planning of soil-sensitive field operations. *Decision Support Systems*, Accepted Dec 2011, DOI: 10.1016/j.dss.2011.12.005

Fröba, N. & Funk, M. (1995). Teilzeitspezifische Dieselbedarfskalkulation bei Arbeiten in der Außenwirtschaft. *KTBL-Arbeitsblatt: Landtechnik und Pflanzenbau Nr. 0255 'Benötigte Traktormotorennleistung bei landwirtschaftlichen Arbeiten' (N. Fröba, 1995)* (in Germany).

Hameed, I. A., Bochtis, D. D. & Sørensen, C. G. (2011). Driving angle and track sequence optimization for operational path planning using genetic algorithms. *Applied Engineering in Agriculture* (in press).

Hameed, I. A., Bochtis, D. D., Sørensen, C. G. & Nøremark, M. (2010). Automated generation of guidance lines for operational field planning. *Biosystems Engineering*, 107(*4*), 294–306.

Hameed, I. A., Bochtis, D. D., Sørensen, C. G. & Vougioukas, S. (2012). An object oriented model for simulating agricultural in-field machinery activities. *Computers and Electronics in Agriculture*, 81(1), 24–32.

Jin, J. & Tang, L. (2010). Optimal coverage path planning for arable farming on 2D surfaces. *Transactions of the ASABE*, 53(1), 283–295.

Jin, J. & Tang, L. (2011). Coverage path planning on three-dimensional terrain for arable farming. *Journal of Field Robotics*, 28(3), 424–440.

Oksanen, T. & Visala, A. (2009). Coverage path planning algorithms for agricultural field machines. *Journal of Field Robotics*, 26(8), 651–668.

Sulebak, J. R. (2000). *Applications of Digital Elevation Models*. Department of Geographic Information Technology, SINTEF Applied Mathematics, Oslo, Norway.

Tavares, G., Zsigraiova, Z., Semiao, V. & carvalho, M. G. (2009). Optimization of MSW collection routes for minimum fuel consumption using 3D GIS modelling. *Waste Management*, 29(3), 1176–1185.

Chapter 7

Field Robotics in Sports: Automatic Generation of Guidance Lines for Automatic Grass Cutting, Striping and Pitch Marking of Football Playing Fields

Hameed, I. A., Sørensen, C. G., Bochtis, D. D., & Green, O.

International Journal of Advanced Robotic Systems, 2011, 8(1), 113-121.

INTECH OPEN ACCESS PUBLISHER

Field robotics in sports: automatic generation of guidance lines for automatic grass cutting, striping and pitch marking of football playing fields

Ibrahim A. Hameed, Claus G. Sorrenson, Dionysis Bochtis and Ole Green

Aarhus University, Foloum Research Center, Denmark

Abstract Progress is constantly being made and new applications are constantly coming out in the area of field robotics. In this paper, a promising application of field robotics in football playing fields is introduced. An algorithmic approach for generating the way points required for the guidance of a GPS-based field robotic through a football playing field to automatically carry out periodical tasks such as cutting the grass field, pitch and line marking illustrations and lawn striping is represented. The manual operation of these tasks requires very skilful personnel able to work for long hours with very high concentration for the football yard to be compatible with standards of Federation Internationale de Football Association (FIFA). In the other side, a GPS-based guided vehicle or robot with three implements; grass mower, lawn stripping roller and track marking illustrator is capable of working 24 h a day, in most weather and in harsh soil conditions without loss of quality. The proposed approach for the automatic operation of football playing fields requires no or very limited human intervention and therefore it saves numerous working hours and free a worker to focus on other tasks. An economic feasibility study showed that the proposed method is economically superimposing the current manual practices.

Keywords field robotic, sports, FIFA, GPS.

1. Introduction

Field Robotics have been proved reliability in many different areas such as in rehabilitation and surgery (Casals, 1999; Hockstein and O'Malley, 2008), endoscopic surgery (Terris and Amin, 2008), at home personal manipulation (Beetz et al., 2010), mining (Devy et al., 1993), manipulation and assembly in space and in industry (Lueth et al., 1995; Sujan et al., 2002), underwater, construction, and service environments (Khatib, 1999; Zavadskas, 2010), in agriculture such as weed control (Bak and Jakobsen, 2004; Slaughter et al., 2008; Bakkera et al., 2010), mobile cow milking (Rossing et al., 1994), forest fire monitoring (Casbeer et al., 2006), and in hazardous environments such as welding (Lee et al., 2010; Liu et al., 2010) and in nuclear industry (Wehe et al., 1989; Gelhaus and Roman, 1990; Briones et al., 1994).
Automatic guidance system of field robotics and autonomous vehicles usually consists of the following three parts; navigation sensors that supply the system with the position of the vehicle and hence the position deviation from target position, a steering controller which generates a system specific correction control signal and finally an actuator which is combined with the forward movement and steering system of the vehicle to transform guidance information into changes in position and direction (Li et al., 2009; Keicher and Seufert, 2000).

Various guidance technologies, including mechanical guidance, optical guidance, radio navigation, and ultrasonic guidance have been deeply investigated (Reid et al., 2000; Tillett, 1991). High accuracy guidance systems based on global positioning systems (GPS) and real-time kinematic (RTK) GPS are also developed and investigated (Sun et al., 2010; Nørremark et al., 2008; Gan-Mor et al., 2007; Yao et al., 2005). A new generation of equipment based on small, fully autonomous machinery is developed (Blackmore et al., 2005; Schafer et al., 2006). The main benefits of these platforms lie in the reduction of soil compaction and power consumption. The objective is to develop smaller, less intrusive, specialized (Slaughter et al., 2008) and cooperating (Nogucgi et al., 2004) autonomous mobile robots capable of working 24 h a day, in most weather and in harsh soil conditions. Accurate field operations such as weeding in high-value crops or field input applications (seeds, fertilizer, chemicals) may then advantageously be done by these small, light vehicles with economic benefits and less environmental impact. To take advantage of such potentialities, these systems have to be precise enough and act at relatively high speed (from 1 to 5 m/s). Numerous tracking control algorithms are designed leading to less tracking error (Cariou et al., 2009; Pota et al., 2007; Wang and Low, 2006). Experimental results demonstrate that despite sliding phenomena, the mobile robot is able to automatically and accurately achieve a desired pass, with lateral and angular errors, respectively, within ±10 cm and ±2 deg, whatever its shape and whatever the terrain conditions (Cariou et al., 2009). In flat terrain such as football playing fields, better line tracking accuracies could be easily obtained.

In this paper, a promising application of field robotics for doing periodical tasks in football playing fields such as cutting the grass field, pitch and line marking illustrations and lawn striping, is introduced. These tasks are done manually in regular bases and require very high qualified and expensive personnel who have to keep very high concentration during the whole process in order to verify standards and qualities set by FIFA (FIFA, 2007). For the automated operation of these tasks, an approach for generating way points representing the passs of the autonomous vehicle through the football field is introduced. Different sets of way points are obtained for each individual operation. The developed approach is not only limited to football but also applicable to different games and different field sizes. The proposed approach will enable a 24 h a day operation of such tasks without loss of quality. It will also save many working hours and free manpower to focus on other tasks and improve grass quality due to less soil compaction.

2. Standard FIFA dimensions of football playing field

For all football matches at the top professional level and where major international and domestic games are played, the playing field should have dimensions of 105×68 m². These dimensions are obligatory for the FIFA World Cup™ and the final competitions in the confederations' championships (FIFA, 2007). However, other matches can be played on playing fields with other dimensions stipulated by the laws of the game; it is strongly recommended that new stadiums have a 105×68 m² playing field area. In this paper, standard dimensions of a football playing field are adopted; however, other dimensions can be incorporated easily. Additional flat areas are required beside the playing field, ideally behind each goal line, where players can warm up. This area also allow for the circulation of assistant referees, ball boys and girls, medical staff, security staff and the media. It is recommended that there should be a minimum of 8.5 m on the sides and 10 m on the ends of a playing field resulting in an overall playing and auxiliary area of 125×85 m². In this area, a minimum of 5m on the sides or touch lines and 5m behind the goal lines must be of the same surface material as the playing field (grass or artificial turf). The remainder of the auxiliary area can be either of the same surface material as the playing field or it can be a concrete-type surface material which facilitates the movement of service and security vehicles and ambulances. Any part of this additional auxiliary area that will be used as a warm-up area should have the same surface as the playing field and as a result, the grass area of the playing field will have a dimension of 115×78 m². The playing field consist of a center line and center circle of radius 9.15 m, two goal areas of dimensions 18.32×5.5 m², two penalty areas of dimensions 40.32×16.5 m² centered at both field ends. It has also two penalty arcs of radius 9.15 m and four corner arcs of 1 m length. The standard dimensions of a typical playing field are shown in Figs. 1 and 2. For pitch and line marking illustration, a line of thinness 0.12 m is recommended.

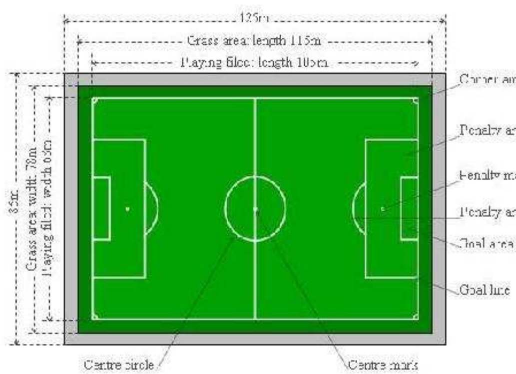

Figure 1. Dimensions of the playing field (FIFA, 2007).

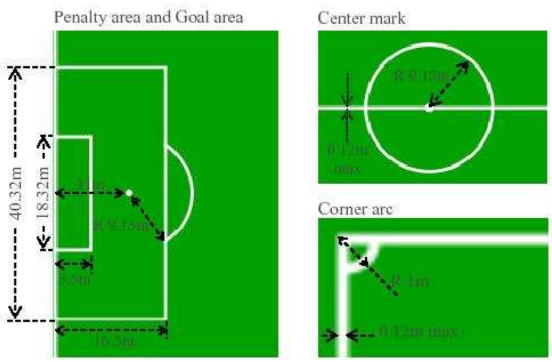

Figure 2. Dimensions of penalty and goal area (left), central mark (up right) and corner arcs (bottom right) (FIFA, 2007).

3. A football's grass field representation

Three different tasks are required to be done in a football grass field, namely, grass cutting, lawn striping, and pitch and line marking illustration and hence three representations, one for each task, are required. For basic lawn striping patterns and if the required width of a lawn stripe is set equal to the operating width of the grass mower, grass cutting and lawn striping tasks could be done simultaneously by attaching a striping roller to the rare side of the mobile robot or the autonomous vehicle. For each individual task, a different driving course or what we call a field representation for guiding the vehicle through this specific task is obtained. A driving course is defined by a set of tracks or segments each is defined by a set of waypoints in 2D coordinates. The outer boundary of a grass field of a playing field is defined by a closed polygon (i.e., n vertices) represented in Universal Transverse Mercator (UTM) coordinate system in meters or in latitude/longitude coordinate systems in degrees. The vertices of the grass field outer boundary could be manually obtained by walking around the grass field and collecting enough number of points using a handheld GPS device or RTK-GPS device for better accuracy. It could also directly be obtained from shape files or from Google® maps. These coordinates are used as an input to the developed tool, along with, the operating width of the grass mower, the operating width of the lawn striping roller and the required striping pattern. The output will be three different driving courses, one for each task, represented as a set of way points in degrees (i.e., in latitude and longitude) stored in a KML file which is generally used to display geographic data in an earth browser such as Google maps®. The obtained KML file will be delivered to the vehicle computer control system in order to execute each individual task by the simple point-to-point driving. A general flowchart of the process used to generate these driving courses or task-based field representation is shown in Fig. 3. In the following sections, obtaining the way points for each driving course is explained in details.

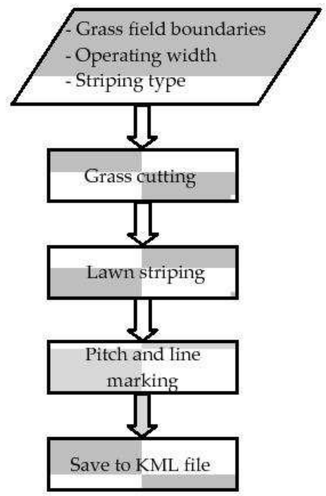

Figure 3. Flow chart of in-football field operations.

3.1 Waypoints generation for grass cutting

According to the standards of the FIFA (FIFA, 2007), the grass area of a football field is defined as a rectangle of an area of 115×78 m^2 but some grass fields have different shapes and different areas. The vertices of the outer boundary of the grass field could be given in the form of a shape file containing the outer boundaries of the grass field of the football stadium as a closed polygon in UTM coordinate system (i.e., in meters) or it could be obtained manually by collecting enough number of vertices to accurately represent the outer boundaries of the grass field in degrees using a handheld GPS device or RTK-GPS device for better accuracy. In case of manual collection of field vertices and since all calculations are done in meters, a conversion from latitude/longitude coordinate system (i.e., in degrees) into UTM coordinate system (i.e., in meters) is required. A tool for geometrical field representation for operational planning, developed by Hameed et al. (2010), is used to obtain the driving course for grass cutting operation. The inputs to the tool are the grass field outer boundary, the operating width of the robot or the autonomous vehicle used for grass cutting, the required driving direction and the number of headland passes. The tool allows for a driving direction defined by the angle between horizontal right-axis and the given line representing that direction. In this paper and for the sake of simplicity, the driving direction is defined as the line connecting any two different vertices of the grass field outer boundary. A flowchart showing the developing process of a driving course for grass cutting process is shown in Fig. 4.

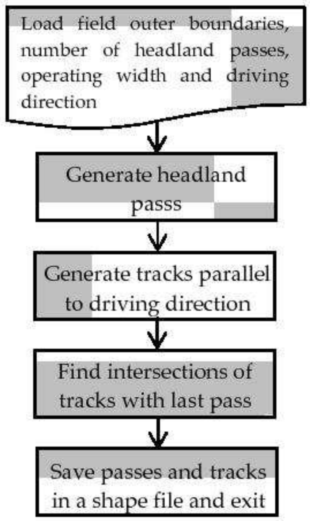

Figure 4. Flow chart of developing a driving course for grass cutting operation.

The developed tool reads the field's outer boundary from field shape file, the required number of headland passes, the driving direction and the operating width of the implement used for grass cutting (i.e., mower). The headland passes are generated by producing lines parallel to the field outer boundaries. Sharp edge and loop removal filters which remove possible sharp edges and possible loops in the generated headland pass are applied in order to produce smoother pass, see Fig. 5(a and b). The remaining field area, after the headland area, is then used for producing tracks parallel to the decided driving direction. The resultant waypoints are then saved in a shape file or KML file in order to be used by the robot or the autonomous vehicle for the automatic grass cutting operation. A good strategy to increase the life time of grass is to cut in different directions each time mowing is required and shift tracks a little in order to avoid tracks course by repeated passes. Fig. 6 shows the grass mowing process using 2 tracks in headland area and covering other field area by generating tracks parallel to the goal lines.

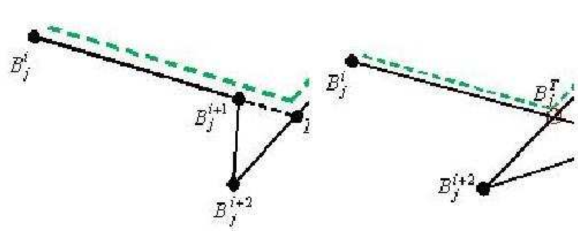

(a) (b)

Figure 5. Filters applied to field headland passes in order to remove noises and irregularities for smoother headland passes: Sharp edge removal filter (a) and loop removal filter (b).

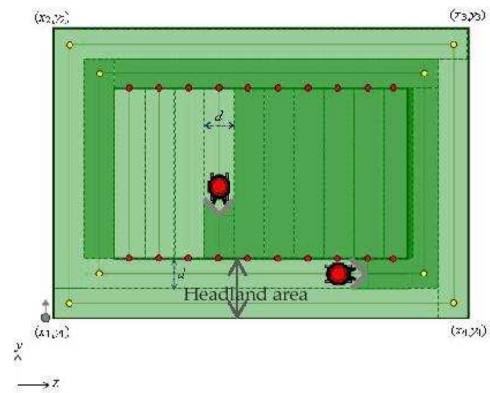

Figure 6. Basic grass cutting operation: 2 tracks in the headland area, d is the operating width of the mower implement/striping roller and driving direction is parallel to one of the field edges.

3.2 Waypoints generation for lawn striping

Intensifying lawn stripes to obtain different patterns is an optional step. Light and dark colored stripes are simply caused by light reflection off the blades of grass. It has not been cut at a different height nor is it a different breed of grass. The stripes are made by bending the blades of grass in different directions. The direction that the grass is bent determines the *light* or *dark* colored stripe. When the blades of grass are bent away from the viewer, the grass appears lighter in color because the light is reflecting off of the wide, lengthy part of the blade. When the blades of grass are bent towards the viewer, the grass appears darker as the viewer is looking more of the tips of the blades (a smaller reflective surface) and the shadows under the grass. So cutting a lawn in an opposing pattern (up/down, right/left, north/south, east/west etc) provides the most contrasting stripe effect. Interestingly, as the color of the stripe is dependent upon what direction the viewer is looking at it from, a light colored stripe will appear dark from the opposing direction. The easiest way to intensify the stripe is to bend the grass farther. The best way to do that is to physically contact the grass with a roller and press it to the ground. Some common stripe patterns, but not restricted to, are as follows (Scag Power Equipment, 2010):

(a) Basic stripe pattern (BSP): tracks are generated parallel to one of the field sides, shown in Fig. 7. In this case, it is not required to intensify lawn stripes in a separate step if it is possible to attach the roller to the vehicle's three-point-linkage while grass is being mowed.

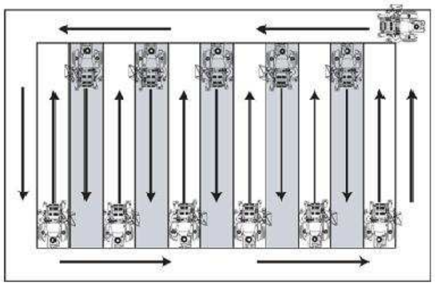

Figure 7. Baisc lawn stripe pattern (Scag Power Equipment, 2010).

(b) Checkerboard stripe pattern (CSP): this pattern is obtained by applying the stripes parallel to one side of the field and then in perpendicular direction (i.e., parallel to the other side of the field), shown in Fig. 8.

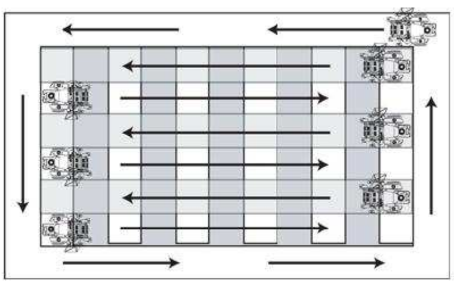

Figure 8. Checkerboard stripe pattern (Scag Power Equipment, 2010).

(c) Diagonal stripe patterns (DSP): this pattern is achieved using the same techniques as the CSP listed above. Simply apply the stripes in a diagonal direction, shown in Fig. 9.

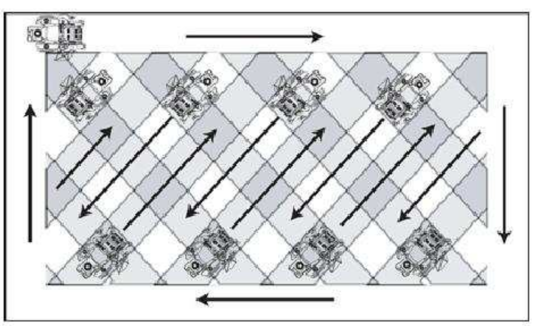

Figure 9. Diagonal stripe pattern (Scag Power Equipment, 2010).

Other patterns could be easily designed and obtained. The waypoints for these patterns are generated by using the automatic route planning algorithm described in Section 3.1 by selecting the appropriate driving direction to generate each specific pattern.

3.3 Pitch and line marking illustration algorithm

In this section, the algorithm for generating waypoints for the vehicle to navigate through the field for pitch and line marking illustrations is introduced. The input to the algorithm is the UTM coordinates of the grass field outer boundaries. The outputs are the vertices of the playing field, penalty area, goal area, central mark and corner arcs in UTM coordinate system. The coordinates are then converted into degrees and saved in a KML file for navigation.

According to standards of FIFA, the playing field is a rectangle of length l_p = 105 m and width w_p = 68 m. The dimensions for the center circle and penalty kick arcs are measured from the center of the field and penalty spot respectively, to the outside of the lines. The radii of corner arcs are 1 m and the radii of the center circle and goal circle are 9.15 m. The inside faces of the goal-posts should be 7.32 m apart and the distance between the ground and the underside of the crossbar is 2.44 m. The width of the playing lines should be 120 mm maximum and the goal-line should be marked the same width as the depth of the goal posts which should be considered in the design of the pitch and track marking implement. Line color is not specified but is traditionally white. The external dimensions should include the width of the lines. The center of the penalty spot is measured from the outside of the goal line. The UTM coordinates of the playing field for pitch and line marking illustrations are obtained as follows.

(a) Boundaries of the playing field

The dimensions of a playing field, according to standards of FIFA, are 105×68 m², as shown in Fig. 1. In order to obtain the UTM coordinates of the four corner points (i.e., vertices) of the rectangle-shaped playing field, if the grass field is rectangle, the grass field is de-expanded by distance r m, given by Eq. (1) where l_g, w_g are the length and width of the grass field, respectively, and l_p, w_p are the length and width of the playing field, respectively.

$$r = (l_g - l_p)/2 = (w_g - w_p)/2 \quad (1)$$

If the grass field is not a rectangle, it must be rectanglized first by finding the intersection points between each touch (i.e., longest edge of the playing field) and goal (i.e., shortest side of the playing field) lines and repeating this process until we obtain the four vertices of the rectangle-shaped playing field. The de-expanded field is obtained by applying the automatic route planning algorithm described in Section 3.1as the process of obtaining a headland pass.

(b) Center line
Center line is the line connecting the two center points located exactly at the middle of each of the two opposite touch lines. A center point is obtained by finding the UTM coordinates of the point dividing the touch line by two (i.e., $l_p/2$).

(c) Center mark
Center mark is the point located exactly at the middle of the center line. It is obtained by finding the UTM coordinates of the point located on the center line and dividing it by two. The center mark is illustrated by a circle of 0.15 m radius.

(d) Center circle
The center circle is illustrated by a circle of 9.15m radius centered at the center mark with a line of 0.12 m thickness.

(e) Penalty area
Penalty area is the area bounded by the penalty lines forming a rectangle of area of 40.32×16.5 m^2. There are two opposing penalty areas in the field, each consists of penalty lines, penalty mark and penalty arc.

(1) Penalty lines
There are three penalty lines; one line, of length 40.32 m, parallel to the goal line and two parallel lines, of length 16.5 m, perpendicular to the goal line and at distance of 40.32 m from each other. The two vertices of the perpendicular penalty lines are located on the goal line at distance of (68-40.32)/2 m and (68+40.32)/2 m from each end of the goal line, respectively. The other two vertices are located at the parallel penalty line and at distances of (68-40.32)/2 m and (68+40.32)/2 m from each end of the parallel penalty line, respectively. The parallel penalty line is the line parallel to the goal line and at distance of 16.5m from it.

(2) Penalty mark
Penalty mark is a circle of 0.15 m radius centered at a point located at distance of 11 m from the end point of a line parallel to the touch line (i.e., longest edge of the playing field) and at the center (i.e., at distance of 68/2 m from the touch line) of the side line.

(3) Penalty arc
Penalty arc is an arc of a circle of radius 9.15 m centered at the penalty mark.

(f) Goal area
Goal area is the area bounded by the goal lines (forming a rectangle of area 18.32×5.5 m^2). Goal lines are three; one of length 18.32 m parallel to the goal line and two of length 5.5 m perpendicular to the goal line. The UTM coordinates of the vertices of this rectangle are obtained by allocating two points on the goal line at distances of (68-18.32)/2 m and (68+18.32)/2 m from each of its ending points. The other two vertices are allocated on the line parallel to goal line (i.e., the short side of the playing field) at distance of 5.5 m and at distance of (68-18.32)/2 m and (68+18.32)/2 m from each of its ending points.

(g) Corner arcs
There are four corner arcs in the field located at each corner point of the playing field with radius of 1 m.

A computer program to generate the above vertices has been developed using Matlab® programming language and it is available for free for interested readers by contacting the corresponding author.

4. Economic feasibility study

In this section, the costs of the manual practices of the above operations are investigated. As an example, in Viborg football stadium, Stadion Alle 1-3, 8800 Viborg, Denmark (http://viborg.dk/stadion), grass mowing, intensifying lawn stripes and pitch and line marking illustrations cost from 40 to 50 working hours per week. One working hour costs on average 350.0 Danish Krone so totally 672,000.0 to 840,000.0 Danish Krone (1.0 Danish krone = 0.18 USD) per year. In addition, new workers require especial and expensive training which is not considered here. Using the developed system, stadiums will invest only in machines and it will be able to save extra working hours and cost of training new employs. The developed system will allow a worker to focus on other works, save time and able to work 24 hours/7 days per week.

5. Simulation results

In this section, the developed algorithms are successfully applied to several international and national football stadiums in Denmark and the world. Due to the limited space and to avoid repeatability, the resultant waypoints of applying the developed algorithms to Viborg Stadium, Stadion Alle 1-3, 8800 Viborg, Denmark, will only be introduced. The latitude/ longitude coordinates (in degrees) of the outer boundaries of the grass field of Viborg Stadium is shown in Table1. A satellite image of Viborg Stadium, Stadion Alle 1-3, 8800 Viborg, Denmark, is shown in Fig. 10.

Points	Easting	Northing
1	56.456359	9.402698
2	56.456339	9.40272
3	56.455373	9.402473
4	56.455357	9.402434
5	56.455438	9.401313
6	56.455455	9.401286
7	56.456427	9.40154
8	56.456447	9.401577

Table 1. The UTM coordinates of the grass field of Viborg football stadium.

The grass field of Viborg stadium is not rectangular and therefore it is described by eight vertices. Two different driving courses can be followed by the autonomous vehicle or the robot in its point-to-point motion in order to cut the grass field; the first driving course is obtained by driving parallel to the touch line of the grass field (i.e, parallel to the longest side of the grass field) while the second driving course is obtained by driving parallel to the side line of the grass field (i.e., perpendicular to the touch line of the grass field or parallel to the goal line). The resultant driving courses for a grass mowing implement of 2 m working width are shown in Fig. 11. Basic lawn striping patterns can be easily obtained by combining a striping roller with a grass mower and by using the same driving courses shown in Fig. 11. Checkerboard striping pattern is obtained by driving parallel and then perpendicular to the longest side of the grass field, while, the diagonal striping pattern is obtained by driving parallel and then perpendicular to diagonal of the grass field, as it is shown in Fig. 12(a) and (b), respectively, for a striping roller of 2 m operating width. The way points of these striping patterns can be saved into KML files which can be easily used for the auto-steering of the autonomous vehicle or simply for visualizing the resultant driving course on Google maps as it is shown in Fig. 13 (a) and (b) for the checkerboard and diagonal striping patterns, respectively. The course for pitch and line marking illustrations is shown in Fig. 14(a) for the waypoints in UTM coordinate system (i.e., in meters) and in Fig. 14(b) for the waypoints converted into lat/lon coordinate system (i.e., in degrees) and stored in a KML file for the easily representation of the resultant on Google maps.

Figure 10. Satellite image of Viborg Stadium (Stadion Alle 1-3, 8800 Viborg, Denmark).

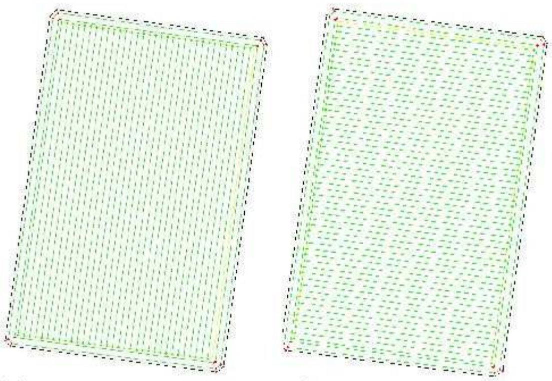

(a) (b)

Figure 11. Way points for mowing Grass field of Viborg Stadium and the classical stripe pattern in two different driving directions.

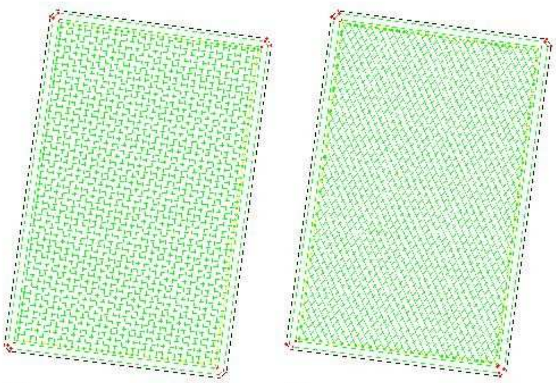

(a) (b)

Figure 12. (a) Checkerboard stripe pattern, and (b) diagonal stripe pattern of Viborg stadium.

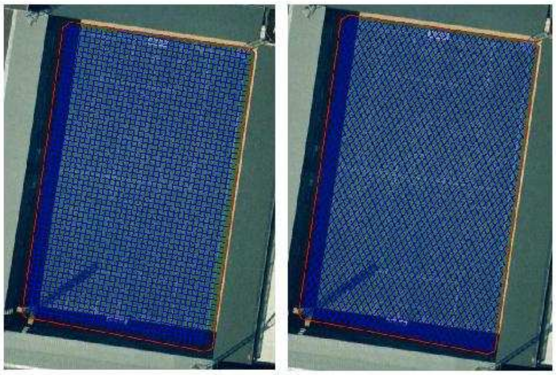

(a) (b)

Figure 13. (a) Checkerboard stripe pattern, and (b) diagonal stripe pattern of Viborg stadium.

Figure 14. Pitch and line marking illustrations of Viborg Stadium operated using the algorithm: (a) waypoints in meters, (b) a KML file of waypoints in degrees.

Simulation results showed that the proposed method is able to automatically provide waypoints with very high accuracy without exhausting on-ground measurements. For the current GPS-guided autonomous vehicles, the navigation accuracy on a straight line motion is approximately ±2 cm. it has been proved that the system can perform better under good conditions and terrain (Keicher and Seufert, 2000). When the proposed method applied to other stadiums, it was able to detect that some stadiums such as the Danish National Stadium and the Egyptian army stadium are not compatible with the dimensions approved by FIFA for international games.

6. Conclusions

The developed tool provides simple algorithms able to automatically carry out the periodical operations which are used to be done manually in regular bases in football stadiums. These operations require very high qualified and expensive personnel who have to keep very high concentration during these operations in order to match the standards set by the FIFA. The developed tool provides the waypoints for each operation in meters and in degrees and store it in a standard KML files to be later used by the vehicle computer control system for navigation. The developed approach is not limited to football playing fields but can also be used for other games such as hockey, tennis, etc. It also can operate playing fields of different sizes and produce very complex lawn striping patterns with no human intervention and with very high accuracy. The tool is implemented using Matlab® from Mathworks™ and is available for free for interested readers.

Acknowledgements

The authors are gratefully acknowledging Mr. Torben Simonsen, Viborg stadium, 8800 Viborg, Denmark and the constructive comments of anonymous referees.

7. References

Alakukku, L., Poyhonen, A., Sampo, M. (1997). Soil compaction control with a light, unmanned tractor in two tillage systems. *In proceedings of the 14th Conference "Agroecological and economic aspects of soil tillage"*, Pulawy, Poland.

Bak, T. and Jakobsen, H. (2004). Agricultural robotic platform with four wheel steering for weed detection. *Biosystems Engineering*, 87(2), pp. 125-136.

Bakkera, T., Asselt vana K., Bontsemab, J., Müllerc, J. and Straten vana, G. (2010). Systematic design of an autonomous platform for robotic weeding. *Journal of Terramechanics*, 47(2), pp. 63-73.

Beetz, M., Jaina, D., Mösenlechnera, L., and Tenortha, M. (2010). Towards performing everyday manipulation activities. *Robotics and Autonomous Systems*, 58(9), pp. 1085-1095.

Briones, L., Bustamante, P., and Serna, M. A. (1994). Robicen: A wall-climbing pneumatic robot for inspection in nuclear power plants. *Robotics and Computer-Integrated Manufacturing*, 11(4),pp. 287-292.

Cariou, C., Lenain, R., Thuilot, B., and Berducat, M. (2009). Automatic Guidance of a Four-Wheel-Steering Mobile Robot for Accurate Field Operations. *Journal of Field Robotics*, 26(6-7), pp. 504-518.

Casals, A. (1999). Medical robotics at UPC. *Microprocessors and Microsystems*, pp. 69-74.

Casbeer, D. W., Kingston, D. B., Beard, R. W., McLain, T. W., Li, S. M., Mehra, R. (2006). Cooperative forest fire surveillance using a team of small unmanned air vehicles. Int. J. Syst. Sci. 37(6), 351.

Devy, M., Orteu, J. J., Fuentes-Cantillana, J. L., Catalina, J.C. , Rodriguez, A., Dumahu, D. and Villeneuve de Janti, P. (1993). Mining robotics: Application of computer vision to the automation of a roadheader. *Robotics and Autonomous Systems*, 11(2), pp. 65-74.

Diekhans, N. (1999). Claas Industrietechnik product information, CIT development department.

FIFA (2007). Football stadiums: technical recommendations and requirements (http://www.fifa.com/mm/51/54/02/football_stadiums_technical_recommendations_and_requirements_en_8211.pdf).

Gan-Mor, S., Clark, R. L., and Upchurch, B. L. (2007). Implement lateral position accuracy under RTK-GPS tractor guidance. *Computers and Electronics in Agriculture*, 59(1-2), pp. 31-38.

Gelhaus, F. E., and Roman, H. T. (1990). Robot applications in nuclear power plants. *Progress in Nuclear Energy*, 23(1), pp. 1-33.

Hameed, I. A., Bochtis D. D., Nørremark M., Sørensen C. G. (2010). Automated generation of guidance lines for operational field planning. *Biosystems Engineering*, doi:10.1016/j.biosystemseng.2010.09.001.

Hockstein, N. G., O'Malley, B. W. (2008). Transoral robotic surgery. *Operative Techniques in Otolaryngology*, 19, pp. 67-71.

Keicher, R. and Seufert, H. (2000). Automatic guidance for agricultural vehicles in Europe. *Computers and Electronics in Agriculture*, 25 (2000), pp. 169–194.

Khatib, O. (1999). Mobile manipulation: The robotic assistant. *Robotics and Autonomous Systems*, 26(2-3), pp. 175-183.

Lee, D., Lee, S., Ku, N., Lim, C., Lee, K.-Y., Kim, T.-W., Kim, J. and Kim, S. H. (2010). Development of a mobile robotic system for working in the double-hulled structure of a ship. *Robotics and Computer-Integrated Manufacturing*, 26(1), pp. 13-23.

Li, M., Imou, K., Wakabayashi, K., and Yokoyama, S. (2009). Review of research on agricultural vehicle autonomous guidance. *International Journal of Agriculture and Biological Engineering*, 2(3), pp. 1-16.

Liu, Z., Bu, W., and Tan, J. (2010).Motion navigation for arc welding robots based on feature mapping in a simulation environment. *Robotics and Computer-Integrated Manufacturing*, 26(2), pp. 137-144.

Lueth, T. C., Nassal, U. M., and Rembold, U. (1995). Reliability and integrated capabilities of locomotion and manipulation for autonomous robot assembly. *Robotics and Autonomous Systems*, 14(2-3), pp. 185-198.

Nieminen, T., Sampo, M., Mononen, J. (1996). Development of a control system for autonomous agricultural vehicles. *Agricultural Engineering*, Paper (096A-094).

Nørremark, M., Griepentrog, H. W., Nielsen, J., Søgaard, H. T. (2008). The development and assessment of the accuracy of an autonomous GPS-based system for intra-row mechanical weed control in row crops. *Biosystems Engineering*, 101(4), pp. 396–410.

Nørremark, M., Olsen, H. J. and Lund, I. (2009). The development of a computer vision based and real-time plant tracking system for dot spraying. *In proceedings of the Joint International Agricultural Conference*, book of abstracts, Wageningen Academic Publishers.

Rossing, W., Devir, S., Hogewerf, P.H., Ipema, A.H., Ketelaar-de Lauwere, C.C. and J. Metz-Stefanowska, J., 1994. Robotic milking: State of the art. In: *Proc. 33rd Ann. Meeting Natl. Mastitis Council*, pp. 212–221.

Scag Power Equipment (2010). Lawn Striping and Lawn Patterns - How Do They Work? Retrived from http://www.scag.com/lawnstriping.html.

Slaughter, D.C., Gilesa, D.K. and Downeya, D. (2008). Autonomous robotic weed control systems: A review. *Computers and Electronics in Agriculture*, 61(1), pp. 63-78.

Stoll, A., Kutzbach, H. D. (1999). Concept of a guidance system for agricultural vehicles. *In proceedings of the 2nd Europ. Conf. On Precision Agriculture*, Odense, 11-15 July 1999, Sheffield, Academic Press, pp.825-835.

Stoll, A., Kutzbach, H. D. (2000). Guidance of a Forage Harvester with GPS. *Precision Agriculture*, 2, pp. 281–291.

Sujan, V. A., Dubowsky, S., and Ohkami, Y. (2002). Robotic Manipulation of Highly Irregular Shaped Objects: Application to a Robot Crucible Packing System for Semiconductor Manufacture. *Journal of Manufacturing Processes*, 4(1), pp. 1-15.

Sun, H., Slaughter, D. C., Perez Ruiz, M., Gliever, C., Upadhyaya, S. K. and Smith R. F. (2010). RTK GPS mapping of transplanted row crops. *Computers and Electronics in Agriculture*, 71, pp. 32-37.

Terris, D. J. and Amin, S. H. (2008). Robotic and endoscopic surgery in the neck. *Operative Techniques in Otolaryngology-Head and Neck Surgery*, 19(1), pp. 36-41.

van Zuydam, R. (1999). A drivers steering aid for an agricultural implememt, based on an electronic map and Real Tine Kinematic DGPS. *Computers and Electronics in Agriculture*, 24, pp. 153–163.

Wehe, D. K., Lee, J. C., Martin, W. R., Mann, Hamel, W. R. and Tulenko, J. (1989). Intelligent robotics and remote systems for the nuclear industry. *Nuclear Engineering and Design*, 113(2), pp. 259-267.

Wulf, B. (1997). Automatische Seitensteuerung bei Pflegegeraten und Erntemaschinen. *VDI Landtechnik*, 3, pp. 130–131 (in Dutch).

Yao, L., Li, L., Zhang, M. and Minzan, L. (2005). Automatic Guidance of Agricultural Vehicles Based on Global Positioning System.*IFIP International Federation for Information Processing, Artificial Intelligence Applications and Innovations*, 187, pp. 617-624.

Zavadskas, E. K. (2010). Automation and robotics in construction: International research and achievements. *Automation in Construction*, 19(3), pp. 286-290.

Chapter 8
General Discussion

8.1. Introduction

In this Chapter the developed methods and the results obtained from the separate Chapters which make up this Thesis are discussed. The main objective guiding the dedicated research as outlined in the Introduction Section was to investigate and conclude if the developed planning algorithms significantly will advance optimized autonomous or semi-autonomous operations of various fieldworks in bio-production. The developed algorithms and models included:

1. A field geometrical representation for a user defined driving angle and number of headland passes or polygons.
2. A coverage pattern generator as a sequence of waypoints in UTM coordinates in the form of KML or shape file to be manipulated by the vehicle's on-board control computer or for visualization purposes.
3. An optimized driving angle and track sequence generator for field operations under various criteria functions involving minimised operational time, minimised fuel consumption, etc.
4. A clustering of field tracks into blocks followed by an optimum sequence of blocks that minimizes the connection distances between blocks and avoids obstacles.
5. An inclusion of 3D field terrains and terrain elevation as additional information to further advance energy efficiency of field operations
6. A simulation model integrating the individual coverage path planning components as part of a dedicated decision support system (DSS) capable of testing operational scenarios.

8.2. Optimized coverage path planning on 2D surfaces

A set of 2D field geometrical representation algorithms were developed to provide straight and curved field work tracks. The developed algorithms can deal with field as a single block or as multi-blocks. In multi-block operation, concave field shapes are divided into a number of simple convex sub-fields and provide the optimal driving direction in each sub-field. These algorithms were based on the minimum bounding box (MBB) principal that enable full field coverage regardless of the field's shape complexity and without any human intervention (Hameed et al., 2010). A genetic algorithm based approach for optimizing driving angle and track sequencing was developed (Hameed et al., 2011a). The resultant optimized path enables field operations to be carried out in a manner that minimizes operational time, nonworking travelled distance and skipped and overlapped area over the entire field area. Simulation results showed the superiority of the developed algorithms in reducing total operational time and hence fossil fuel consumption by an amount in the range of 10-15% when applying the optimized routes. For dealing with the presence of in-field obstacles a method has been developed in which field tracks are clustered into independent blocks and the sequence of blocks is optimized in a manner that minimizes the connection distance between blocks. Simulation results showed a systematic and complete coverage regardless of the number and arrangement of these obstacles (Hameed et al., 2011b).

8.3. Coverage path planning in 3D field terrain

The terrain structure of many farms has considerable influence on the design and optimization of the path planning. A three-dimensional (3D) representation of field terrain will not only provide more information to supported automated farming operations but also improve the presentation of crop information in GIS (Rovira-Mas et al., 2005). For some of the 3D terrain surfaces, there could be problems applying 2D coverage path planning algorithms, which assume that fields are flat and ignore elevation changes. Elevation changes or slopes have considerable influence on soil erosion, skips and overlaps between furrows, and vehicle's fuel consumption in driving over rolling terrains (Jin and Tang, 2011).As mentioned in the introduction, the only reported 3D terrain field coverage path planning is the work of Jin and Tang (2011) where an optimized 3D terrain field coverage path planning algorithm has been developed. The developed algorithm classifies field terrain into flat and slope areas and then apply the most appropriate path planning strategy to each region so as to achieve the minimum coverage cost in terms of headland turning cost, soil erosion cost and skipped and overlapped area cost. In this approach, a decomposition algorithm is applied to classify the terrain into only flat areas and slope areas where the proper planning method can be applied to each sub-region and therefore a global solution can not be achieved. In the present Thesis, a new 3D coverage path planning approach is presented based on an optimization algorithm which finds an optimized driving angle enabling an agricultural vehicle carrying time-depended load to cover the entire field in a manner that minimizes the total amount of energy requirements. The developed approach results the solution is capable of optimizing fuel consumption for three roadway or soil conditions (i.e., good, medium and bad) in relatively short time by using low computational resources regardless of the field shape and terrain complexity.

8.4. Energy optimization

Fuel consumption is playing a significant economical and environmental role in arable farming and efforts are directed toward reducing the energy consumption in field work (i.e., tractors, combines, mowers, balers, etc.) and hence the overall costs of agricultural production (Schnepf, 2004). The agricultural vehicles used in various field work activities can emit significant levels of undesirable atmospheric pollutant emissions, which include carbon dioxide (CO2) and nitrogen oxide (NO), both of which are of major concern due to their contribution to the greenhouse effect and to acid rain. Reducing pollutant outputs through fuel economy therefore yield both environmental and financial benefits (Tavares et al., 2009). An optimised energy usage in arable farming involves the reduction of fuel consumption through the efficient use of the available machinery system in terms of efficient operational planning and execution and hence, the invoking of optimal field area coverage becomes necessary. Research into the potential savings from the implementation of B-patterns (i.e., optimal track sequences) has shown that the savings in terms of operational time ranged from 8.4% to 17.0%, while the mean savings in terms of fuel consumption, and consequently the CO_2 emissions and other greenhouse gases was in the order of 18% (Bochtis et al., 2010). In the presented Thesis, it was shown that the implementation of the optimal driving direction in the 3D approach of the coverage planning leads to even more fossil fuel potential savings relative to normal practices. By reducing the fuel consumption by the above mentioned percentages, there is the perspective of roughly savings of 25 million l of fuel and 60 million kg greenhouse gasses per year (based on rough estimates using Denmark Statistics (2011) and Iowa State University report (2011)).

Farmers, lacking alternatives, usually select an intuitive driving angle based on their own experience, usually following the longest border of the field. The selected driving pattern is usually not the optimal one, resulting in excessive use of time and fuel mainly because of turnings in the beginning and end of the tracks (over the headland area of the field). Significant reduction in fuel consumption can be achieved as a result of the direct application of the optimized coverage path planning.

8.5. Decision support system

Planning of field operations is essential for the operational efficiency in terms of time and cost, especially in complex operations involving capacity constraints and cooperating units. In order to deal with such type of planning problems an object oriented simulation which simulates in detail in-field machine activities during the execution phase, was developed and applied. The simulation model was developed in combination with optimized coverage path planning algorithms. It was shown that the simulation model provides all the key operational parameters necessary for the evaluation of a selected operational scenario. This makes it feasible to be used as an integral part of a decision support system (DSS) for advising farmers about infield operational decisions (e.g., traffic system, driving direction, refilling position) and machinery dimensioning (e.g., tank capacity, operating width, etc.). As an example, simulation results showed that the adoption of the controlled traffic farming (CTF) system increases the operational time approximately 5% while at the same time decreases the field efficiency by an amount of about 8.25%, based on selected field scenarios involving organic fertilising. Another example, regarded the selection of the driving direction, where the results showed a decrease in operational time by 4.5% and an increase in the field efficiency by 6.6% when comparing selected scenarios with different driving directions. The developed system can be used by farmers in selecting the mechanical specifications of the farm machinery system by testing it for different operating widths and tank capacities and selecting the most appropriate one.

8.6. General conclusions

The main goals of the Thesis were achieved through the development of algorithmic approaches and models for field area geometrical representation and field coverage planning. The developed algorithms can be applied on both 2D and 3D field terrains and, in principle, for any field shape with any number of obstacles and regardless of the complexity of its shapes. The developed methods help in carrying out field operations in a manner which reduces operational time and fuel consumption and hence reduces the environmental impact in terms of a proportional reduction in the emissions of CO_2 and other greenhouse gases. The developed tools are able to provide the optimized coverage plan as a sequence of waypoints which can be used directly by the control system of the vehicle. In case of in-field obstacles, a complete field coverage approach was developed which involves clustering of field tracks into blocks and then arranging these blocks in a manner which minimizes the connection distance between blocks. The developed tool enables an agricultural vehicle to avoid collision with field permanent obstacles without any human intervention and in a manner that reduces nonworking distance and time. It has been shown that the developed approaches can also be used in non-agricultural applications that involve area coverage planning. Finally, the developed farm machinery system simulator can be used as decision support systems (DSS) to help farmers to better understand complex operations and also using it to test various operational scenarios and selecting the most appropriate one.

References

Acar, E. U., Choset, H., Zhang, Y. & Schervish, M. (2003). Path Planning for Robotic Demining: Robust Sensor-based Coverage of Unstructured Environments and Probabilistic Methods. The International Journal of Robotics Research, 22(7–8), 441-466,

Arkin, E. M., Fekete, S. P., & Mitchell, J. S. B. (2000). Approximation algorithms for lawn mowing and milling. *Computational Geometry*, 17, 25–50.

Bochtis, D. D., Vougioukas, S. G., Sørensen, C.G., Hammed, I.A. and T. Oksanen. 2010. *Fleet Management: Assessment of Potential Savings*. Report, EU project: Integration of Farm Management Information Systems to support real-time management decisions and compliance of management standards, WP 3: Analysis Influences of robotics and biofuels on economic and energetic efficiencies of farm production.

Choset, H. & Pignon, P. (1997). Coverage path planning: The boustrophedon decomposition. In: *Proceedings of the International Conference on Field and Service Robotics*, Canberra, Australia.

Choset, H. (2000). Coverage of Known Spaces: The Boustrophedon Cellular Decomposition. Autonomous Robots, 9, 247–253.

Choset, H. (2001). Coverage for robotics – A survey of recent results. *Annals of Mathematics and Artificial Intelligence*, 31, 113–126.

Domnitcheva, S. (2004). Smart vacuum cleaner - an autonomous location-aware cleaning device. In: *Adjunct proceedings of 6th International Conference on Ubiquitous Computing*.

Hameed, I. A., Bochtis, D. D. & Sørensen, C. G. (2011a). Driving angle and track sequence optimization for operational path planning using genetic algorithms. *Applied Engineering in Agriculture* (in press).

Hameed, I. A., Bochtis, D. D. & Sørensen, C. G. (2011b). An optimized obstacle avoidance approach for complete field coverage. (Submitted).

Hameed, I. A., Bochtis, D. D., Sørensen, C. G. & Nøremark, M. (2010). Automated generation of guidance lines for operational field planning. *Biosystems Engineering*, 107(4), 294–306.

Jin, J. & Tang, L. (2010). Optimal coverage path planning for arable farming on 2D surfaces. *Transactions of the ASABE*, 53(1), 283–295.

Jin, J. & Tang, L. (2011). Coverage path planning on three-dimensional terrain for arable farming. *Journal of Field Robotics*, 28(3), 424–440.

Land, S. & Choset, H. (1998). Coverage path planning for landmine location. In: *Proceedings of the 3rd International Symposium on Technology and the Mine Problem*, Monterey, CA.

Oksanen, T. & Visala, A. (2009). Coverage path planning algorithms for agricultural field machines, *Journal of Field Robotics*, 26(8), 651–668.

Optimal route for slurry spreading with umbilical hose (2011). Retrieved November 29, 2011, from http://130.226.173.223/agromiljoe/map.html.

Ryerson, A. E. F. & Zhang, Q. (2007). Vehicle path planning for complete field coverage using genetic algorithms. *Agricultural Engineering International: CIGR Ejournal*, 4, manuscript ATOE 07 014.

Conclusions

Optimized coverage planning provides the ability to accomplish various field operations in a manner that minimizes operational time, driving over field surface, fuel consumption and the consequent environmental implications. Complete and optimized coverage path planning is a key challenge for automated and (future) autonomous agricultural vehicles. Algorithms for generating coverage paths should be able to deal with any field regardless of its shape complexity and on both 2D and 3D terrains. These algorithms should be fast and suitable for on-board calculations.

The general objective of this PhD assignment, therefore, was to develop a set of coverage planning algorithms to enable the automatic execution of various field operations, such as seeding, spraying, harvesting, etc.. To accomplish this goal, the following framework has been applied:

1. A set of complete field area geometrical representation algorithms have been developed. The developed algorithms can deal with a field as a single block or as multi-blocks where the field area is divided into sub-areas. All these algorithms works on 2D field terrain.
2. g. Based on this geometrical representation a GA-based optimization tool was developed to optimize the field area coverage by finding the driving angle and track sequence which minimizes operational time, and skips and overlaps in covered area..
3. It has been observed that important information is lost when working on 2D terrain and therefore, a tool was developed which can produce coverage planning on 3D terrain minimizing fuel consumption and environmental impact.
4. Finally, it was necessary to combine the developed algorithms in a tool able to provide farmers with the optimal machinery specifications required to carryout material handling operations through the development of an object oriented model to simulate these operations.

During the course of this research, the relationship between efficiency of field operations and the applied coverage planning was indicated. From simulation results, it was shown that applying an optimized driving pattern can significantly improve the energy efficiency of the field operations, e.g. fuel savings could be in the range of 10 to 15% (Hameed et al., 2011) relative to normal practices. This provides a significant environmental impact represented in reduced emissions of CO_2 and other greenhouse gases as a result of the reduced combustion (Dinica, 2002).

References

Denmark Statistics, 2011. Danmarks Statistik. Retrieved from www.dst.dk/stattabel/868.

Dinica, V. (2002). Energy policies for CO_2 emissions reduction. In: *Yotova, A. (Ed.), 'Natural resource system challenge II – Climate change, human systems and policy', Encyclopedia of life support systems*, EOLSS Publishers Co., Oxford, UK (retrieved from http://www.eolss.org).

Hameed, I. A., Bochtis, D. D. & Sørensen, C. G. (2011). Driving angle and track sequence optimization for operational path planning using genetic algorithms. *Journal of Applied Engineering in Agriculture*, ASABE (in press).

Iowa State University report, (2011). Fuel required for field operations. Retrieved from http://www.extension.iastate.edu/Publications/PM709.pdf.

Future Perspectives

Based on the research conducted in this thesis, it was shown that a significant increase in the efficiency of field operations can be achieved through the applications of optimized coverage planning methods. Regarding the optimization methods adopted in the approach, coverage planning is computationally complex (NP-Hard) and the solutions obtained using GAs are near optimal. Therefore, the adoption of other optimization approaches is needed.

Working on 2D important information about field terrain might be lost as a result of ignoring the elevation variations. Working on 3D surfaces is very promising in the regard of minimizing fuel consumed and environmental implications. Soil erosion and can be further considered in future work.

As a future work, the developed algorithms and approaches have to be implemented in web environment in order to evaluate its efficiency in real field operations and to attract farmers' attention to use and apply this technology. This can be accomplished by implementing the algorithms on a web server where the user can use existing web-based services, like Google Maps, for the selection of field and the visualisation of the coverage plan.

List of scientific publications

Journal articles

Bochtis D. D., Sørensen C. G., Jørgensen R. N., Nørremark M., Hameed I. A. & Swain K. C. (2011). Robotic weed monitoring. *Acta Agriculturae Scandinavica, Section B - Plant Soil Science*. 61(3): 195-201

Hameed, I. A., Bochtis D. D., Sørensen C. G , & Nørremark M. (2010). Automated generation of guidance lines for operational field planning. *Journal of Biosystems Engineering*, 107(4), 294-306.

Bochtis, D. D., Sørensen, C. G., Busato, P., Hameed, I. A., Rodias, E., Green, O., & Papadakis, G. (2010). Tramline establishment in controlled traffic farming based on operational machinery cost. *Journal of Biosystems Engineering*, 107(3), 221-231.

Hameed, I. A., Sorrenson, C. G., Bochtis, D. D. & Green, O. (2011). Field robotics in sports: automatic generation of guidance lines for automatic grass cutting, striping and pitch marking of football playing fields. *International Journal of Advanced Robotic Systems*, 8(1), 113-121 (ISSN 1729-8806).

Hameed, I. A., Bochtis, D. D. & Sørensen, C. G. (2011). Driving angle and track sequence optimization for operational path planning using genetic algorithms. *Applied Engineering in Agriculture*, ASABE, 27(6), 1077-1086.

Hameed, I. A., Bochtis, D. D., Sørensen, C. G. & Vougioukas, S. (2012). An object oriented model for simulating agricultural in-field machinery activities. *Computers and Electronics in Agriculture*, 81(1), 24-32.

Hameed, I. A., Bochtis, D. D., Sørensen, C. G. Jensen, A. L., & Larsen, R. (201x). Three-Dimensional Field Representation for Complete Automation and Optimization of Autonomous Agricultural Operations. (To be submitted in *Computers and Electronics in Agriculture*).

Hameed, I. A., Bochtis, D. D., Sørensen, C. G. (201x). A simplified two-dimensional field area coverage planning involving obstacles. (submitted).

International conferences

Bochtis, D. D., Sørensen, C. G., Nørremark, M., Hameed, I. A. and Swain, K. C. 2009. Field Monitoring System Using a Small Robot. *Conference "Technology and Management to Increase the Efficiency in Sustainable Agricultural Systems"*, Rosario, Argentina.

Swain, K. C., Nørremark, M., Bochtis, D., Olsen, H. J., Sørensen, C. G., Green O., Hameed, I. A. 2009. Automated Blob Spraying System for Agricultural Robots. *International Agricultural Engineering Conference* (IAEC2009), Bangkok, Thailand.

Hameed, I.A., Bochits D. D., Swain K.C., Green O., Sorensen C.G. 2009. Evaluation of field coverage algorithms for agricultural machines. *International Agricultural Engineering Conference* (IAEC2009), Bangkok, Thailand.

Green O., Larsen, J. J., Kristensen, E. F., Nadimi, E. S., Jørgensen, J. R., Hameed, I. A., Bochtis D. D., Sørensen C. G. 2010. Automated monitoring of variations of drying conditions in a seed drying facility. *XVIIth World Congress*, Quebec City, Canada.

Green O., Larsen, J. J., Jørgensen, J. R., Nadimi, E. S., Jensen, M., Hameed, I. A., Bochtis D. D., Sørensen C. G. 2010. Wireless sensors for process monitoring of seed storage. *XVIIth World Congress*, Quebec City, Canada.

Oudshorn, F.W., Sørensen, C.G., Green, O., Bochtis, D., Munkholm, L., Hameed, I.A. (2010). Design of research platform for integrating ICT and automation in organic arable cropping. *ASABE Annual International Meeting*, Pittsburgh, Pennsylvania, USA, Paper Number 1009325.

Sørensen, C.G. Oudshorn, F.W., Green, O., Bochtis, D., Munkholm, L., Hameed, I.A. (2010). Platform for integrated ICT and automation. *NJF seminar 438*, Page 65.

Hameed, I.A., Sørensen, C.G., Green, O. (2011). Role of a vehicle's driving angle in an agricultural field. *NJF seminar 441, Automation and System Technology in Plant Production, CIGR section V & NJF section VII conference, 30 June - 2 July 2011,* Hammerum, Denmark.

Hameed, I. A. & Green, O. (2011). Preface – Automation and system technology in plant production. *Abstract from CIGR/NJF seminar 441 – Automation and system technology in plant production*, Herning, Denmark.

Contribution to scientific report

Bochtis, D. D., Vougioukas, S. G., Sørensen, C. G., Hammed, I. A. & Oksanen, T. (2010). Fleet Management: Assessment of Potential Savings. *EU project: Integration of Farm Management Information Systems to support real-time management decisions and compliance of management standards, WP 3: Analysis Influences of robotics and biofuels on economic and energetic efficiencies of farm production*.

Poster sessions and seminars

Nørremark, M. and Hameed, I. A. (2009). Pant nursing field robotics: the hortibot. *Field Robot Event 2009 July 6, 7 & 8*, Wageningen University, Netherlands.

Hameed, I. A. (2009). An automated GPS guided vehicle model for evaluating agricultural field coverage algorithms. *Green Agricultural Robotics conference*, September 9, Odense, Denmark.

Hameed, I. A. Bochtis, D. D., Nørremark, M. & Sørensen, C. G. (2010). On-line field-track generation tool. 10-11 Jun, Nordunet Agri seminar, Helsinki, Finland.

Hameed, I. A., Green, O., Nørremark, M., Sørensen, C. G. (2010). Field robotics in sports: automatic grass cutting, striping and pitch making of football fields. *Opening of new research facilities*, August 16, Foulum, Denmark.

Hameed, I. A. (2010). *A platform for the optimization and automation of autonomous vehicles in field operations. Jensen, AL & Pesonen, L (Eds.), 2010, Proceedings of Nordunet Agro Seminar on Mobile internet services for online support of agricultural machinery*, 10-11 June 2010, Helsinki

and Vihti, Finland, Aarhus University DJF Internal Report, Markbrug no. 28 2010, 150pp (http://www.agrsci.dk/Nordunet_Agri_Seminar_2010).

Curriculum Vitae

Ibrahim A. Hameed was born in March 1976 in Damietta, a city located in the north east part of the Delta of the river Nile in Egypt. He was graduated in May 1998 with the first honour grade from Department of Industrial Electronics and Control Engineering, Faculty of Electronic Engineering, Menofia University, Egypt. In December 1999, he completed his military service at the Egyptian Second Field Army (652th Signal Regiment). In January 2000, he joined Menofia University as an Assistant Faculty member. In May 2005, he completed his MSc in the area of intelligent control and automation. In September 2005, he joined College of Agriculture and Life Sciences (CALS), at Seoul National University (SNU), Seoul, South Korea, as a Research Assistant. In March 2006, he joined Dept of Industrial Systems and Information Engineering at Korea University, S. Korea and started a PhD project in the area of artificial intelligence and expert system and its applications in control and decision support system. In November 2008, he joined Aarhus University and started a PhD project in the area of autonomous navigation and optimization of autonomous vehicles in agriculture. In August 2010, he obtained his first PhD degree from Korea University. During his second PhD, he worked with the automation and system technology group within the Department of Biosystems Engineering which has been lately become Department of Engineering (DoE).

Ibrahim Abdel Fattah Abdel Hameed, Intelligent Behavior of Autonomous Vehicles in Outdoor Environment, 2012

Department of Engineering
Aarhus University
Edison, Finlandsgade 22
8200 Aarhus N
Denmark

Tel.: +45 4189 3000